World Renewable Energy Congress – Sweden

8–13 May, 2011
Linköping, Sweden

Editor

Professor Bahram Moshfegh

Copyright

The publishers will keep this document online on the Internet – or its possible replacement –from the date of publication barring exceptional circumstances.

The online availability of the document implies permanent permission for anyone to read, to download, or to print out single copies for his/her own use and to use it unchanged for non-commercial research and educational purposes. Subsequent transfers of copyright cannot revoke this permission. All other uses of the document are conditional upon the consent of the copyright owner. The publisher has taken technical and administrative measures to assure authenticity, security and accessibility.

According to intellectual property law, the author has the right to be mentioned when his/her work is accessed as described above and to be protected against infringement.

For additional information about Linköping University Electronic Press and its procedures for publication and for assurance of document integrity, please refer to its www home page: http://www.ep.liu.se/.

Linköping Electronic Conference Proceedings, 57
Linköping University Electronic Press
Linköping, Sweden, 2011

http://www.ep.liu.se/ecp_home/index.en.aspx?issue=057
ISBN: 978-91-7393-070-3
ISSN 1650-3740 (online)
ISSN 1650-3686 (print)

© The Authors

Volume 6

Hydropower Applications

Table of Contents

Low Head Pico Hydro Turbine Selection using a Multi-Criteria Analysis

S.J. Williamson*, B.H. Stark, J.D. Booker

Faculty of Engineering, University of Bristol, Bristol, UK
** Corresponding author, Tel: +44 (0)117 954 5499, E-mail: sam.williamson@bristol.ac.uk*

Abstract: Turbine types suit specific ranges of head, flow rate and shaft speed and are categorised by specific speed. In the pico range, under 5kW, the requirements are often different to that of larger scale turbines and qualitative requirements become more influential. Pico hydro turbines can be applied beyond these conventional application domains, for example at reduced heads, by using non-traditional components such as low speed generators. This paper describes a method to select which turbine architecture is most appropriate for a low-head pico hydro specification using quantitative and qualitative analyses of 13 turbine system architectures found in literature. Quantitative and qualitative selection criteria are determined from the particular requirements of the end user. The individual scores from this analysis are weighted based on perceived relative importance of each of the criteria against the original specification and selects a turbine variant based on the total weighted score. This methodology is applied to an example of a remote site, low head and variable flow specification and used to select a propeller turbine variant or single-jet Turgo turbine for this specification.

Keywords: *Pico hydro, Turbine selection, Low head, Application Range, Turgo*

1. Introduction

Typically, selecting hydro turbines is based on the specific speed of the turbine, a non-dimensional parameter that includes head, output power and output shaft speed [1]. From this, the commonly used application domain for turbines is used to aid selection, as in Fig. 1, which has been compiled from [2], [3] and [4]. This leads to the choice of Pelton and Turgo turbines at high heads, crossflow and radial (Francis) turbines at mid heads and propeller turbines and waterwheels at low heads. This is also reflected in the commercially available turbines for these heads.

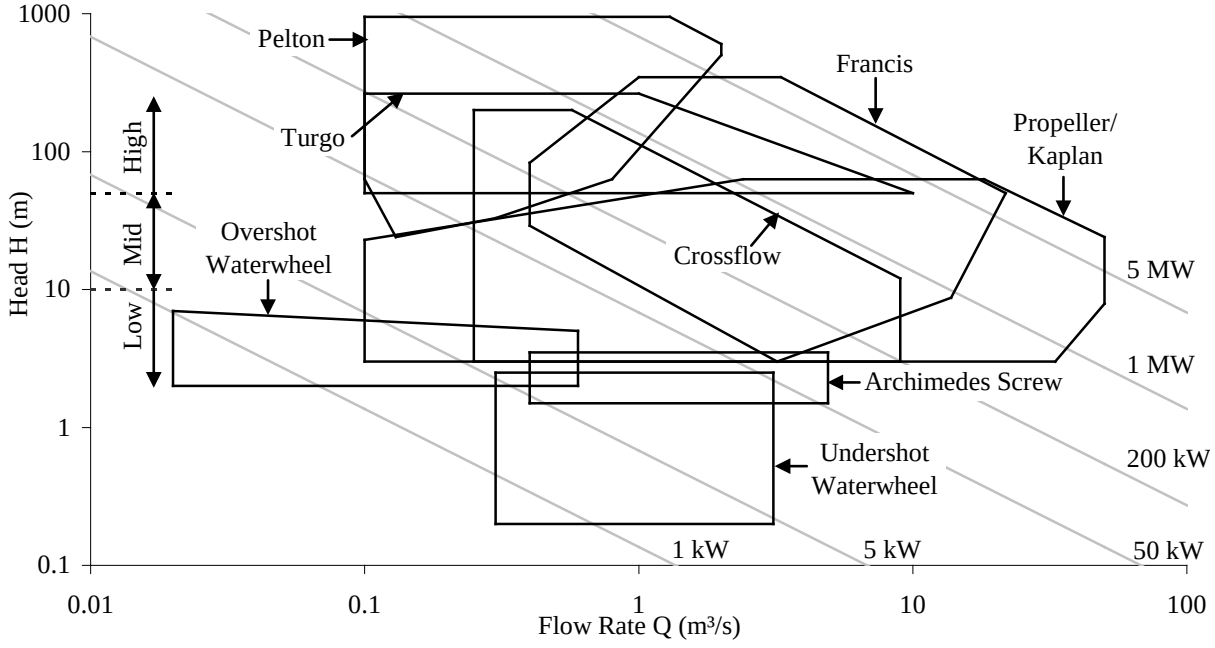

Fig. 1. Turbine application range chart, adapted from data in [2], [3] and [4].

As can be seen in Fig. 1, the pico range, under 5 kW generation, appears to be sparsely covered by reported application domains. There are several commercially available pico hydro products at high, mid and low head, and these tend to follow the topology of the larger scale turbines. The use of traditional 4 or 6-pole generators and direct generator-grid interfaces restricts the application domains for pico hydro turbines. However, introducing technologies such as low speed generators or inverter based grid interfaces generally extends a turbine's application domain, thus providing alternative turbine solutions. In addition, the requirements on a pico hydro turbine tend to be different to those of a larger scale turbine; pico hydro generators cannot carry the cost of unique designs for each location, requiring instead off-the-shelf solutions. It can be located in remote locations, several hours walk from the nearest road and have no skilled labour locally to operate and maintain the system. The application domain selection method of turbine selection does not take these more qualitative factors into account. The method proposed in this paper is used to select a pico hydro turbine for a low head specification using both quantitative and qualitative criteria.

2. Methodology

2.1. Selection Criteria

Each turbine system will have a set of requirements and specification. This will include either site conditions, such as head and flow rate, or output power requirements. There will be environmental requirements, for example the site may be in an inaccessible location, be subject to extremes in temperature or have to comply with fishery regulations. The turbine may be able to have regular maintenance checks from an onsite operator, or it may be required to be operated remotely and therefore should require minimal maintenance and have a high reliability. Using the requirements, a set of selection criteria can then be developed. Table 3 shows the selection criteria used in the method example in Section 3. Some of the criteria can be assessed through a quantitative analysis, whilst others are less quantifiable, and so will require a qualitative analysis. These analyses are then combined to give each turbine type a final score.

2.2. Quantitative Analysis

Basic fluid flow equations are used to derive simple performance characteristics about the turbine option for the quantitative analysis. The performance variables are turbine power P, overall turbine system efficiency η, flow rate Q, and gross head H_g, two of which will need to be defined, leaving two unknowns. These variables are combined using Eq. (1) [1] for a general turbine system.

$$P = \eta \rho g Q H_g \tag{1}$$

where ρ is density and g is the gravitational constant. The two unknowns are solved using a second equation, which is derived from further analysis of the turbine torque generation mechanism. This analysis may result in the power available at a specific site and the turbine system efficiency or the efficiency and flow rate required to produce a specified power depending on the variables defined. There are 13 turbine types commonly used which are divided into 4 categories: Impulse, Reaction, Archimedes Screw, and Waterwheel. Each category has a different torque generation mechanism and is analysed in a different manner, as summarised in the following Sections. The performance modelling used here is simplified, neglecting fluid mechanic non-linearities, and assumes linear geometric scaling. For some turbines considered, impractical geometries are generated at the extremes of their head range.

2.2.1. Impulse Type – Pelton and Turgo (single and multiple jet), Crossflow

Velocity triangles of the water jet impacting with the blade of the turbine are used to analyse the impulse turbines [1]. The head loss in the penstock H_{l1} reduces the inlet jet velocity. The change in whirl velocity Δv_w is used to calculate the rate of change in momentum of the water, generating a force at the blade. The force is concentrated at the jet impact point, radius r, assuming the flow enters and exits at the same radius, which causes a torque T on the wheel. The power is then the product of the rotational speed at maximum power ω by the torque

$$P = T\omega = Q\rho\Delta v_w r\omega \,. \tag{2}$$

2.2.2. Reaction Type – Axial, Radial

The gross head H_g in Eq. (1) is reduced by head losses in the penstock H_{l1}, the draft tube H_{l2}, and from the outflow kinetic energy H_{l3}. These head losses are functions of the speed of the water passing through the component and a factor dependent on the geometry of the component [1]. The power generated is then dependent on the net head and the estimated turbine hydraulic efficiency η_t, which is different to η in Eq. (1),

$$P = \eta_t \rho g Q\left(H_g - H_{l1} - H_{l2} - H_{l3}\right). \tag{3}$$

2.2.3. Archimedes Screw

The Archimedes screw operates on a hydrostatic pressure difference across the blades [5]. The efficiency η is a function of the geometry of the screw n, the diameter D, and the flow passing through it Q

$$\eta = \left(\frac{2n+1}{2n+2}\right)\left(1 - \frac{0.01125D^2}{Q}\right). \tag{4}$$

2.2.4. Waterwheels – Overshot, Breastshot, Undershot

The analysis for the waterwheels is based on the losses in the system, as described in [6]. For the Overshot and Breastshot Waterwheels it is assumed that the losses are only the kinetic energy loss from the water entering the wheel H_{l4}, and the swirl in the water on the exit of the wheel H_{l5}, and the efficiency is then

$$\eta = \left(\frac{H_g - H_{l4} - H_{l5}}{H_g}\right). \tag{5}$$

For an Undershot Waterwheel, two efficiency losses are considered. First the inlet efficiency η_{th} represents the non-ideal flow entrance due to fixed wheel geometry, second the friction on the water bed h_{l6} ($=H_{l6}/H_g$), which models friction loss as a function of inlet water velocity. The efficiency is then

$$\eta = \eta_{th} - h_{l6} \,. \tag{6}$$

2.3. Qualitative Analysis

The qualitative analysis uses clearly defined criteria to score the qualitative aspects of the turbine selection, as in [7]. Each criterion is given an unambiguous definition and a defined scoring system between 1 (poor) and 5 (excellent). Each turbine is then scored against this scoring system as a part of a team discussion. An example of the scoring system is shown in Table 1, which was developed as part of the research methodology and used in Section 3.

Table 1. Example qualitative scoring definition and criteria.

Scope for Modularity

Definition - Modules that allow the system to be broken into carryable/shippable units and allow line replaceable for easy servicing and fault identification, with the ability to interchange identical modules.

Scoring Criteria	**Score**
Few, but standard, interfaces; few system elements; simple coupling mechanisms between elements; simple element architecture orientation	5
Few non-standard interfaces, some standard interfaces; manageable architecture; some non-standard coupling between system elements	3
Many non-standard interfaces; many separate system elements; complex coupling mechanisms between system elements; unusual element architecture orientation	1

A scoring system is defined for each of the different selection criteria. If within a criterion there are several different aspects, then sub criteria are used to fully define all the different aspects. These are combined to form a single score for the criterion, through either an arithmetic or weighted mean.

2.4. Combining Analyses

The results from the quantitative analysis are normalised against the maximum value, and the qualitative scores are normalised against the maximum value, 5. A weighting for each of the criteria is decided by project stakeholders, as recommended by [7]. These weightings are multiplied by normalised scores from the quantitative and qualitative analyses to give a final score for each turbine solution. The scores can then be analysed and an appropriate solution chosen. In the following Sections, the method described above is shown through an example.

3. Example of Pico-Hydro Turbine Selection Using Multi-Criteria Analysis

The village of Bhanbhane in central Nepal has several low head sites for turbines. The heads at the sites vary from 0.5 m to 3.5 m, the flow available at the sites also varies depending on the season and the location in the river. There are two different rivers that would supply the sites. The villagers would like to install the same turbine in all of the locations, making savings in bulk buying and allowing them to stockpile spares. At each turbine site, they do not require more than 1 kW of electric power, so allowing for inefficiencies in the system, such as drive and generator losses, the turbine should produce 1.3 kW of mechanical power. Bhanbhane is a rural village, and the sites lie several kilometres from the nearest road, so the units need to be portable, ideally able to be carried by villagers. Also, with the rural location and the distance from a road, cement is expensive and difficult to obtain, therefore the civil works should be minimised. The villagers intend to carry out on-site maintenance and servicing themselves, so the unit should be simple to maintain and have a modular design allowing faulty modules to be easily identified and replaced. Any faulty modules that cannot be repaired onsite are to be returned to the manufacturer or a service centre for repair. It is

assumed that the generator output is 50 Hz, with a direct interface to the distribution system. From this, the specification for the turbine is derived (Table 2), and the selection criteria developed (Table 3).

Table 2. Turbine specification

Power:	1.3 kW
Head:	Range from 0.5 to 3.5 m
Portability:	Able to be transported to locations with limited transport infrastructure
Reliability:	High reliability for low maintenance operation
Output Frequency:	50 Hz output from generator
Maintenance:	Maintenance and servicing carried out by unskilled labour
Flow rate:	Large variation across the seasons
Modularity:	Turbine in modules to allow for easy fault identification and module replacement
Civil works:	Small civil works

Table 3. Selection criteria

Efficiency:	Efficiency of the unit at rated flow/head and at part flow/part head
Power:	Power of the unit must be 1.3 kW
Portability:	Minimised volume for easy transportation
Civil Works:	Minimised civil works – concrete sparsely available in site locations
Modularity:	Scope to incorporate modularity into the design for line replaceable units and to disassemble the unit for ease of portability
Maintenance & Serviceability:	The ease of maintaining and servicing the unit, especially with unskilled labour.

Here, power and head are the known variables, with the efficiency and flow rate required from the quantitative analysis. The volume of the unit is estimated as a function of the flow rate and using existing designs and rules, for example [8]. The portability and power are dealt with by deriving a power density metric (rated power/volume) which provides the volume required to generate 1.3 kW. This volume includes the penstock, turbine and casing. The power density and rated flow efficiency are thus treated by the quantitative analysis, whilst the part flow/part head efficiency, civil works, modularity and maintenance will be analysed qualitatively. The quantitative analysis designs a set of turbines for heads from 0.5 m to 3.5 m in 0.5 m steps. Power density is chosen to be the most important criterion, as if the unit is too large and unwieldy then the villagers will not be able to implement it in their chosen sites. The maintenance and serviceability and modularity in the design are considered less important, which is reflected in the weightings, shown in Table 4.

Table 4. Weighting scheme for example.

Selection Criteria	**Weighting**
Power Density	0.30
Rated Flow Efficiency	0.25
Part Flow, Part Head Efficiency	0.20
Civil Works	0.15
Maintainability & Serviceability	0.05
Scope for Modularity	0.05

The turbines assessed represent the four main different turbine types described in Section 2.2. Impulse and reaction turbines require a penstock, which is assumed to have a 5% head loss.

The multiple jet turbines are assumed to have four jets which give it a volume and efficiency penalty. It is assumed that the turbine is connected to a generator that can produce 50 Hz as long as the rotational speed is between 200 and 3000 rpm (commercially available generators). If the rotational speed is less than or greater than these limits, a gearbox is required to bring the speed within these limits and so gearbox efficiency is taken into account.

4. Results

The results from the quantitative analysis are shown in Fig. 2. The summary of the results from the combined analysis are shown in Fig. 3 and 4.

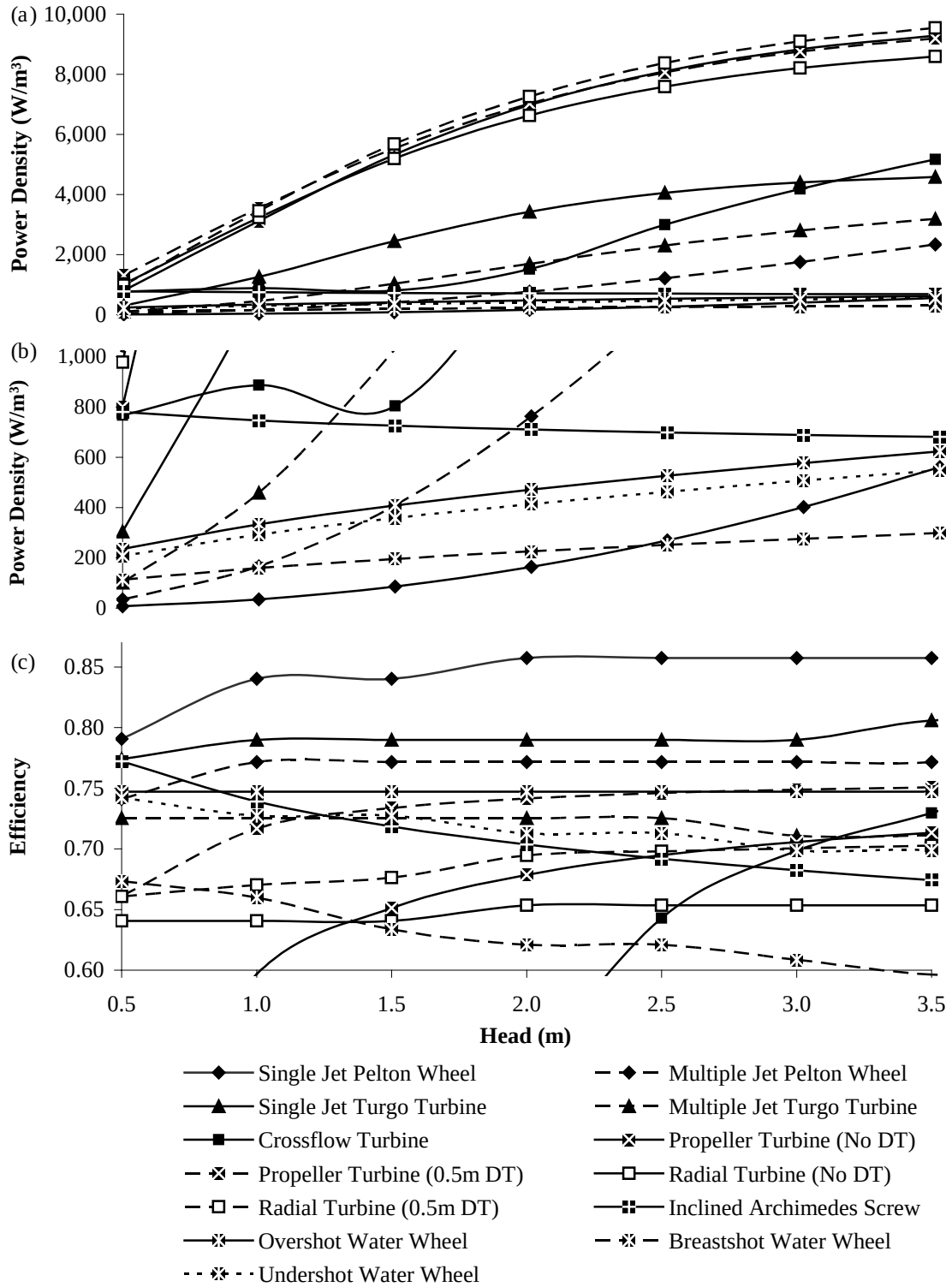

Fig. 2. The output of the quantitative analysis: (a) power density (b) power density zoomed in at low power density (c) efficiency variation over the head range 0.5 to 3.5m, 'DT'=Draft Tube.

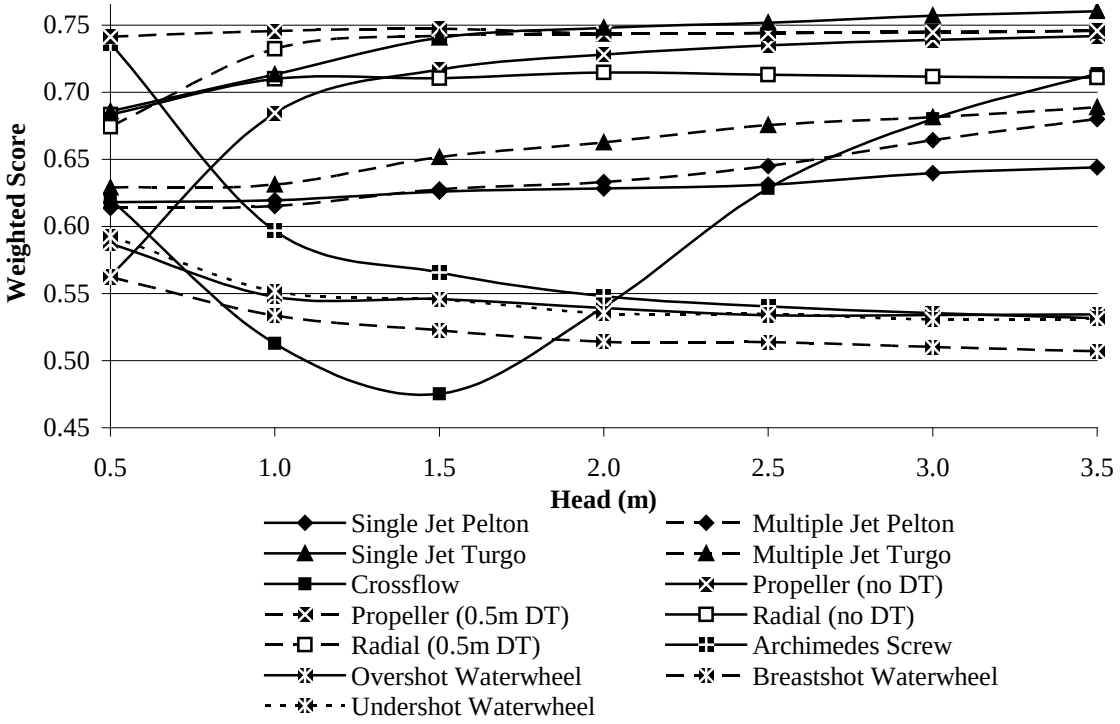

Fig. 3. The weighted scores for the 13 turbine choices over the head range 0.5 to 3.5m, 'DT'=Draft Tube.

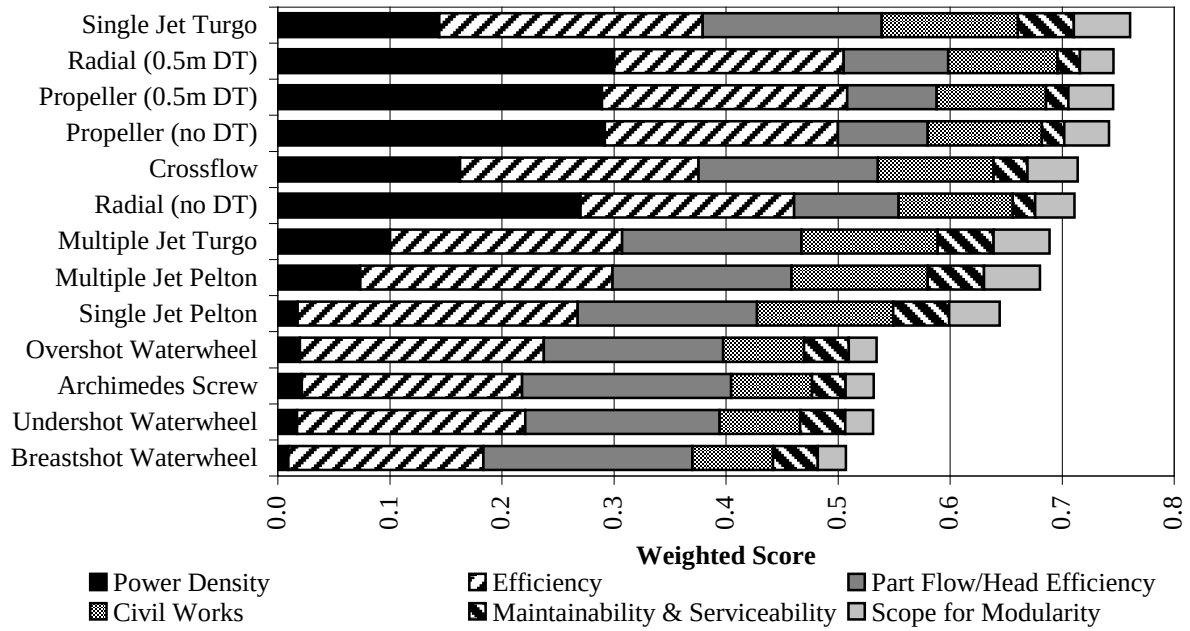

Fig. 4. The weighted score at 3.5m head for the 13 turbine choices with the contributions from each of the different selection criteria, 'DT'=Draft Tube.

Using this selection method and the specification in Table 2, the propeller turbine with draft tube (DT) should be selected if the typical head is between 0.5 and 1.5 m, and the single-jet Turgo turbine should be selected if the typical head is between 1.5 and 3.5 m.

5. Discussion

Fig. 2 (a) shows that the reaction turbines have a superior power density. As the head increases, the power density of the impulse turbines and waterwheels improves, whilst that of

the Archimedes Screw decreases. The conventional solution of adding multiple jets for Pelton and Turgo turbines at low heads is penalised in the power density, as the extra pipe work required to feed the jets takes up a large amount of volume. The efficiency of the single jet impulse turbines is superior to all the other turbines, as shown in Fig. 2 (c). As the head increases then the speed of the impulse turbine increases, so removing the need for a gearbox, increasing the overall efficiency of the turbine. Fig. 3 shows the variation in the weighted scores over the head range. This shows that a propeller turbine with a draft tube is the most suitable solution between 0.5 and 1.5 m typical head, with the single-jet Turgo turbine the best solution above 1.5 m typical head. The propeller and radial turbines with draft tubes have a similar weighted score to the single-jet Turgo turbine above 1.5 m head and therefore are viable choices for the specification. The reaction turbine result is expected, as many of the low head commercial turbine systems available are propeller turbines with draft tubes. The surprising result in this analysis is the Turgo turbine which is usually only used in medium to high heads – as indicated in the application range graph in Fig. 1, and stated in several literature resources such as [2]. However, as Harvey points out in [8], the Pelton turbine, and therefore the Turgo turbine, can be used in low heads if low speed and runner size do not pose problems. Using the calculations in the previous section, the runner diameter for a single-jet Turgo turbine generating 1.3 kW at 3.5 m head would be 435 mm, which would therefore not pose a portability problem in rural areas.

6. Conclusion

This research is part of a project to develop a low head pico-hydro off-grid network. The turbine selection is the first phase of the project which will look at developing the network technology requirements. This paper has presented a method of selecting low head pico hydro turbines through a multi-criteria analysis, using the specification of the turbine to assess the turbine types through quantitative and qualitative analyses. Using this method, a propeller turbine with a draft tube or a single-jet Turgo turbine has been shown to be the best solution for a given low head, variable flow specification.

Acknowledgements

This research is funded by Renishaw plc, and supported by Engineers Without Borders, UK.

References

[1] B. Massey, Mechanics of Fluids, Stanley Thornes Ltd, 7th Edition, 1998.

[2] O. Paish, Micro-hydropower: status and prospects, Proceedings of the Institution of Mechanical Engineers, Part A: Journal of Power and Energy, 216(1), 2002, pp.31-40.

[3] G. Muller and K. Kauppert, Old Watermills - Britain's new source of energy?, Proceedings of the ICE: Civil Engineering, 150, November 2002, pp.178-186.

[4] European Small Hydropower Association, A Layman's Guidebook on How to Develop a Small Hydro Site, 2nd Edition, 1998.

[5] G. Muller and J. Senior, Simplified Theory of Archimedean Screws, Journal of Hydraulic Research, 47(5), 2009, pp.666-669.

[6] F. C. Lea, Hydraulics for Engineers and Engineering Students, Edward Arnold, 1945.

[7] S. Pugh, Total Design, Prentice Hall, 1st Edition, 1991.

[8] A. Harvey et al, Micro-Hydro Design Manual, ITDG Publishing 1st Edition, 1993.

Small scale hydropower: generator analysis and optimization for water supply systems

Guilherme A. Caxaria[1,*], Duarte de Mesquita e Sousa[2,**] , Helena M. Ramos[3,***]

[1] *Electrical and Computer Engineering Department, Instituto Superior Técnico, Technical University of Lisbon, Lisbon, Portugal.*
[2] *Electrical and Computer Engineering Department and CIE[3], Instituto Superior Técnico, Technical University of Lisbon, Lisbon, Portugal.*
[3] *Civil Engineering Department and CEHIDRO, Instituto Superior Técnico, Technical University of Lisbon, Lisbon, Portugal.*
** Av. Rovisco Pais, 1049-001, Lisbon, Portugal , E-mail: gui.caxaria@gmail.com*
*** Av. Rovisco Pais, 1049-001, Lisbon, Portugal , E-mail: duarte.sousa@ist.utl.pt*
**** Av. Rovisco Pais, 1049-001, Lisbon, Portugal , E-mail: helena.ramos@civil.ist.utl.pt*

Abstract: This work focuses on the analysis of the power generation feasibility of both a pump as turbine (PAT) and an experimental propeller turbine, when applied to water supply systems. This is done through an analysis of the electrical generation aspects of the PAT's induction motor and of a permanent magnet DC motor, which was connected to the propeller turbine. The collected data allows for parameter optimization, adequate generator choice and computational modeling. These tests constitute a good sample of the range of applicability of small scale turbines as valid solutions for micro-hydro. It is also possible to consider multiple scenarios, such as rescaling/resizing, for larger turbines and systems, and the use of power electronics for further efficiency enhancing.

Keywords: *Small-scale hydropower, water supply systems, low power turbines, behavioral analysis*

1. Introduction

Starting from a scientific research base in the field of hydraulics, the objective of this work is to study the applicability and performance of electrical generators when connected to low power hydro turbines, for use in water supply systems (and others with similar characteristics). The generated power has a broad range of application, namely in the field of decentralized production (either on or off-grid) for use in rural or isolated areas, as well as in urban areas. It is possible to use the generated power to supply devices related with the small-scale industry (e.g. hydro-mechanical systems in pumping stations), communication stations, data acquirement, control or telemetry systems, or even observation posts in isolated areas.

Through the use of computer models, laboratorial tests and prototype analysis, a solution for a certain micro-hydro scheme is chosen. Behavioral analysis is then undertaken, allowing for further generator parameter optimization.

1.1. Water supply systems

Water supply systems aren't built with a power generation purpose. However, due to the type of infrastructure which is used for their normal operation (pressure reducing and flow control valves, reservoirs, pumps, and piping), they offer a multitude of power generation scenarios while assuring an almost constant flow rate 24h/day. It is then possible to generate power in the following manners: replacing (or assembling a joint installation with) pressure reducing valves; taking advantage of the hours where there's an increased demand for water (hours which coincide with an increase in demand for electrical power); piping water between

reservoirs, in hours of lower demand, and storing the produced energy. All of these are subject to the installation of adequate equipment in the piping.

1.2. Micro-hydro turbines

The existing micro-hydro conversion equipment is based on impulse turbines (i.e. *Pelton*, *Turgo*, and *Cross-flow*) and on reaction turbines (i.e. *Francis* and *Kaplan/propeller*). Their main problem is the low efficiency values (typically 30% to 60%) that are obtained regarding small scale schemes. In this case optimization is needed, in order to increase their efficiency. This type of work, however, will not be discussed in depth in this document.

The application of commercially available small scale turbines to water supply systems is conditioned by a series of restrictions, namely head, flow, pressure, and the need for piping adaptation, which can make them unsuitable for application in a vast majority of sites. Therefore, it is necessary to optimize and/or develop power generation solutions for water supply systems.

2. Pump as Turbine (PAT)

Given the information in the introductory chapter, a PAT was the first of the two solutions that have been considered for power generation in water supply systems. This was due to its simplicity in installation, only requiring small adaptation procedures. In water supply systems, a PAT is to be installed in a bypass circuit.

2.1. Theoretical considerations

Pumps as Turbines have, for the past three decades, been tested and considered for micro-hydro generation. This is due to a number of arguments, those being that PATs are mass produced, for various operating conditions, such as flow, drop, dimensions and rotating speeds. The electromechanical converters that usually equip a PAT are asynchronous machines, optimized for pumping operation, which, as previously mentioned, help to reduce acquisition costs, which, in turn, increase the competitiveness of a PAT in a power generation scenario. Another advantage in the use of a PAT is that its technology is vastly explored and with proven results, adding to the fact that these allow for power values starting at 50W [6].
The main disadvantage in the use of a PAT is that its operation is highly dependent on flow rate, not allowing for medium and high variations of flow. In situations where multiple flow values exist, it is possible to consider the use of two or more PATs [2].

2.2. Laboratorial testing

For laboratorial testing, a PAT (WITH $N_{SPT(M,M^3/S)} = 21\,\text{RPM}$ AND $N_{SPT(M,KW)} = 51\,\text{RPM}$) was acquired, and inserted in a laboratorial system that allowed for head and flow variation, and for grid-connected excitation. The electrical machine that equips the PAT is a six-pole (i.e. with a synchronous speed of 1000rpm) 550W induction motor. The objective was to test the power generation feasibility of the PAT when connected to the grid (i.e. with no additional equipment, such as capacitors for excitation), along with testing the transient response of the induction machine when a hydraulic transient regime occurred (e.g. the closing of a valve). Also analyzed was the behavior of the PAT under runaway conditions.

2.2.1. Power generation testing

Regarding power generation, the results are presentED in Figure 1. Values up to 160W (at a flow of 4.4l/s) were registered. However, due to the fact that the machine was excited

resorting to the main grid, the excitation required 240W of power; this meaning that, in fact, the generator never generated enough power to "counter" the excitation, and thus, the load flow was always done from the grid to the generator.

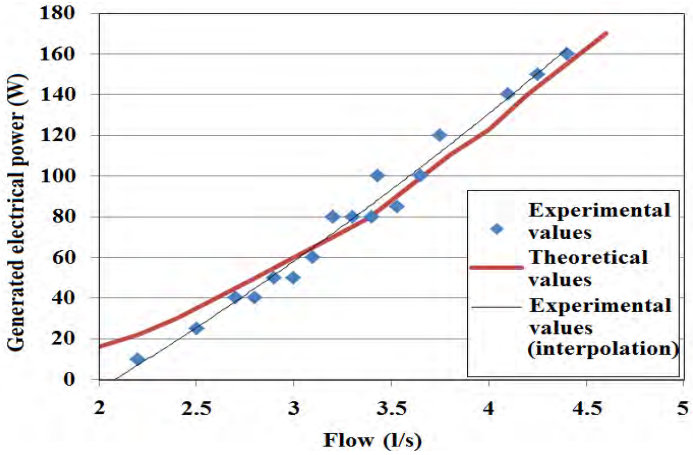

Fig. 1. PAT Power/Flow characteristics.

2.2.2. Transient response analysis

Transient analysis, either electrical or hydraulic, at a micro-hydro scale, is a field of research that is rather unexplored. This field of research, however, is of extreme importance, in order to properly dimension electrical protection methods. In this particular case, a h ydraulic transient regime was created by the sudden closure of a valve which, in turn, originated an electrical transient regime. The testing results are presentED in Figure 2.

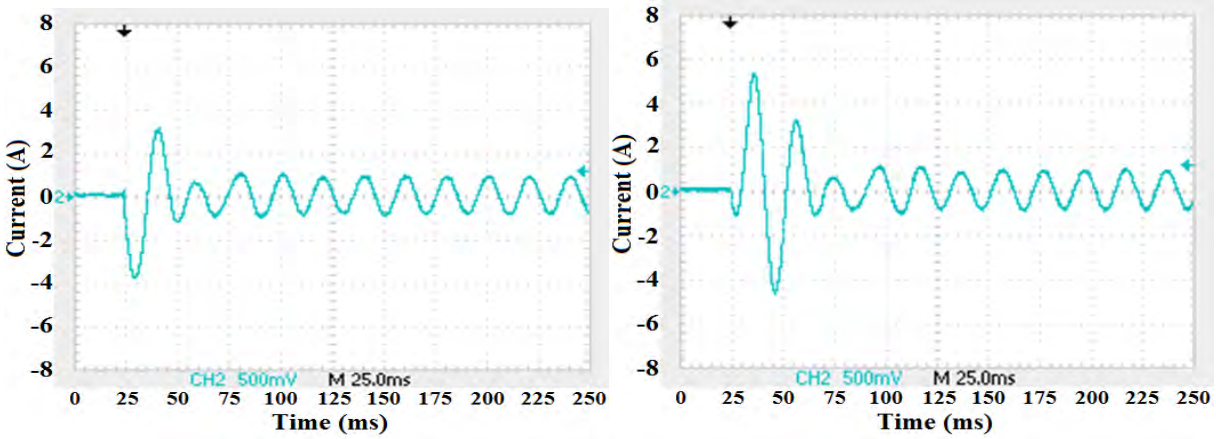

Fig. 2. Electrical transient regimes in the PAT, derived from pressure surges in the piping.

According to the work of [5], it is possible to verify that waterhammer effects induce electrical transients in the generator, thus influencing the power generation. However, it is possible to observe that the duration of the transient regime is, on both cases, under 100ms. Attending to the values of the time constants that are present in the used hydraulic systems, it is possible to claim that the generator doesn't introduce additional dynamic restrictions to the global system.

2.2.3. Runaway conditions analysis

Testing of runaway behavior was also undertaken, in order to properly apply control methods to the system. The results of the mentioned testing are presentED in Figure 3.

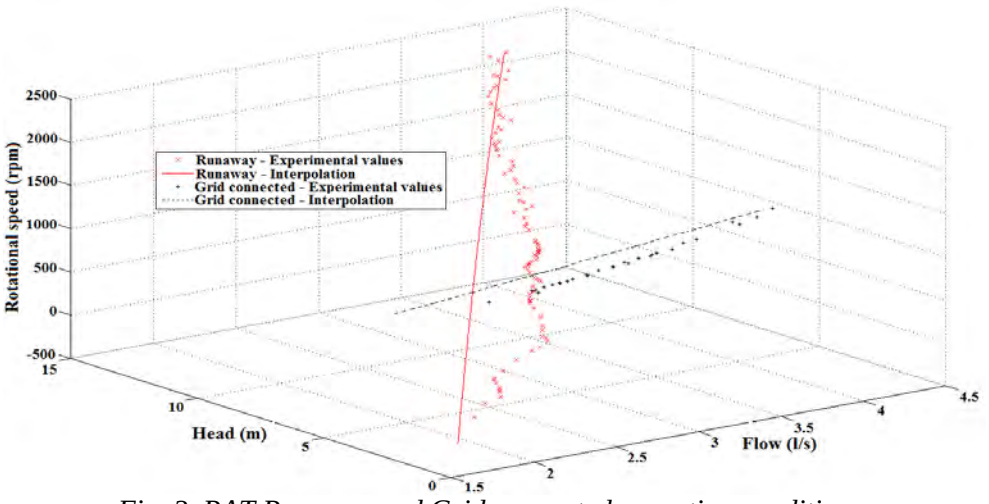

Fig. 3. PAT Runaway and Grid connected operating conditions.

It is possible to observe that, in runaway conditions, for the same flow rate value, pressure surges occur (here described by an increase in the available head). This is coincident with the work of [3] where it is shown that turbines with low specific rotating speeds induce high pressure surges in the piping

2.3. Computational model: control simulation

Given the results obtained in laboratorial testing and due to the nature of water supply systems, the chosen (and simulated) control method was the one resorting to flow control valves. The objective of these simulations was to control and avoid a runaway situation, which results from a load withdrawal on the generator. *MATLAB/Simulink* was used. The control scheme is described in fig 4 and the simulation results are presented in fig 5.

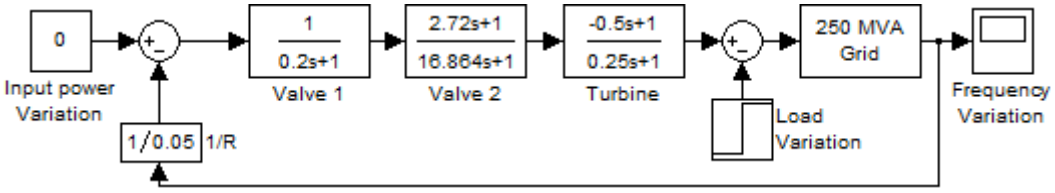

Fig. 4. Control scheme used for the PAT simulations.

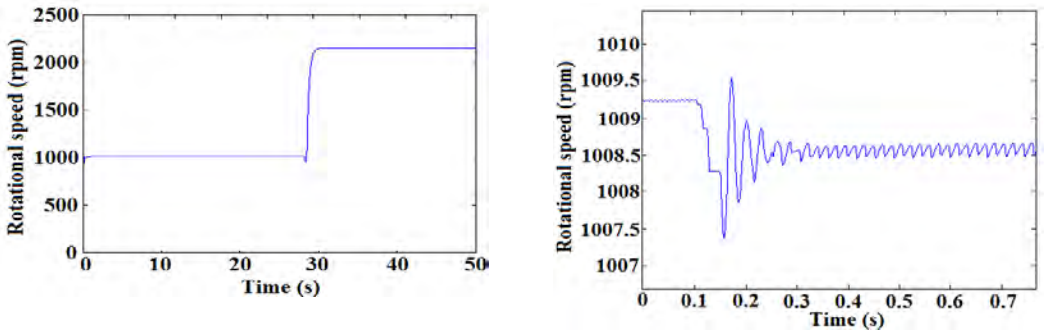

Fig. 5. Simulation results for full and uncontrolled (left), and partial and controlled (right) load removal on the PAT.

3. Five blade propeller turbine (5BPT)

A propeller turbine was the second of the two solutions chosen for micro-hydro generation in water supply systems. Again, equipment and installation simplicity were key factors regarding the choice.

3.1. Theoretical considerations

Propeller turbines are axial turbines, adequate for operation under low head (up to a minimum of 1.5m) and high flow rates. These have been mainly used in small (<10MW) and mini (<2MW) hydro schemes. Only recently, due to developments in scientific research (which, in turn, have resulted in an increase of the turbines' efficiency), has the application been extended to the field of micro-hydro.

Given the difficulties on applying commercially available micro-hydro turbines to water supply systems, a 100mm diameter prototypical propeller turbine was developed specifically for this purpose (under the HyLow project of the 7th Framework Program of the European Union) and (through the work of [7]) optimized for small scale (i.e. blade shape, number, and orientation). This type of turbine can be installed in either a bypass to, or directly in the main piping circuit. Its main disadvantages are that it is still experimental equipment, and there's very little knowledge regarding its long time operation in water supply systems.

3.2. Laboratorial testing

For laboratorial testing, similarly to what was done with the PAT, the 5BPT (with $N_{SPT(M,M^3/S)} = 238\,\text{RPM}$ AND $N_{SPT(M,KW)} = 118\,\text{RPM}$) was inserted in a laboratorial system that allowed for head and flow variation, and that mimicked the conditions found on a real water supply system. Being experimental equipment, the maximum obtained speed was of 1550rpm. For power generation purposes a 500W DC permanent-magnet machine, derived from an electrical scooter, was acquired. Due to the nature of the generator, and to the lack of additional power electronics, no grid connection was done. The turbine's characteristic curves are shown in Figure 5, the DC machine's characteristics and curves are shown in Table 1 and Figure 6.

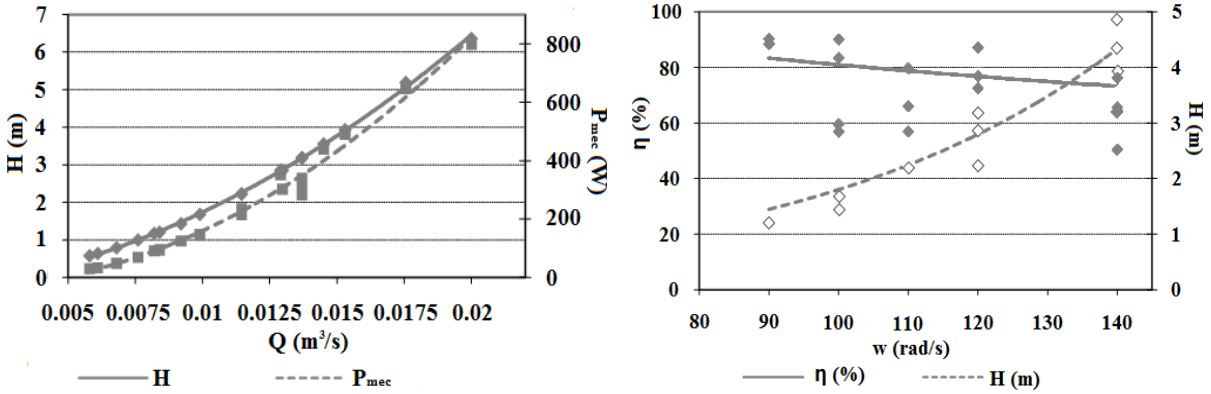

Fig. 6. Five blade propeller turbine characteristic curves

Table 1. DC motor manufacturer's parameters

Rated voltage (V)	Rated power (W)	No-load Current (A)	No-load Speed (rpm)	Rated Torque (N.m)	Rated Speed (rpm)	Rated Current (A)	Rated efficiency (%)
36	500	2.2	3150	1.9	2500	17.8	78

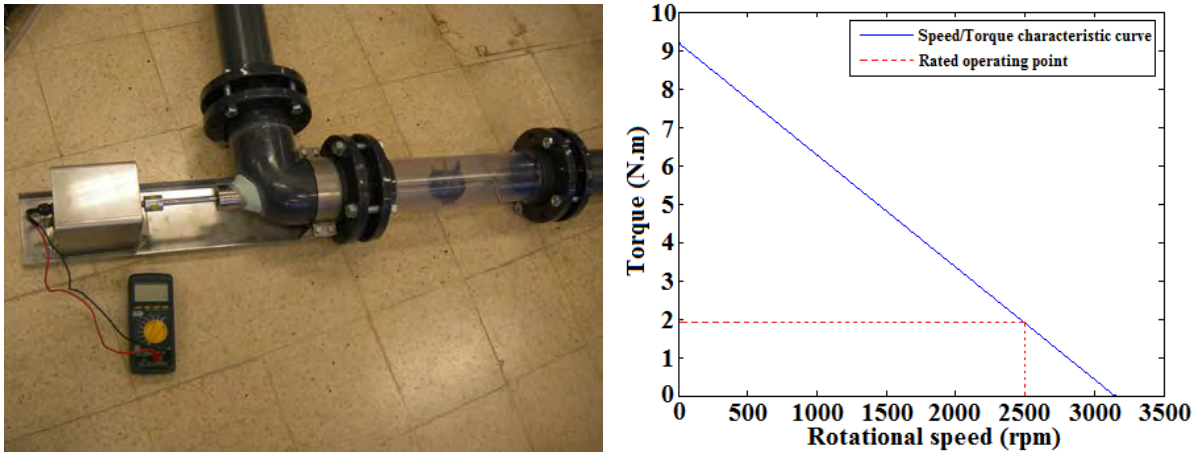

(a) *(b)*

Fig. 7. (a) The turbine+generator group (b) DC motor manufacturer's Torque/Speed curve.

From the data provided by the manufacturer, it was possible to calculate the machine's theoretical characteristic parameters, namely the armature resistance and the k_ϕ constant, to be used for computational simulations:

$$k_{\phi(manufacturer)} = 0.1091 \qquad R_{a(manufacturer)} = 0.4267\Omega$$

3.2.1. Power generation testing

For power generation testing purposes a 6Ω, 16A rheostat was used, in order to emulate the behavior of "normal" electrical loads. The testing was done by varying the resistive load while maintaining a fully open admission valve. The testing was done in three separate sessions, being that, on the first session, there was a constraint in terms of head and flow, and on the second and third sessions, that constraint was eliminated. The best efficiency points for the experimental sessions are presentED in Table 2.

Table 2. Best efficiency points for the three experimental sessions.

Experimental session	Maximum Generated power (W)	Rotational speed (rpm)	Flow rate (l/s)	Generator efficiency (%)	Overall efficiency (%)
#1	3.64	182.5	3.6	35.6	32.8
#2	34.4	719.7	8.8	50.3	46.8
#3	36.2	619.8	10.4	68.2	60.7

From the testing results, it w as possible to calculate the machine's real characteristic parameters, and while the armature resistance corresponded to the manufacturer's value, the k_ϕ constant greatly differed:

$$k_{\phi(experimental)} = 0.1443 \qquad R_{a(experimental)} = 0.4267\Omega$$

3.2.2. Computational model: power generation simulations

Given the obtained conclusions regarding the DC machine's characteristic parameters, simulation was undertaken, again using *MATLAB/Simulink*, in order to test the power generation under optimal conditions (i.e. with $k_\phi = k_{\phi(manufacturer)}$). Due to the nature (i.e. size)

of the turbine, a transfer function similar to the Pat's was used. The simulation results are presented in figures 7 and 8.

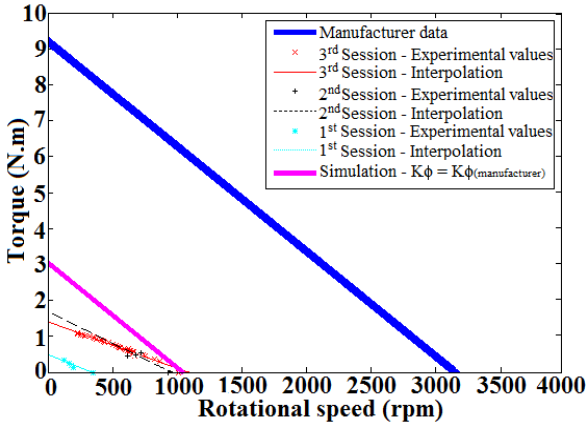

Fig. 8. Manufacturer's, experimental, and simulation Torque/Speed curves

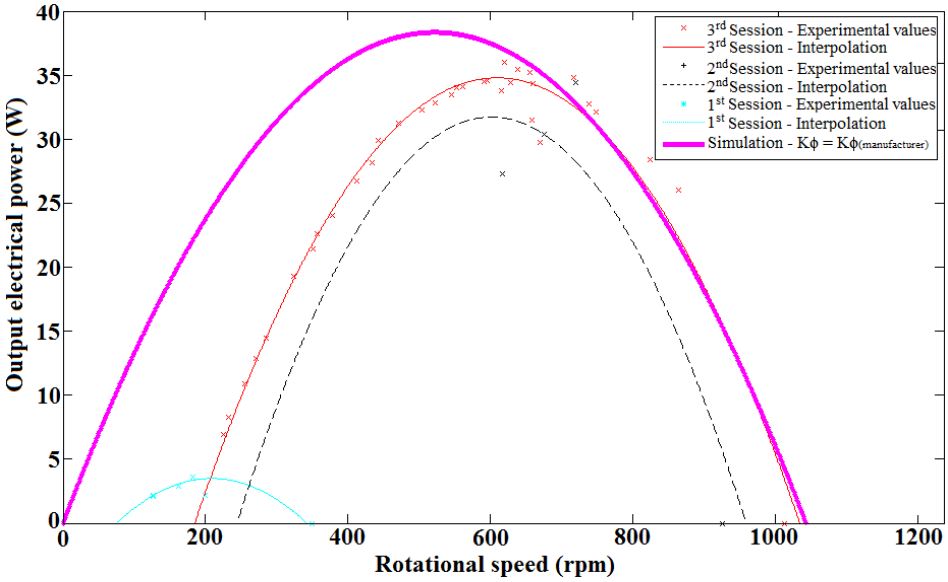

Fig. 9. Simulation and experimental turbo-generator group Output power/Speed curves

4. Conclusions and recommendations

4.1. Pump as Turbine

4.1.1. Main conclusions

From the power generation testing results, it is possible to conclude that the application of PATs for micro-hydro generation in water supply systems is viable. However, using grid-connected excitation may not be viable in all cases, namely the ones regarding lower power values. Control methods using valves, although efficient, may not be viable, namely in situations where there's a g eneration scheme directly applied to the main piping. In these cases, reducing the water flow, for control purposes, in hours of greater water need, may be prejudicial for the populations.

4.1.2. Recommendations

To avoid the excitation related issues, and according to [2] and [11], using "motor run" capacitors (either star, delta, or C-2C connected) for excitation purposes is an alternative, and more efficient way, than resorting to the main grid. As mentioned, for main piping connected

generation schemes, control methods using ELCs, or other electronic devices, may eliminate the issues related with control methods using valves.

4.2. Five blade propeller turbine

4.2.1. Main conclusions

Despite the power values that were generated, the 5BPT, regarding its use in water supply systems, is a very promising solution, with high hydro-mechanical efficiency values. The generated power values using the DC machine, although low, are still viable in a battery charging, or in a low power consumption equipment supply context. The turbo-generator group, when applied to water supply systems, doesn't interfere with the normal flow behavior in the piping.

4.2.2. Recommendations

Regarding power generation in a real system (opposed to a laboratorial one), for testing purposes, a permanent-magnet synchronous generator (or an induction motor) should be used. For laboratorial purposes, a lower power generator should be used, more adequate to the rotational speed and torque values present in the experimental piping system. Testing under better flow and head conditions, for improved power generation, is also recommended for future work.

References

[1] A. Williams, Pumps as Turbines: a user's guide, 2nd Edition, Practical Action Publishing, 2003.

[2] H. Ramos, Guidelines for design of small hydropower plants, 2000, WREAN/DED, ISBN 972-96346-4-5.

[3] H. Ramos, A.B. Almeida, Dynamic effects in micro-hydro modeling, 2003, pp. Water Power & Dam Construction, ISSN 0306-400X.

[4] H. Ramos, A.B. Almeida, Parametric analysis of waterhammer effects in small hydropower schemes, 2001, Journal of Hydraulic Research, IAHR, Vol. 39 (4), pp. 429-436, ISSN-0022-1686.

[5] H. Ramos, A. Borga, Pumps as turbines: unconventional solution to energy production, Urban Water International Journal, Elsevier Science Ltd, 2000, pp.261-265.

[6] H.M. Ramos, A. Borga, M. Simão, New design solutions of low power for energy production in water pipe systems, Water Science and Engineering, 2009, 2(4): 69-84, doi:10.3882/j.issn.1674-2370.2009.04.007.

[7] H.M. Ramos, M. Mello, P. De, Clean power in water supply systems as a sustainable solution: from conceptual to practical analysis, IWA Publishing, Water Science and Technology, 2010.

[8] H.M. Ramos, F. Vieira, D. Covas, Energy efficiency in a water supply system. Water Science and Engineering, 2010, pp.331-340.

[9] J.S. Ramos, H.M. Ramos, Sustainable application of renewable sources in water pumping systems: optimized energy system configuration, 2009, (doi:10.1016/ j.enpol. 2008.10.006), Energy Policy 37, 633-643.

[10] N. Smith, Motors as generators for micro-hydro power, 2nd Edition, Practical Action Publishing, 2008.

Performance evaluation of cross-flow turbine for low head application

Bryan Ho-Yan[1], W. David Lubitz[1,*]

[1] *School of Engineering, University of Guelph, Guelph, Ontario, Canada. N1G 2W1*
** Corresponding author. Tel: +1-519-824-4120 ext. 54387, Fax: +1-519-836-0227, E-mail: wlubitz@uoguelph.ca*

Abstract: Pico hydro generators are a promising means of providing cost-effective electricity to locations with limited or no availability of grid-supplied electricity. The Firefly design has been employed throughout rural areas of Cameroon and used as a light battery charger. It is hoped to extend the turbine capacity to provide steady baseload output between 100-500 W operating at low head sites (2-10 m). Suitability of the Firefly under these conditions is currently unknown, and the turbine has not been evaluated under conditions of very low head. The study objective was to characterize the performance through laboratory testing under conditions of low head and variable flow rate, in order to determine if the Firefly turbine meets the requirements of users in Cameroon. At this time, construction has been completed of the Firefly turbine and testing apparatus. The testing process and initial Firefly performance results, as well as lessons learned to date, are the focus of this paper. This is the first phase of a larger project seeking to design an optimized pico hydro turbine that balances performance, reliability and ease of manufacture and installation. The Firefly results will be used as a baseline in comparisons to new turbine designs.

Keywords: *Pico hydro, Cross-flow turbine, Low head, Remote power generation, Firefly.*

1. Introduction

Rural electrification enhances welfare through increased productivity, health, media access, and education. Studies by the Independent Evaluation Group of the World Bank (2008) have demonstrated this empirically and have also found that the benefits from rural electrification outweigh the cost of investment.

1.1. Introduction

Pico hydro systems harness the energy in flowing water at capacities smaller than 5 kW. They are recognized as a viable option to electrify remote areas with regard to economical, environmental, and social perspectives. Pico hydro yields one of the lowest generating costs amongst off-grid energy options (Williams & Simpson, 2009). Unlike large scale hydropower, there is low environmental impact with pico hydro systems, mainly due to the exclusion of large water containment. Associated large civil works and the displacement of habitats are not required for the commissioning of pico hydro systems. In addition, negative impacts of large reservoirs such as siltation, increased mercury levels, and off-gassing of green house gases from submerged decomposing organic material are avoided (Gunkel, 2009).

1.2. GREEN STEP e.V in Cameroon

GREEN STEP e.V. (http://www.green-step.org) is a non governmental organization originating from Germany with the objective to improve rural livelihoods through providing training and co-financing of renewable energy projects, building environmental awareness through education, and sustainable agriculture extension. In 2007, the organization connected with the M'muock village situated in south western Cameroon. The majority of the 70,000 residents of M'muock to do have access to grid-supplied electricity.

Pico hydro technology has been one of the main focuses and to date, 40 craftsmen have been trained and nearly 10 turbines successfully built. However, after a year in use, only 2 turbines remained in operation at a limited capacity. Observations (Hertlein, 2010) made from these implemented systems include:

- Concerns regarding ownership have arisen, especially in situations where multiple stakeholders (ie. community or multiple household ownership) are involved. The need for smaller systems targeted towards single dwellings has been identified as lines of responsibility are defined more clearly and free-rider issues are mitigated.
- Improvements are needed to reduce the complexity of the design and also increase robustness. End-users may not be made aware of the importance of maintenance; in addition, distances to workshops are far.
- The current systems employ expensive car alternators, car batteries and inverters. These components are also prone to failures, with the wearing down of alternator brushes being the main concern.
- The willingness-to-pay for a pico hydro system is estimated to be €150.
- Training is required for local construction of pico hydro systems.

Based on the above lessons-learned, the overall project objective is to design a robust and reliable pico hydro system that is affordable at the household level, suitable for household electricity demand, uses locally sourced materials, and can be manufactured locally at a small industrial scale. The operational range is to be 2 m to 10 m head, with flow rates of 5 L/s to 100 L/s, and electrical output in the range of 100 W to 500 W. The initial phase of the project is to characterize the performance of the existing systems at 2-10 m head and variable flow rates, in order to determine the degree to which the current Firefly turbine meets the targets that are required by users in Cameroon, and provide a baseline for comparisons to future designs.

1.3. Purpose

The purpose of this report is to present the low-head and variable-flow-rate laboratory test rig implemented at the University of Guelph (Canada) that is used for testing a pico hydro system built to the same specifications as those used in Cameroon. Results from the tests are tabulated. In addition, lessons learned from the Firefly construction process, and recommendations for improving the testing process are identified.

2. Methodology

The existing pico hydro systems employed by GREEN STEP e.V. in the field are known as the "Firefly" design. A Firefly unit was constructed in Guelph (Canada) for laboratory testing, according to the instructions of Portegijs (2003). Laboratory testing was conducted on a rig with the ability to vary flow rates and heads within the low head range. Focus was placed on the low head range as the Firefly documentation did not provide performance for heads below 3 m (Portegijs, 2003).

2.1. Firefly

The Firefly was designed by Jan Portegis for use in rural Philippines. It consists of a cross-flow turbine attached to a car alternator, and was intended strictly for battery charging.

The turbine has 27 blades supported by circular side plates with a 75 mm diameter and turbine height of 55 mm (Fig. 1). A 51 mm wide nozzle guides the flow to the turbine. The range of operating head is 3 m to 7 m, and 8 m to 25 m with governed flow (Portegijs, 2003).

In the original Firefly design, the field current of the alternator is controlled by 4 incandecsent light bulbs (3 x 20 W and 1 x 10 W) and switches connected in parallel. Six different resistance values are possible, which allows for optimization of the field current (Portegijs, 2003).

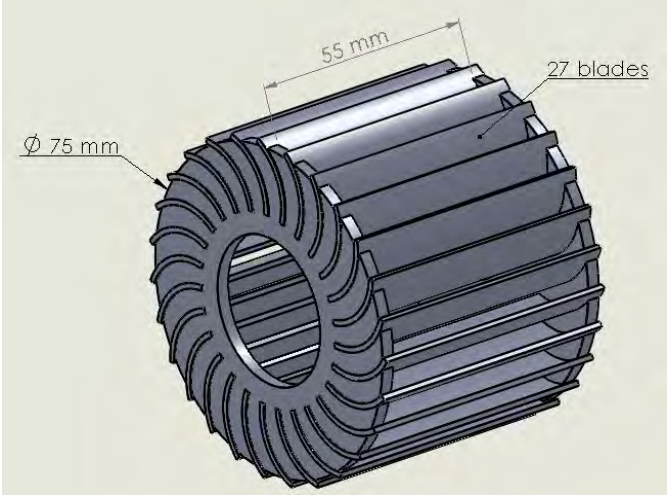

Fig. 1. Runner assembly.

2.2. Firefly construction

Construction of the Firefly for testing in Guelph generally followed the design manual (Portegijs, 2003). The cross-flow sidewalls were laser cut rather than hand cut. The blades were manually sheared and formed as per instructions. The turbine assembly was welded instead of soldered, as detailed in the design manual, however this is in agreement with practices used for the Cameroonian units. The nozzle and frame were also fabricated as per instructions. The casing was excluded as the test unit would not be exposed to a harsh field environment. A Valeo model AB180128 automobile alternator was used. All construction (except for laser cutting) took place within the engineering machine shop facilities at the University of Guelph.

Considerable lessons were learned from the build process. Significant skill on the part of the fabricator is required to build these units. Difficulty would be further accentuated by limited resources. The use of jigs, especially for blade cutting and bending, could improve consistency from blade to blade and simplify the turbine assembly: additional practical advice on fabrication would be a useful addition to an updated construction manual. The turbine sidewall fabrication involves cutting multiple curved slots for the attachment and soldering/welding of the curved blades. Consistently cutting the curved slots in the side walls is extremely difficult for unskilled workers (such as university students), which lead us to laser cut these components. It should be noted that skilled workers with metal working experience using appropriate jigs could mitigate much of this concern.

Variability between individual Firefly is also introduced if different models of alternators are used. For example, the joining of the turbine to the alternator shaft differs slightly between the Guelph unit and the instruction manual, owing to a different configuration of the alternator

shafts. This need to adapt to different alternator models affects the standardization of the build process, complicating construction by forcing builders to veer away from the design manual.

2.3. Test Apparatus

The Guelph laboratory test apparatus (shown in Fig. 2) consists of an 1135 L (0.9 m x 1.9 m plan, 0.6 m height) reservoir elevated on a 3.3 m high platform. A 10 cm (4 in) diameter ABS plastic penstock connects the drainage hole at the base of the reservoir to the Firefly. The total length of the penstock pipe from the reservoir to the Firefly is approximately 4 m. The Firefly is located above a receiving reservoir. An electric pump is used to return water to the supply reservoir between tests. With the Firefly in place, the system has a nominal head of 3 m, however, the head can be varied by changing the height of the Firefly while adjusting the length of the penstock.

The Firefly's alternator field circuit was connected to a high capacity 12 V deep discharge lead acid battery. A resistor was included in the circuit. Changing the resistance of this resistor allowed the field strength to be varied. The power output of the alternator was directly connected to a 2.0 ohm dynamic braking resistor with a 2 kW capacity.

A Medusa Scientific PowerPro power meter capable of measuring voltage, current and power was connected to the alternator. The PowerPro was connected to a desktop PC, which recorded data at a rate of 4 Hz.

Flow rate is controlled by throttling a needle valve installed at the penstock inlet at the base of the reservoir. Instantaneous reservoir level, and by extension, flow rate out of the reservoir, is measured using a float connected to an ultra-low friction potentiometer (adapted from an anemometer) by a swing arm. The potentiometer is connected to the PowerPro via a voltage divider circuit, so that head and flow rate are recorded simultaneously with voltage, current and power. Before testing, the output of the float sensor is calibrated and a transfer function is derived that outputs reservoir level as a function of the recorded signal.

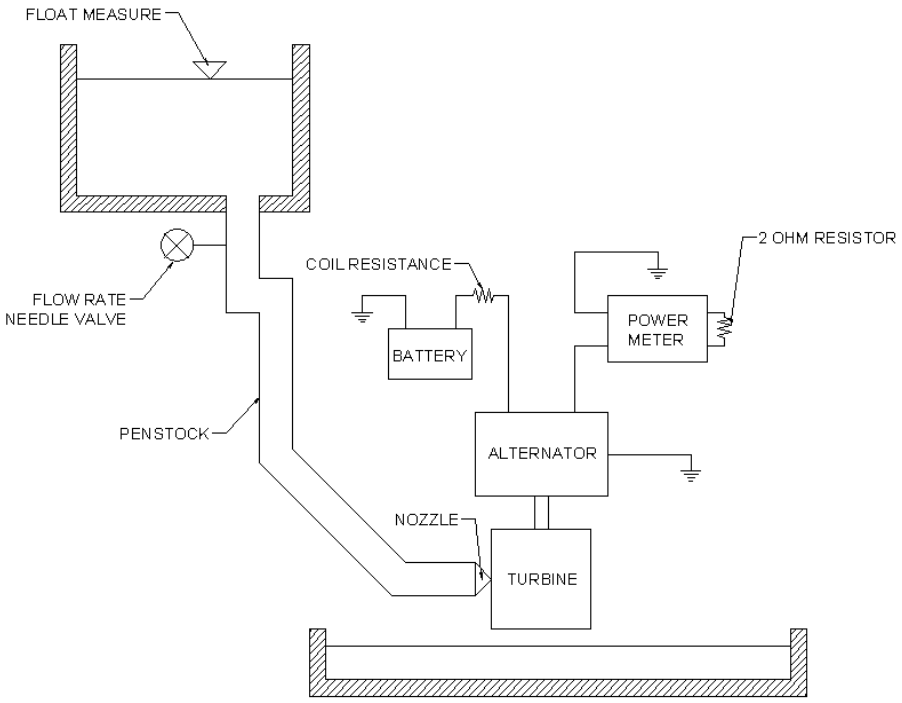

Fig. 2. Layout of test apparatus.

2.4. Test Method

Tests were conducted with flow rates ranging from 5.52 to 5.81 L/s and average heads of 3.4 m. The field circuit resistance was varied to determine the optimum resistance to include in the field coil circuit. Resistances used were 0, 5, 10, 20, and 47 ohm.

3. Results

The results of the tests are tabulated below in Table 1. Power output from the Firefly under a generally consistent flow rate and head is reported, with varying field resistance.

Table 1. Experimental results

Coil Resistance [ohm]	Flow Rate [L/s]	Average Head [m]	Average Power Output [W]	Efficiency
0	5.61	3.40	9.39	4.8%
5	5.81	3.39	12.15	5.9%
10	5.52	3.39	11.60	6.0%
20	5.73	3.39	10.70	5.3%
47	5.58	3.39	10.14	5.2%

Based on the test results, a 5 ohm to 10 ohm field circuit resistance was observed to be the optimal resistance, resulting in a higher average power output than was achieved with higher or lower resistances in the field circuit. The field current control recommended in the design manual is calculated to range from 2.1 ohm to 14.4 ohm, which is consistent is consistent with these test results.

Over the entire range of resistances, power output and efficiencies were lower than the predictions of Portegijs (2003). Portegijs predicted but could not test that the Firefly would produce 46 W at 3 m head and 5.3 L/s. It should be noted that a typical alternator would be below its normal operating range, and likely to underproduce the predicted value. Portegijs identified this as a concern, and suggested that his calculated values would be high because of this, for the combination of head and flow rates tested here. This is believed to be one reason for the lower than expected performance during testing.

4. Discussion

Given the lower than expected power outputs and efficiency, it is believed that the test Firefly requires modifications to enhance the test results. Construction of the Guelph Firefly must be revisited: it appears that the gap between the nozzle and turbine is higher than other examples of the Firefly. Inspection of the unit after testing showed that realignment is needed of the nozzle with respect to the cross-flow turbine, and that a small amount of nozzle movement was possible. This is considered to be the root of the matter. This demonstrates the criticality of construction training and the need for simplistic designs.

The test results also confirm that at the combinations of head and flow rate tested, the direct drive automobile alternator may not be the ideal type of generator to utilize, due to inefficiencies when operating at low rotational speed, and utilization of a large fraction of the power generated to energize the coils that provide the magnetic field. One recommendation is to consider the use of a permanent magnet alternator that can provide power over a greater range of rotation speeds, and critically, not consume power in its operation.

5. Conclusions

Following adjustments to nozzle position and mounting of the Guelph Firefly unit, testing will recommence with varied flows and heads.

Modeling the alternator is difficult: in addition to rotation speed and torque, performance is impacted by field strength. This makes it difficult to separate the effects of alternator performance from turbine performance. Future testing will separate the Firefly from the alternator. The Firefly turbine will be characterized by testing on a dynamometer over a range of torque and rotation rates. Separate dynamometer testing of the alternator will allow determination of the relative importance of alternator optimization (e.g. field strength) compared to turbine configuration (e.g. nozzle alignment). Alternative turbines of different configurations and lower parts counts will also be designed and tested, and compared to the Firefly.

This paper has described the initial stages of this research project. Additional testing of the current Firefly unit is currently being conducted, and work has begun on the design of different turbines with the goal of further optimizing ease of construction, performance and reliability. The results of the continued testing will be used to draw conclusions on the appropriateness of the current Firefly, and improved designs, in M'muock, Cameroon.

References

[1] International Evaluation Group – World Bank, The Welfare Impact of Rural Electrification: A Reassessment of the Costs and Benefits, 2008, URL: http://siteresources.worldbank.org/EXTRURELECT/Resources/full_doc.pdf [last accessed January 11, 2011].

[2] A.A. Williams and R. Simpson, Pico hydro – Reducing technical risks for rural electrification, Renewable Energy 34, 2009, pp. 1986 – 1991.

[3] G. Gunkel, Hydropower - A green energy? Tropical reservoirs and greenhouse gas emissions, Clean - Soil, Air, Water 37 – 9, 2009, pp. 726 – 734.

[4] J. Hertlein, Project start document – Small Scale Water Turbine for Cameroon. Report. Green Step e.V., 2010.

[5] J. Portegijs, J. The Firefly Micro Hydro System, 2003. URL: http://www.microhydropower.net/mhp_group/portegijs/firefly_bm/ffbm_index.html [last accessed January 11, 2011]

Water supply lines as a source of small hydropower in Turkey: A Case study in Edremit

S.Kucukali[1,*]

[1] *Cankaya University, Department of Civil Engineering, Balgat, 06530 Ankara, Turkey*
** Corresponding author. E-mail: kucukali78@hotmail.com*

Abstract: Hydropower has the highest share among the renewable energy sources of Turkey by 94% with a total installed capacity of 14,553 MW for the year 2009. Turkish government has based its energy policy on maximizing hydropower potential to be evaluated in next 15 years. In this context, private sector is expected to build hydroelectric power plants having a total capacity of 27,500 MW. Besides these hydropower plants, there is also a considerable hydropower potential in existing water supply systems. The most convenient locations for hydropower generation in water supply systems are water supply lines located before the water treatment or distribution network. In water supply lines, the excess pressure is dissipated by creating water jet in the pressure reduction tank. However, the excess pressure can be removed from the system by installing a hydro-turbine and it can be converted into useful energy by means of electricity. For a case study, the hydropower potential of the water supply system of Edremit in Turkey has been analyzed. There are 12 pressure reduction tanks along the water supply line of the city and the system has an electric energy potential of 4.08 GWh/year, corresponding to about 560,000 Euro/year economic benefit.

Keywords: *Hydropower, Water supply lines, Turkey.*

1. Introduction

The need for saving water and energy has grown as one of the world main concerns over the last years and it will become more important in the near future. Increase in oil and natural gas prices by 500% in last 15 years has made renewable energy sources become important than ever. Hydropower is a renewable energy source most widely used all around the world [1]. Installation of hydropower plants on water supply network has found a wide usage area in Europe (Table 1). For example, in Switzerland 90 small hydropower plants were installed on the municipal water supply network of the country (Table 2). The advantages of these facilities compared to river-type hydropower plants could be summarized as follows: (i) all civil works are present, which will reduce the investment cost in the order of 50% [2], (ii) the facility has no significant environmental impacts and it has a guaranteed discharge through the year, (iii) the generated electricity is used in the water supply system and the excess electricity is sold to the government, (iv) there is no land acquisition and significant operating costs [3]. In this context, this study aims to show the possible benefits of the installation of a water turbine in water supply line. This could be an alternative clean energy solution to reduce the consumption of energy supplied by the national electric grid mostly fed by fossil fuels and to induce the minimization of CO_2 emissions to the atmosphere. In the present study, utilization of the hydropower plants in existing water supply systems has been discussed. As a case study, the hydropower potential of the water supply system of Edremit, Turkey has been analyzed in detail.

Table 1. Some examples of hydropower plant installation on water supply lines in Europe. Data source: [1]

Plant Name	Country	Design discharge (m^3/s)	Gross head (m)	Output (kW)	Production (MWh/year)
Vienna Mauer	Austria	2	34	500	364
Mühlau	Austria	1.6	445	5750	34000
Shreyerbach	Austria	0.02	391	63	550
Poggio Cuculo	Italy	0.38	28	44	364
La Zour	Switzerland	0.30	217	465	1800

Table 2. Multipurpose schemes in Switzerland: operating and remaining potential. Data source: [1]

Water network type	Potential type	Number of sites	Output (MW)	Production (GWh/year)
Drinking water	Operating	90	17.8	80
	Remaining	380	38.9	175
Treated waste water	Operating	6	0.7	2.9
	Remaining	44	4.2	19

2. Methodology

A typical water supply system is composed of water source and storage, supply lines, water treatment plant, storage tank and distribution network (Fig. 1). The objective of water supply systems is to guarantee the delivery of adequate amount of good quality water to the inhabitants of the region. However, energy is needed to achieve this objective which requires operate water pumping and operation of treatment plants. The supply lines transport the water from storage to treatment facilities and treated water to storage tanks. It should be noted that the supply lines have limitations for pressure. For example, In Turkey, the static pressure should be in the range of 20-80 m head [4] and if the upper limit of the pressure is exceeded along the pipe line, pressure reduction valves or tanks are used to dissipate the excess pressure head. Based on the estimations of Bank of Provinces, there is a 30 MW hydropower potential in the existing pressure reduction and storage tanks in Turkey.

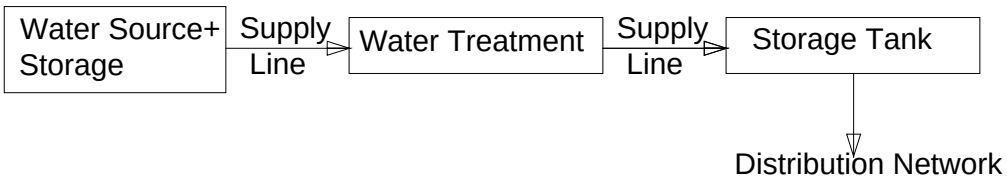

Fig. 1. Flow diagram of a typical water supply system

The shares of water supply sources in Turkey, with a capacity of 5.16 billion m^3 in 2006, are as follows: 36% dam reservoirs, 27% groundwater reservoirs, 27% springs, %6 rivers and 4% lakes [5]. The domestic water demand is expected to increase from 6.2 billion m^3 in 2007 to 26 billion m^3 in 2030 (Fig.2). There are totally 43 municipal water supply dams in operation and the distribution of these dams across the country is shown in Fig.3. The municipal dams

are distributed over 23 cities and the most of them are in the big cities like Ankara, Istanbul and Izmir [6].

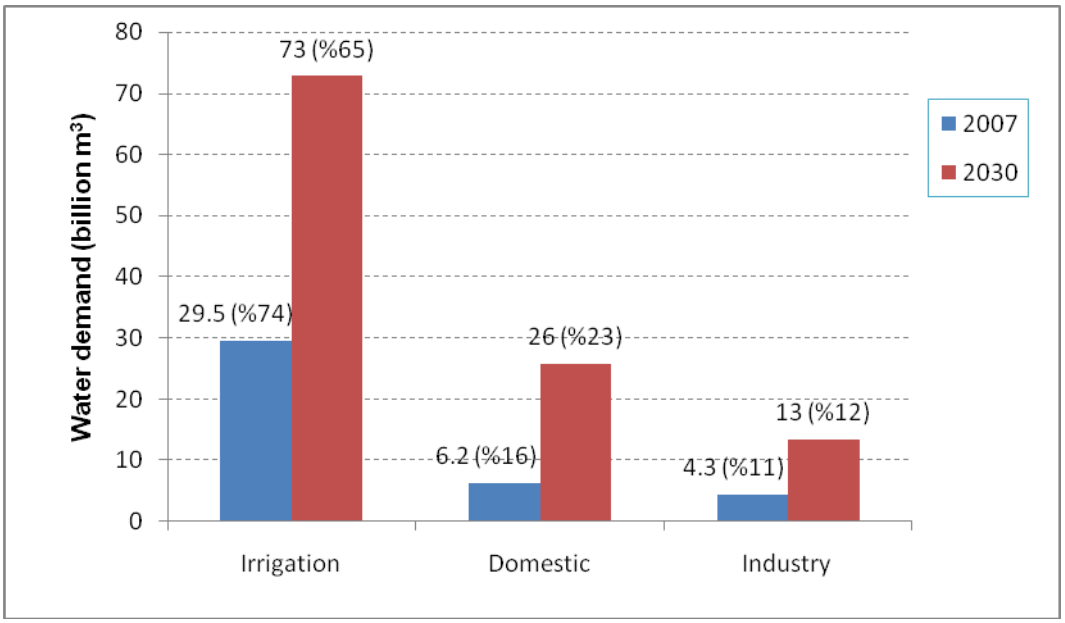

Fig. 2. Water demand of Turkey by sectors for 2007 and 2030 (projection by DSI)

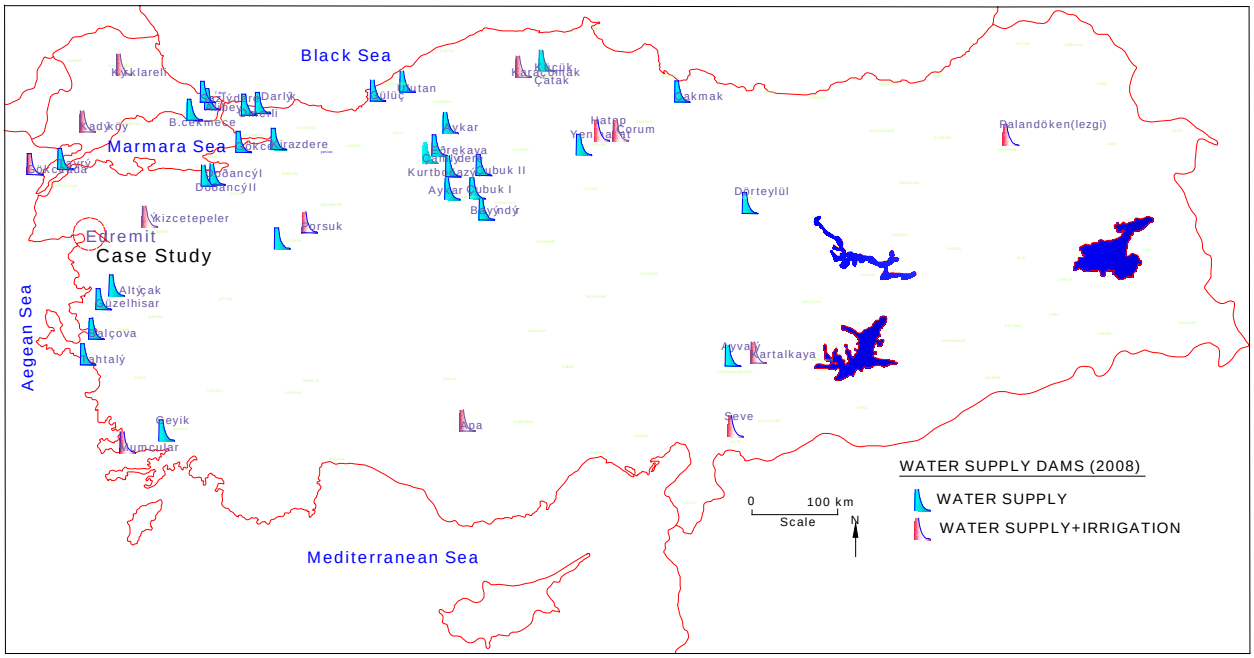

Fig.3. Municipal water supply dams in Turkey by 2008 and the location of the case study.

Hydro-turbines convert the water pressure into mechanical shaft power, which can be used to drive an electricity generator, or other machinery. The available power is proportional to the product of pressure head and water discharge. Modern hydro-turbines can convert as much as

90% of the available energy into electricity. The installed capacity P (kW) of a hydropower plant is calculated from

$$P = \gamma \times Q \times H_n \times \eta \quad (1)$$

where γ is the specific weight of water, Q (m^3/s) is the discharge, H_n (m) is the net head (m), η is the sum of the turbine and generator efficiency. The annual energy generation E (kWh/year) of a hydropower plant is obtained from

$$E = P \times t \quad (2)$$

where t is the operating hours in a year. The most convenient locations for hydropower generation in water supply systems are water supply lines located before the water treatment or distribution systems. In water supply lines, using the Bernoulli energy equation between sections 1 and 2 (Fig.4) and employing a velocity head correction factor of 1 gives

$$\frac{U_1^2}{2g} + \frac{p_1}{\gamma} + z_1 = \frac{U_2^2}{2g} + \frac{p_2}{\gamma} + z_2 + \Delta H \quad (3)$$

where, U is the average velocity, p is the pressure, z is the elevation above an arbitrary datum, g is the acceleration of gravity, ΔH (m) is the hydraulic head loss between 1 and 2. The head loss occurs because of the frictional and local energy losses. The velocity head is constant through the supply line and the excess pressure head equals to

$$\Delta H = \frac{p_1 - p_2}{\gamma} + (z_1 - z_2) \quad (4)$$

In water supply lines, the pressure head increases rapidly in the system where the elevation difference between two points is high and the excess pressure head is dissipated in pressure reduction tanks. In these structures, the pressure head is dissipated to atmospheric pressure by creating water jets. However, the pressure head could be removed from the system by installing a hydro-turbine. Then, the excess energy will be converted into useful energy by means of electricity.

3. Edremit Water supply System: A Case Study in Turkey

Edremit is situated on the north Aegean coast of Turkey (Fig. 4). Edremit's economy relies largely on the production of olives and tourism. The water used in the city is supplied from a spring located at Mount Ida and the supply line has an elevation range between 80-868 m. Water is carried at a rate of 0.16 m^3/s by a polyethylene pipeline which has a diameter of 450 mm and a length of 32.7 km (Fig.3). There are 12 pressure reduction tanks along the supply line to regulate the pressure of the flow. The pressure heads of the pressure reduction tanks are presented in Table 3.

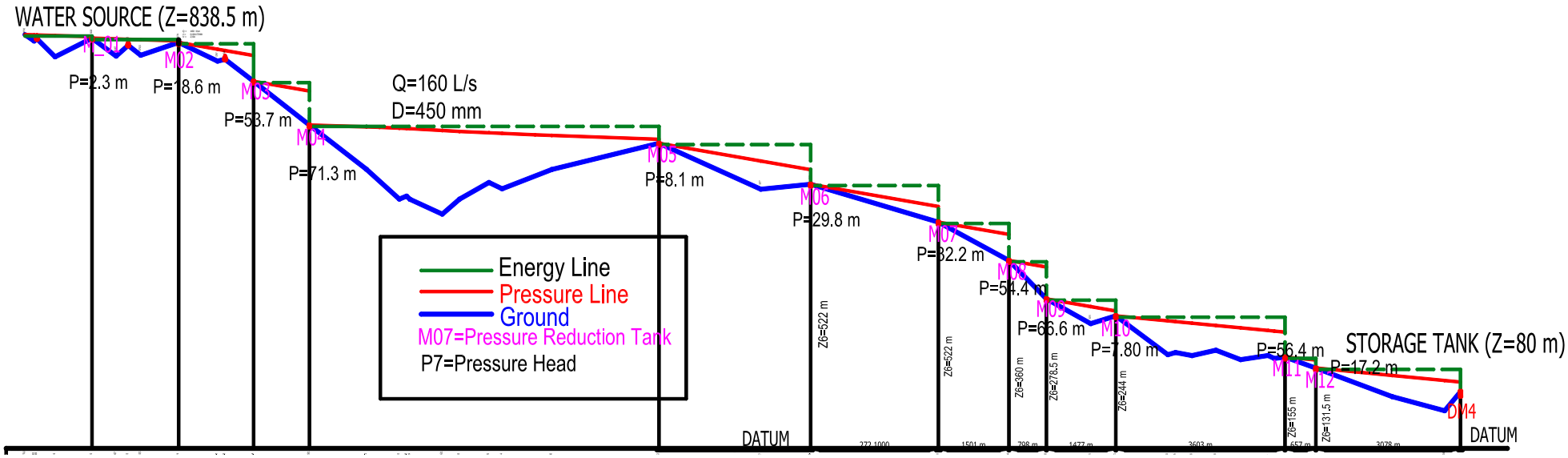

Fig.4 Water supply system of Edremit and the variation of pressure along the supply line

Table 3. Hydropower design characteristics of pressure reduction tanks of Edremit

Tank No	Head (m)	Discharge (m^3/s)	Output (kW)	Energy (kWh/year)	Benefit (Euro/year)
1	2.3	0.16	3	24,524	3,433
2	18.6	0.16	25	198,321	27,765
3	53.7	0.16	72	572,571	80,160
4	71.3	0.16	95	760,229	106,432
5	8.1	0.16	11	86,365	12,091
6	29.8	0.16	40	317,740	44,484
7	32.2	0.16	43	343,329	48,066
8	54.4	0.16	73	580,035	81,205
9	66.6	0.16	89	710,116	99,416
10	7.8	0.16	10	83,167	11,643
11	56.4	0.16	75	601,359	84,190
12	17.2	0.16	23	183,393	25,675

The excess pressure heads are dissipated to the atmospheric pressure by creating free water jets in these tanks (Fig. 5). However, the excess pressure can be removed from the system by installing a hydro-turbine and it can be converted into useful energy by means of electricity (Fig.6). The pressure head of the pressure reduction tank was taken as design head for the hydro turbine installation and the design discharge is selected as 0.16 m^3/s (Fig.7). The electricity price is about 14 Eurocent/kWh in Turkey for the May 2010 and the price was used in determining the economic benefit of the hydropower schemes. The operation of water supply system already exists. So there will be no e xtra operation cost. The annual maintenance cost is estimated to be 1% investment cost of hydropower plant [7]. This cost has been considered in the calculations of economic benefit in Table 4.

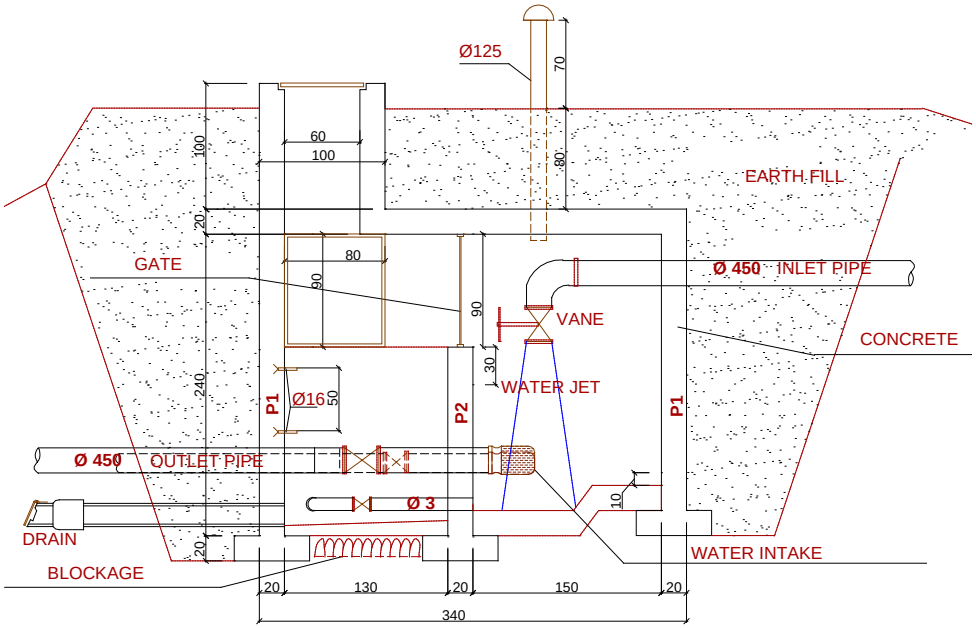

Fig.5 Longitudinal profile of the pressure reduction tank.

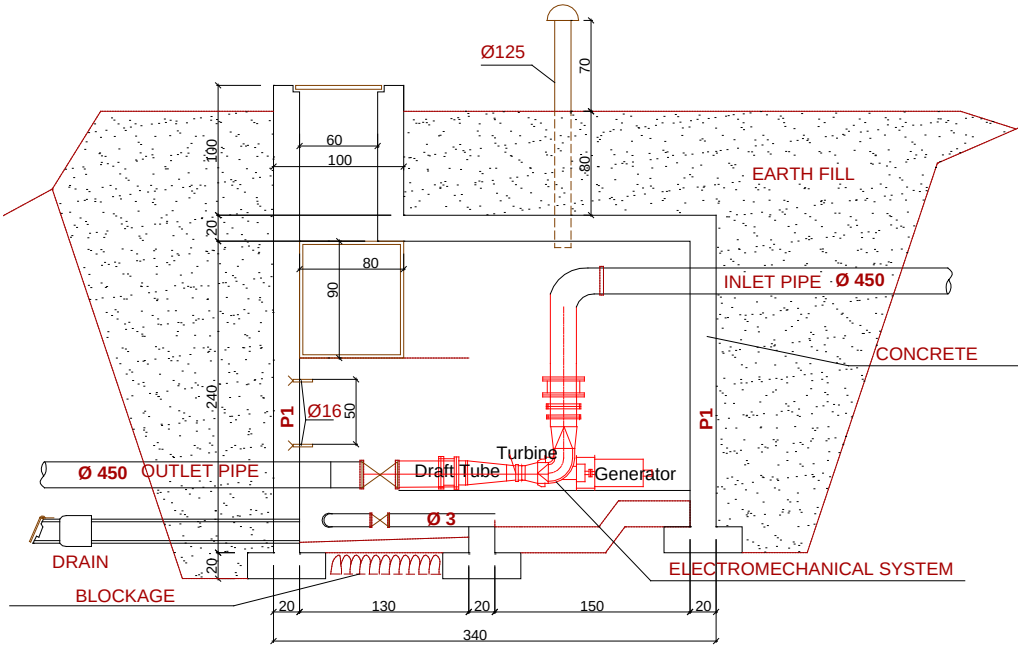

Fig.6 Hydropower generation in the pressure reduction tank.

The water supply system of Edremit has an electric energy potential of 4.08 GWh/year, corresponding to about 560,118 Euro/year economic benefit. The financing of the project would be supplied from international funding organizations like World Bank and European Union.

Table 4.Economic Analysis of The Proposed Project

Total Installed Capacity (kW)	559
The hours in operation (h/year)	7300
Annual Energy (kWh/year)	4,080,700
Cost of the investment (EUR)	1,118,000
Annual Benefit (EUR)	560,118
Payback period (year)	2.00

4. Conclusions

Utilization of the existing hydropower potential in water supply networks has been analyzed. The proposed facility has numerous advantages compared to river-type hydropower plants. The new energy laws and the economic aspects of Turkey create opportunity to develop this potential. For a case study, the water supply system of Edremit has been investigated in a detailed manner. There are 12 pressure reduction tanks along the water supply line and they have an power capacity of 559 kW. The proposed project is ecologically sustainable and it will produce clean and feasible energy.

References

[1] ESHA-European Small Hydropower Association, Energy Recovery in Existing Infrastructures with Small Hydropower Plants: Multipurpose Schemes-Overview and Examples, 2010.

[2] Kucukali, S. and Baris, K., Assessment of small hydropower (SHP) development in Turkey: Laws, regulations and EU policy perspective, *Energy Policy,* 37, 2009**,** 3872-3879.

[3] Kucukali, S., Municipal water supply dams as a source of small hydropower in Turkey, *Renewable Energy*, 35(9), 2010, 2001-2007.

[4] Bank of Provinces, Regulation on the Preparation of Water Supply Projects for Cities and Towns, 1992.

[5] Turkstat, Turkish Statistical Institute, 2009. (www.turkstat.gov.tr).

[6] DSI- General Directorate of State Hydraulic Works, Dams and hydroelectric power plants in Turkey**.** DSI**,** Ankara, 2005.

[7] Linsley, R.K., Franzini, J.B., Freyberg, D.L., Water Resources Engineering. McGraw-Hill Publications, 1992.

Concept-H: Sustainable Energy Supply

Jure Margeta[1], Zvonimir Glasnovic[2,*]

[1] *University of Split, Faculty of Civil and Architectural Engineering, 21000 Split, Matice Hrvatske 15, Croatia,*
[2] *University of Zagreb, Faculty of Chemical Engineering and Technology, 10000 Zagreb, Savska 16, Croatia,*
[*] *Corresponding author. Tel.: +385-1-4597108; Fax: +385-1-4597260, E-mail: zvonglas@fkit.hr*

Abstract: The paper presents an innovative solution that combines Pump Storage Hydroelectric (PSH) with power plants that use only Renewable Energy Sources (RES) into a unique energy producing technological system, called *Concept-H*, which combines PV, solar thermal and wind power plants with PSH. The basic difference between *Concept-H* and the previous use of RES, where output energy depends on the fluctuating input energy, lies in the fact that such new concept can continuously and safe supply a consumer with electric energy and power. In this sense RES are put in equal position with conventional energy sources and *Concept-H* promises to be the important building element of the future *sustainable power system* as a *green strategy* of electric energy production. The application of *Concept-H* creates a significantly lower risk for humans and the environment, than when using conventional technologies, especially in possible incidental situations. The proposed solution is flexible for realization and can be applied in different climatic, hydrological and physical conditions where people live.

Keywords: *Concept-H, Renewable Energy, Hydroelectric Energy, Sustainable Energy Supply, Green Energy Scenario*

1. Introduction

This paper analyses the possible development of the renewable electricity scenario, based on the strategy of the use of Renewable Energy Sources (RES), called *Concept-H* [1]. This concept is based on the use of renewable resources and the use, directly or indirectly, of water storage of hydroelectric (HE) plants as energy storage in addition to other technological possibilities which increase continuity of supplies of RES energy to Electric Power System (EPS). In addition to direct connection of RES with EPS and the users, Fig. 1 (a), the proposed approach in the development of continuous green energy supply also requires indirect connection by use of hydro energy power production unit, similar to Pump Storage Hydroelectric Plant (PSH), Fig. 1 (b).

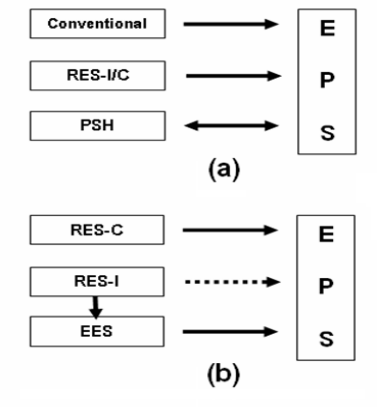

Figure 1. (a) Conventional connection of energy source and storage; (b) principle concept which would enable the green energy scenario (RES-I: intermittent RES; RES-C: continuous RES; EES: Electric Energy Storage, i.e. water storage).

Thus, the approach that enables the realization of green energy scenario would mostly be based on the concept of serial connection between green energy source and EPS through water storage of HE power plant, i.e. PSH, as shown in Fig. 1 (b). In this sense the future sustainable EPS or specific users, i.e. those based solely on RES, would have the configuration as in Figure 2. Solar (PV and solar thermal) and wind power plants, including

other non-continuous energy sources, would connect serially/indirectly to EPS and users through Electric Energy Storage (EES), i.e. water storage, while HE, geothermal and biomass power plants would connect directly, because they can provide continuous supply to consumers.

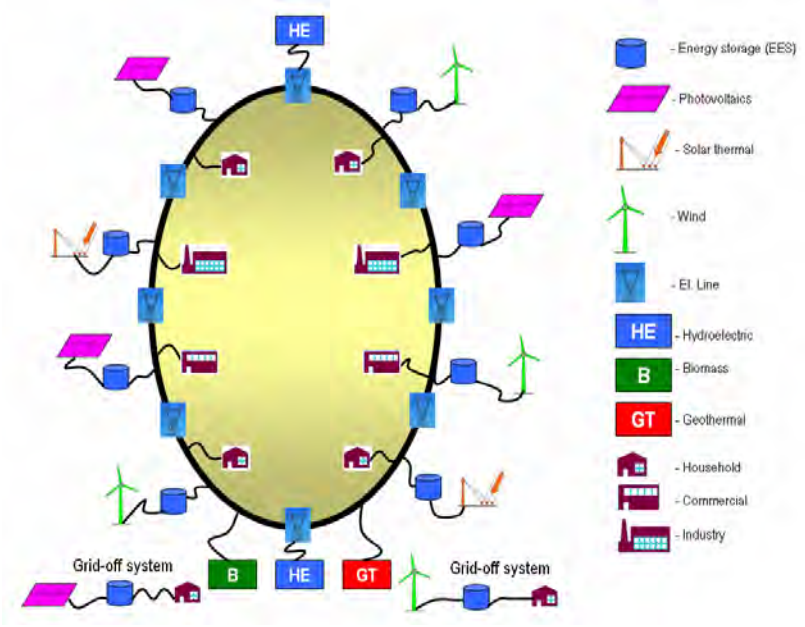

Figure 2. Vision of the future fully sustainable electric power system.

Renewable energy sources with occasional work will also be used directly through global and regional electric supply network, if and when it is acceptable for the electric power system. In this way water storage of hydroelectric power plants has the most significant role in realization of the green system, [2]. Numerous technologies of energy storage are known today (batteries, flywheel, pressure vessels, etc.), which differ in: size, energy storage costs, efficiency, lifetime, costs per cycle, etc., [3, 4]. It is well known that none of the present-day technologies could, in terms of ratings, be compared to storage by PSH, [4]. Precisely because of that, the concept of PSH is still the most significant EES today, which is a mature technology with large volume, long storage period, high efficiency and reliability, while capital cost per unit of energy is low, [5]. For this reason, with the present-day technology, it is possible to achieve the vision of continuous green energy production through *Concept-H* [1].

Implementation of this concept will depend primarily on the policy towards renewable energy sources, RES technological development, and economic conditions. Energy produced from RES is still significantly more expensive than conventional and therefore its production is subsidized. Therefore, the *Concept-H* in its initial implementation should be used primarily for daily energy peak shaving with a tendency towards daliy load leveling. Such implementation strategy would have the greatest ecological and economic effect.

2. Main settings of the proposed concept

2.1. Main elements of Concept-H

In the green scenario (Figure 2) continuous renewable energy sources (RES-C) are exploited directly, while intermittent energy sources, such as marine, wind and solar renewable energy sources (RES-I) are exploited indirectly through *Concept-H*. RES-I power plants deliver their energy to the Pump Station (PS) which pumps water into storage of HE power plants which then serve for daily, weekly and seasonal energy storage, while the consumer is supplied from

the associate PSH power plants, transforming intermittent energy supply into continuous and manageable energy supply as conventional storage of HE power plants, [6, 7]. Serial connection is based on two pipelines in classical concept of PSH. One pipeline pumps water from lower water resource into upper storage when RES produce energy and the other conveys water from the upper storage to turbines for production of hydro energy in accordance with the consumers' needs. In this way intermittent operation of RES-I does not affect hydro energy production according to the consumers' needs. In the proposed *Concept-H*, PSH is used for continuous production of energy, or energy storage for daily and seasonal peak load shaving.

The key driving elements of the solution are: (i) RES-I; (ii) energy storage unit (pump station and water storage); (iii) HE. Production and consumption balancing is performed in upper storage based on balance equation of storage volume and HE productivity, Figure 3. RES power plants are also in parallel (direct) connection with the regional EPS, because it is logical that RES-I power plant will directly deliver its energy excesses into the system, i.e. when the upper storage is full. It is also logical that energy surpluses in EPS are used for PSH operation.

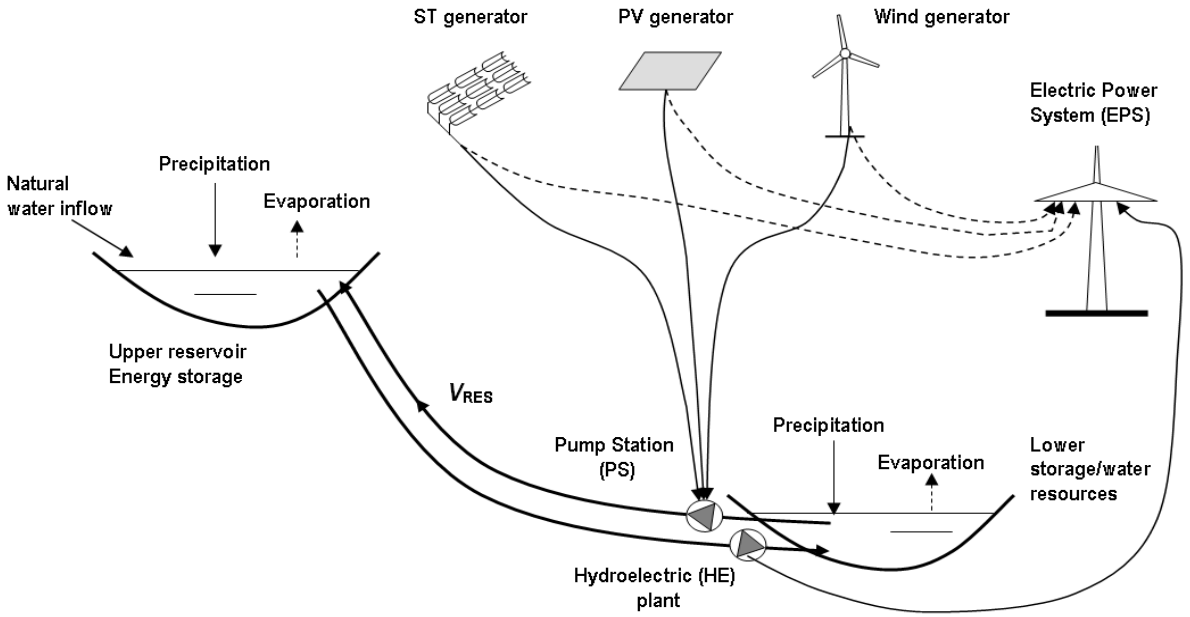

Fig 3. Concept-H: Hybrid power unit as the main building element of the future green energy scenario.

In this concept, water storages in energy power systems operate as energy storage. Hydroelectric power plants are very flexible and manageable in their work and quickly adapt to the needs of EPS. The biggest problems occur when hydrological conditions are not satisfactory. This problem is solved with the proposed *Concept-H,* because new non-natural water resources are created.

The basic unit for continuous production of energy is the hybrid power plant RES-PSH (i.e. *Concept-H)*. Hybridization can be applied to all RES-I energy sources, the most promising being with solar energy because, unlike wind power plants, it is a reliable source of energy, available at all locations where people live. In addition, solar energy enables rational daily balancing of energy production and consumption and thus the need for construction of small storage of PSH. Hybridization can be carried out with other sources of RES indirectly through energy system network.

The proposed solution is characterized by balance of energy and water. Energy balance of the hybrid electric power plant or the single time step is:

$$E_{hyb(i)} = E_{hyb(i-1)} + E_{PSH(i)} + E_{DRES(i)} \quad (1)$$

Where $E_{\mathrm{hyb(i)}}$ and $E_{\mathrm{hyb(i-1)}}$ are hybrid energy production in time stage i and i-1 respectively, $E_{\mathrm{PSH(i)}}$ is energy produced from PSH/HE, $E_{\mathrm{DRES(i)}}$ is energy which RES source supply directly to the energy power system in time period i. However, unlike $E_{\mathrm{PSH(i)}}$ which is reliable and manageable energy production, this energy supply is random, independent and uncontrollable energy production and thus is of minor importance for the EPS. Total energy production is:

$$E_{hyb} = \sum_{i=1}^{T} E_{hyb(i)} \quad (2)$$

Where T is total period used for production of energy (year).

Losses occur in energy transfers from one to the other ($E_{RES\text{-}I}$ into E_{PSH}), as well as in transport from the source to EPS. Total production losses ΔE period T are:

$$\Delta E = E_{RES-I} - E_{PSH} - E_{DRES}\,. \quad (3)$$

Losses due to energy transfer are inevitable and are the price paid for the sustainable and new quality in green energy production, Figure 3.

Water is the second resource needed for constant plant work. Water is necessary for filling of the system and compensation of losses due to evaporation, leakage and the like. Once fully filled, the system needs regular compensation of losses. Given that the system is integrated in the surroundings, part or all losses can be compensated by natural hydrological processes (precipitation, water inflow from catchment areas, etc.), or improved in special situations by external transfer of water mass inflow in the upper storage.

2.2. Water storage as energy storage

The equivalent reservoir energy balance for a single time step i is expressed as:

$$E_{PSH(i)} = E_{PSH(i-1)} + E_{nat(i)} + E_{RES(i)} - E_{prod(i)} - E_{evap(i)} - E_{loss(i)} \quad (4)$$

Where $E_{\mathrm{PSH(i)}}$ is the total equivalent reservoir stored energy in time period i and i-1 (MWh); $E_{\mathrm{nat(i)}}$ is the total natural potential energy inflow over time period i (MWh); $E_{\mathrm{RES(i)}}$ is the total energy inflow over time period i (MWh) generated (pumped) by energy from RES; $E_{\mathrm{prod(i)}}$ is the decision variable or the total energy outflow over time period i (MWh); and $E_{\mathrm{evap(i)}}$ and $E_{\mathrm{loss(i)}}$ is the energy outflow corresponding to the losses (evaporated volume and other losses) from the equivalent reservoir over time period i (MWh).

$E_{\mathrm{nat(i)}}$ during time period i is the sum of all reservoir natural potential energy inflows (river, rain). For a single reservoir, it is calculated by multiplying the natural water inflow discharge ($Q_{\mathrm{nat(i)}}$) by its mean productivity (ξ). Consumptive use water discharges (QC) must be subtracted from the natural inflows. Thus $E_{\mathrm{nat(i)}}$ is expressed as:

$$E_{nat(i)} = \xi(Q_{nat(i)} - QC_{(i)})\,. \quad (5)$$

$E_{\mathrm{RES(i)}}$ during time period i is the sum of all reservoir artificial potential energy inflows (RES). For a single reservoir, it is calculated by multiplying the artificial-RES water inflow discharge ($Q_{\mathrm{RES(i)}}$) by its mean productivity:

$$E_{RES(i)} = \xi \cdot Q_{RES(i)}\,, \tag{6}$$

$$Q_{RES(i)} = \frac{E_{RES}}{CF \cdot t \cdot (\rho \cdot g \cdot H_{n(PS)} \cdot \eta_{PS} \cdot \eta_{INV})} = \frac{E_{RES}}{CF \cdot t \cdot \xi_{MPI}}\,, \tag{7}$$

where $H_{n(PS)}$ is net head of pump station, η_{PS} is total available efficiency of pump station, η_{INV} efficiency of inverter and ζ_{MPI} is motor, pump and inverter productivity and t is time period. The energy outflow from the equivalent reservoir is the decision variable in the optimization problem, i.e. the desired energy production.

2.3. Relation between electric power of the RES generator and storage

The calculation of nominal power P_{el} for pumping water into upper storage and covering the demand for energy in a PSH in time step i is performed according to the characteristics of RES-I power plants (wind, PV and solar thermal). The equation for electric power of a RES-I generator (PV, ST or W) is derived from the equation used for dimensioning of the PV generator, presented in the paper [6] and which can generally be expressed as follows:

$$P_{el(i)} = \frac{2.72 \cdot 10^{-3} \cdot p_{RES} \cdot H_{TE(i)}}{\eta_{RES(i)}(T_a, v, \rho, \varphi) \cdot \eta_{MPI} \cdot E_{RES(i)}} \cdot V_{RES(i)}\,, \tag{8}$$

where p_{RES} (W/m^2) is equivalent value of RES-I power reference value (for solar systems it is 1000 W/m^2); η_{MPI} is efficiency of motor-pump unit and inverter; $\eta_{RES(i)}(T_a,v,\rho,\varphi)$ is exploitation efficiency of a RES, which depends on air temperature T_a, density ρ, wind velocity v and air humidity φ; $H_{TE(i)}$ (m) is total head, $V_{RES(i)}$ (m^3) is total water volume to be pumped by RES-I power plant into upper storage in order to satisfy daily energy consumption; $E_{RES(i)}$(kWh/m^2/day) is average daily energy from RES-I, available for energy production. Optimal power P_{el}* could be calculated in the similar way as is shown in the paper [6].

Apart from E_{RES} and the size of the consumer, expressed in Eq. (8) by $V_{RES(t)}$, it can be seen that upper storage volume V also has a dominant effect on P_{el}. The dependence of P_{el} on operating volume V of the upper storage is:

$$P_{el} = -a \cdot Ln(V) + b\,, \tag{9}$$

Where P_{el} is power of RES-I (W), V is operational volume storage (m^3), a,b – coefficients based on location and technological features. This relationship has been determined by the previous papers for PV and ST hybrid power plants, such papers have not yet been made for the wind power plants.

The interval $V_{min} < V < V_{max}$ which is called the boundary layer, serves as transition from the P_{max} value to the value P_{min}. Minimal value P_{min} is conditioned by the possibility of construction of storage (V_{max}) at a location. Therefore:

$$P|_{V=Vmax} = P_{min}\,. \tag{10}$$

As the period of daily insolation is always shorter than the daily period of planned energy production (24 hours), the minimum period of daily insolation, compared to the planned production of energy, determines the minimum dimensions of the storage volume and thus the maximum required power of solar power plant is:

$$P|_{V=Vmin} = P_{max}\,. \tag{11}$$

The boundary layer defines the size of storage volumes necessary to ensure the continuity of the planned production.

The constant "*b*" represents the maximum power of the plant that provides the total energy needed in the critical time step of the analysis period. The constant "*a*" represents the cumulative impact of factors for production of solar energy (technological and climate) in the period considered.

P_{el} and V are optimized according to characteristics of the problem. Based on the results of modelling it is possible to obtain more detailed information of interest to decision-making. Since the functional relationship between P_{el} and V is known (equation (9)), as well as the relationship between P_{el} and the area of collector field A of PV generator, it is possible to obtain the connection between the required A and V, according to:

$$A = \frac{P_{el}}{1000 \cdot \eta_{oc}} = \beta \cdot \left(-a \cdot Ln(V) + b\right) \ (\mathrm{m}^2) \qquad (12)$$

Where η_{oc} is PV generator efficiency.

In this way, relations are obtained for the size of the three key structures of the hybrid PV-PSH power plant, the area of the collector field (A), power of the PV generator (P_{el}) and the working volume (V). The results for Solar Thermal (ST) power plant can be obtained in the similar way.

Other objects of interest for the sizing of the system are pumping station PS and HE. The capacity of pump station Q_{PV} is obtained based on modelling results as dependent variable used for evaluating the performance of the system, and HE capacity is set by building objectives.

The relation between P_{el} and V can also be observed through the required reserve power supply in the system. It is obvious that the upper storage has the key role in the proposed hybrid power plant management. Relation between P_{el} of RES-I power plants (PV and ST) and reservoir volume V and the required P_{el} depending on power supply reserve, Figure 4.

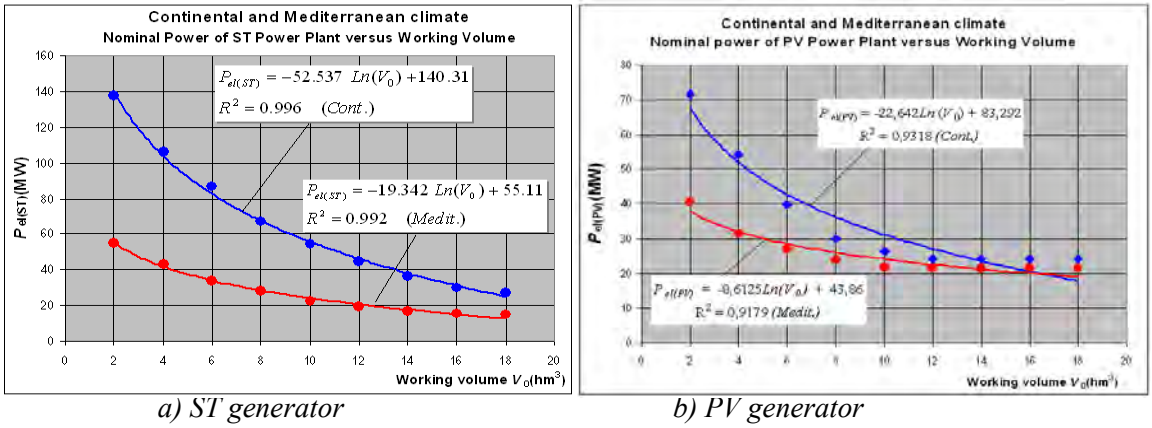

a) ST generator *b) PV generator*

Fig 4. Characteristic curves P_{el}=f(V) for ST and PV power plants for two climates areas.

3. Possible applications

Since this is a completely innovative solution, there are no practical results and the basic relationships of interest for the development and application can be obtained on the basis of previous research, basic theoretical assumptions and literature data. Key data relate to the

basic dimensions of power plant and its parts, production features, as well as economic, social and environmental impacts. Previous research [6, 7] shows that for Mediterranean climate (Island of Vis in Croatia) and continental climate conditions (Osijek, Croatia), the size of the hybrid system in the case of PV generator for these areas can be determined based on equations:

$$P_{PV\,(Medit.)} = -10.497\,Ln(V) + 44.21 \quad (13)$$

$$P_{PV\,(Cont.)} = -19.904\,Ln(V) + 65.123 \quad (14)$$

If these results were applied to the EPS, a general framework and dimensions of the solution could be obtained, using the *Concept-H*. The same was done in the case of Croatia [8], so that the reality of achievement of green energy policies [8] could be seen in Figure 5.

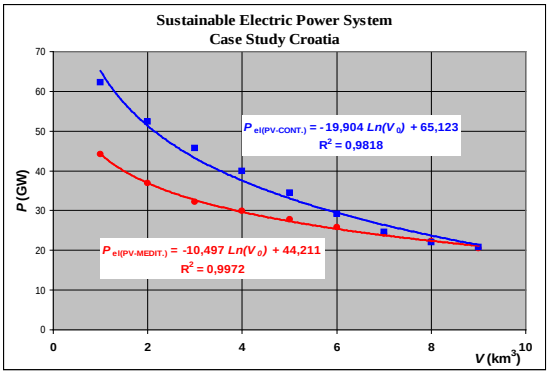

Fig 5. Scenario for Croatia.

In this way the possible applicability of the *Concept-H* at different locations and regions could be analyzed. The proposed *Concept-H* locally imitates the natural hydrological process, essentially generated by the same natural forces (solar energy and gravity), and, as a mostly closed system based on the use of natural renewable solar energy, it has a significantly smaller impact on the environment than other energy sources. In its operation it does not consume water, organic or other substances, does not create harmful residues and CO_2, and therefore provides opportunities to achieve sustainability objectives.

4. Comments and conclusions

This paper points to the possibility of realization of green energy scenario [8, 9, 10] by a concept, the so-called *Concept-H* [1]. It is a technological concept of hybrid RES-PSH systems which provides continuous energy production, the same as conventional energy sources. The solution in the proposed hybrid concept RES+PSH represents a production unit of sustainable energy supply based on natural resources which are free of charge and constantly available. The concept is very flexible in operation and construction. The accent is on hydroenergy, i.e. PSH as the main building unit, because this concept is flexible in implementation and provides continuous supply of „green“ energy and can be built in a wide range of climate areas, locations and water resources (fresh water, water with temporary flow, as well as on the sea). It can be implemented on the existing HE. The proposed production unit usually has very small impacts on the environment because it causes minimal changes in local and global hydrology and eco systems, and has a low level of potential danger for people and environment in case of incidental situations. Starting from the expected progress in the development of RES, especially PV [11], the proposed *Concept-H* may be one of the most promising solutions for achieving sustainable green energy scenario.

References

[1] Z. Glasnovic, J. Margeta, Vision of total renewable electricity scenario, Renewable and Sustainable Energy Reviews, (2011), doi: 10.1016/j.rser.2010.12.016 (in press).

[2] B. Lee, D. Gushee, Massive electricity storage, An AIChE White Paper, American Institute of Chemical Engineers, 3 Park Avenue, New York, NY 10016, 2007.

[3] H.Chen, T.N. Cong, , W. Yang, C. Tan, Y. Li, Y. Ding, Progress in electrical energy storage system: A critical review. Progress in Natural Science, 19, 2009, pp. 291-312.

[4] ESA, Electricity Storage Association, Energy storage technologies. Technologies & Applications – Technology Comparisons, 2009.

[5] J.P. Deane, B.P. Ó Gallachóir, E.J. McKeogh, Techno-economic review of existing and new pumped hydro energy storage plant, Renewable and Sustainable Energy Reviews, 14, 2010, pp. 1293-1302.

[6] Z. Glasnovic, J. Margeta, The features of sustainable Solar Hydroelectric Power Plant, Renewable Energy 34, 2009, 1742-1751.

[7] J. Margeta, Z. Glasnovic, Feasibility of the green energy production by hybrid solar + hydro power system in Europe and similar climate areas. Renewable and Sustainable Energy Reviews, 14, 2010, pp. 1580–1590.

[8] Z. Glasnovic, J. Margeta, Sustainable Electric Power System, Is It Possible? - Case Study Croatia, Journal of Energy Engineering 136, 2010, pp. 103-113.

[9] EREC, European Renewable Energy Council, 2004. Renewable Energy Target for Europe 20% by 2020. <http://www.erec-renewables.org/fileadmin/erec_docs/Documents/Publications/EREC_Targets_2020_def.pdf>

[10] EREC, European Renewable Energy Council, 2006. Renewable Energy Scenario to 2040, Half of the global energy supply from renewables in 2040. <http://www.censolar.es/erec2040.pdf>

[11] M. A. Green, K. Emery, Y. Hishikawa, W. Warta, Solar cell efficiency tables (Version 36), Progress in Photovoltaics: Research and Applications, 18, 2010, pp. 346–352.

Environmentally compatible hydropower potential in the estuary of the river Ems - Analysis for a floating energy converter

Steffi Dimke[1*], Frank Weichbrodt[1], Peter Froehle[1]

[1] *University of Rostock, Coastal Engineering Group, Germany*
** Corresponding author. Tel: +49 381 4983687, Fax: +49 381 4983682, E-mail: steffi.dimke@uni-rostock.de*

Abstract: Within the EC-funded research project *HYLOW - Hydropower converters for very low head differences* a floating energy converter - a so called Free Stream Energy Converter (FSEC) - for the energetic utilisation of currents with slow flow velocities (< 2.0 m/s) has been developed and will be optimized until 2012. In order to estimate the hydropower potential in case of deployment of the *FSEC*, a p otential analysis exemplarily for the northern part of the river *Ems,* at the border between *Netherlands* and *Germany,* was performed. Here, the *environmentally compatible hydropower potential* has a special importance. As expected, *this potential* is much lower than the *theoretical hydropower potential*. In addition to the efficiency of the energy converter, also the required water depth, existing protection areas and other uses are the main reason for the difference between the mentioned potentials in this investigation area.

Keywords: *Estuary River Ems, Environmentally compatible hydropower potential, Flow velocity*

Nomenclature (Optional)

P	*theoretical power* ... *W*	η	*efficiency factor* ... -
A	*flow trough area* ... *m²*	d	*water depth* ... *m*
ρ	*density of water* ... *kg/m³*	$L_{obstruct}$	*length of the obstructed area* ... *m*
v	*flow velocity* ... *m/s*	L_{demand}	*length of the demanded area* ... *m*
n	*number of energy converter like FSEC* ... -	w_{FSEC}	*width of energy converter as FSEC* ... *m*

1. Introduction

According to the European Small Hydropower Association (ESHA) in European rivers an unused small hydropower resource of 5 GW exists. An essential amount of this resource is available in terms of free stream energy with low flow velocities. The utilisation of this hydropower resource still constitutes an unsolved problem, because most current technologies are not cost effective (for low flow velocities and low discharge) and pose ecological risks to fluvial ecosystems due to blocking of the streaming water.

Within the EC-funded research project *HYLOW - Hydropower converters for very low head differences* a floating energy converter - a so called *Free Stream Energy Converter (FSEC)* - for the energetic utilisation of currents with slow flow velocities (< 2.0 m/s) has been developed and will be optimized until 2012. One important objective of the investigation with the *FSEC* is the development of an economic hydropower converter, which minimises the well known adverse ecological effects of small hydropower devices, since the proposed technique should be able to comply with the requirements of the European Water Framework Directive.

To estimate the hydropower potential in case of the deployment of a number of *FSEC´s* a hydropower potential analysis has been performed exemplarily for the northern part of the river Ems. One of the main objectives was the determination of the *environmentally compatible hydropower potential*. In the following paper, first the *FSEC* and the investigation area are described. After this, the results of the performed hydropower potential analysis are

described, the estimation results of the *theoretical* and the *environmentally compatible hydropower potential* are shown.

2. Free Stream Energy Converter

As mentioned before, the *Free Stream Energy Converter (FSEC)* is a floating energy converter for the energetic utilisation of currents with slow flow velocities. It consists of a Hydraulic Pressure Wheel (HPW), which is installed between two floating bodies. The floating bodies are connected with a bottom blade (Fig. 1). The *FSEC* has a length of 8 m, a width of 2.5 m and a draught of approx. 1 m. The width of the HPW is 1.2 m. This results in a flow trough area of 1.2 m². The design velocity is about 1 m/s - 2 m/s. The combined effect of the HPW, the floating bodies and the bottom blade should increase the efficiency by creating a small head differences between up- and downstream of the blade. Therefore, the hydrostatic pressure difference can be used for power generation in addition to utilisation of currents. [1].

Furthermore, within the *HYLOW* project, the expected influences of the *FSEC* on the environment were theoretically assessed and are investigated in field tests. Compared to conventional technologies, the operation of *FSEC* is environmental friendly. For example, the *FSEC* does not occupy the total river cross section, therefore the fauna and flora can migrate as well as sediment can be transported. As first measurements show, the water discharge and the flow conditions around the energy converter is changed only in a minor range. The *FSEC* also does not effect any pollution of the water. Because of that, the FSEC fits better with the ecological requirements according to the Water Framework Directive than the conventional technologies.

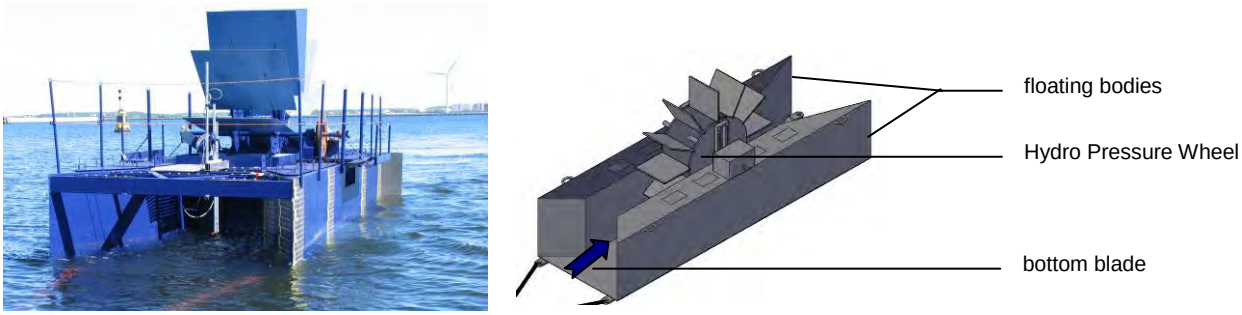

Fig. 1: Free Stream Energy Converter; length = 8 m, width = 2.5 m, draught = approx. 1 m

3. Categories of small hydropower potential

To characterize the areas for potential hydropower sites, different hydropower potentials are described. In publications different definitions for hydropower potential are available. In general the potential is divided into *theoretical, technical* and *realistic potential*. Several further sub-classifications exist.

The total availably energy is the *theoretical hydropower potential*, which can be calculated with following equation, (in which the efficiency factor is 1 for the theoretical potential):

$$P = \frac{1}{2} \cdot A \cdot \rho \cdot v^3 \cdot \eta \qquad (1)$$

The *technical hydropower potential* is only a part of the *theoretical hydropower potential*, which is realizable with existent techniques, at possible sites und complied with legal

regulations. In the range between the *technical* and *realisable hydropower potential*, the *environmentally complaint hydropower potential* and the *environmentally compatible hydropower potential* can be gradated, exemplarily. The definition criteria of mentioned potentials by [2] are mentioned in Fig. 2.

For our investigation within the *technical hydropower potential*, efficiency of the energy converter, requirements caused by dimension and operation of the *FSEC* and existing water uses are considered. The protection areas are taken into account in the *environmentally complaint hydropower potential*. Within the *environmentally complaint hydropower potential,* the impacts on the environment were considered (see chapter 6).

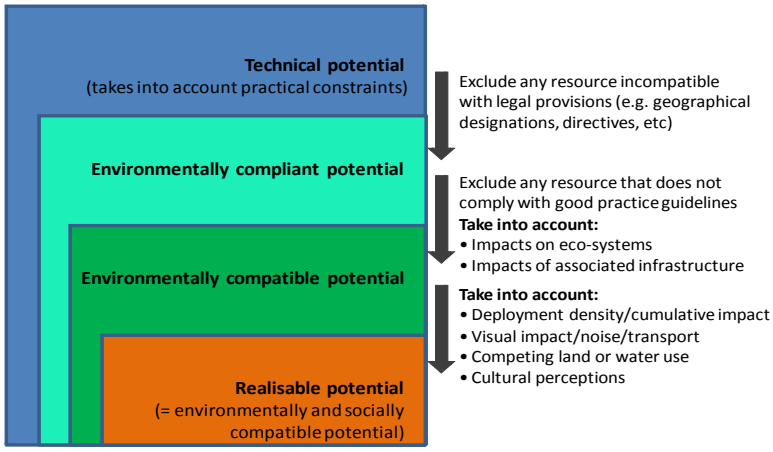

Fig. 2: Constraints to take into account when calculating the hydropower potential (after [2])

4. Investigation area – northern part of river Ems

4.1. Description of the investigation area

The investigation area is in the northern part of the river *Ems*, at the border between Netherlands and Germany. The river *Ems* has a typical river estuary which ends in the *North Sea* (Fig. 3). The river *Ems* is a typical European tidal river with mean tidal range of approx. 3.8 m and a distinctive river estuary. The average annual discharge is much higher than the average annual discharge of the river run-off, therefore not the river run-off but the discharge caused by the astronomical tide is the most important part of the total discharge and, hence, the most important factor influencing the flow velocities, too. The potential analysis for the river *Ems* can be stated to be exemplary for several rivers with tidal impact.

Fig. 3: Overview – investigation area (source: Google earth, modified)

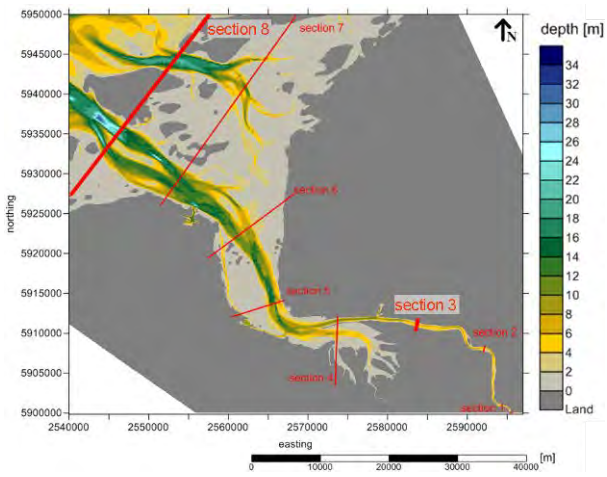

Fig. 4: sections for more detailed investigation, data source BAW

Within a detailed analysis, hydropower potentials were considered along 8 selected cross sections (see Fig. 4). Exemplarily, the investigation is described for the cross section 3 and 8. Section 3 is a typical river section. At this section the river *Ems* has a maximum depth of d = 7.2 m and a width of w = 560 m. The section 8 is typical for an estuary near the sea. The width of this section is about w = 28.000 m and the highest depth is about d = 22 m. Section 8 crosses the border area between Netherlands and Germany and is mainly situated in a protection area, as well as section 4 to section 7.

4.2. Data base

The data for the potential analysis at the *Ems* area is based on results of the Mathematical Model UnTRIM. The Federal Waterways Engineering and Research Institute used this numerical model to emulate and forecast the hydrodynamic conditions in the river *Ems* [2].

For the hydropower potential analysis the results of the simulation scenario with a constant mean run-off of 90 m³/s (average conditions) were used. The available results are representing the mean conditions of the astronomical tide and are available for approx. one day with a temporal resolution of Δt = 10 min and a spatial resolution of Δs = approx. 30 m x 30 m. For the potential analysis the temporal resolution was reduced to Δt = 1 hr and a spatial resolution of Δs = 50 m was used.

It can be assumed that the temporal variability of the natural flow conditions in the river, e.g. neap-spring differences, seasonally changing river run off have only negligible effects on the results of the potential analysis. Hence, the selected average conditions are extrapolated to assess the yearly potential.

4.3. Flow velocity

The mean tidal range is approximately 3.8 m and is varying along the river. The flow velocity varies with the tide and is in maximum about 2 m/s in the whole selected investigation area. Obviously, the flow direction varies also with the tide. The tidal wave is nearly totally reflected in the investigation area which means, that between low tide and high tide, the flow is directed in the upstream direction and between high tide and low tide the flow is directed in the down-stream direction. The mean (surface) flow velocities (on basic of one day) are shown in Fig. 5. As expected, the maximum flow velocities occur in the deep flow channels of the river and, correspondingly, the flow velocities are comparatively low in the shallow water areas.

Because of the bathymetry, the tidal range at section 1 with about 3.8 m is higher than the tidal range at section 8. The tidal range at section 8 is about 2.75 m. At both sections, the highest flow velocities are around v = 1.6 m/s. The flow velocity curves are proportional to the water depth at both sections. Hence, the highest flow velocities are at the sites with high water depth. The mean flow velocity varies along the cross section. A cross section sites with a water depth higher than 4 m, the mean flow velocities are about 1 m/s in section 3 as well as in section 8.

5. Theoretical hydropower potential

The *theoretical potential* is assessed as areal potential and based mainly on the flow velocity. The power output is determined for each grid on basis of the mean flow velocities with equation 1. For the comparison with other results, the flow trough area is defined with 1 m² and the efficiency factor is defined with 1. A bi-directional converter is assumed, which is

able to use the flow in both flow directions of the tide. In Fig. 6 the estimated *theoretical hydropower potential* for the investigation area is displayed. At several locations the estimated power output is higher than 1.2 kW. For most of the areas, the estimated theoretical power is between 0.2 kW and 0.8 kW.

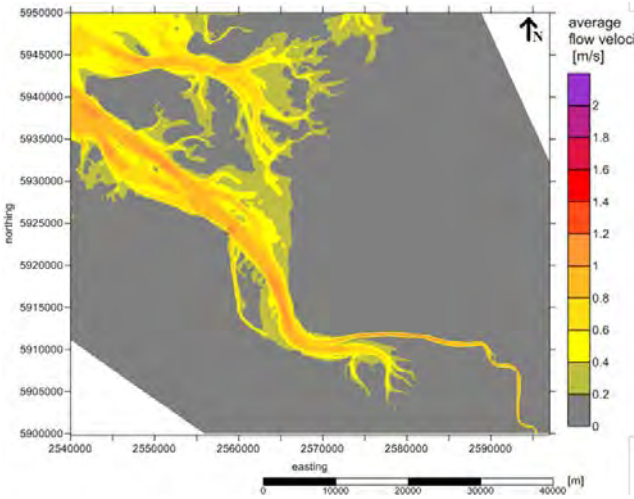

Fig. 5. average flow velocity, data source BAW

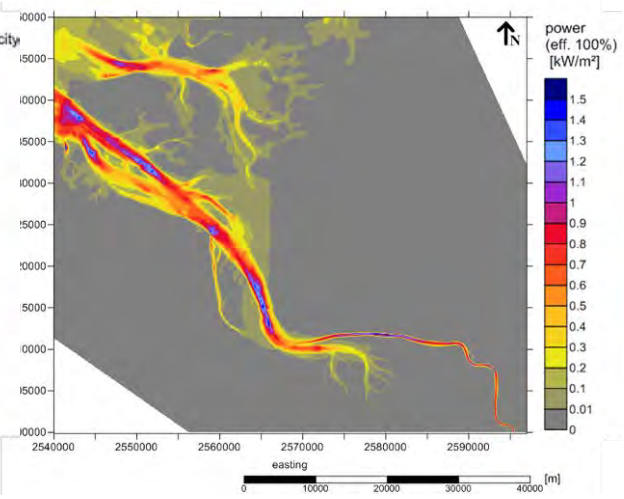

Fig. 6: theoretical power for the investigation area

An assumed realistic efficiency factor leads to decreasing estimates for the technical power. The definition of the efficiency factor for the *FSEC* is an objective of currently investigation and is not determined finally until now. With an assumed efficiency of 30%- 40% the maximum power is about 0.4 kW to 0.5 kW, with is in the range of the *technical hydropower potential*. The further factors, as water depth, other uses of the river or yearly operating hours are neglected, here. It will be considered in the following chapter.

6. Environmentally compatible hydropower potential

6.1. Considered aspects

As mentioned above, the *technical hydropower potential* considered the practical aspect, whether a deployment is possible regarding the technical requirements and other exiting site-uses (see chapter 3). One important aspect is the required space for the energy converter. All 8 considered cross sections are width enough to deploy a *FSEC*. For the *FSEC* (Fig. 1) the depth of the river is a restrictive factor (practical constraint). For the necessary river depth the draught of the *FESC* (1 m), the low water level and a necessary distance between river bottom and *FSEC* ("under keel clearance") have to be considered. The distance between bottom and *FSEC* is necessary, to ensure the floating behaviour of the *FSEC* and also to ensure the pass for the aquatic fauna and sediment below the *FSEC*. Its minimum is defined with 1 m. The low water level is strongly dependent on the local tidal range. The highest tidal range of the section is approx. 4 m, in section 1. Thus, the low water level is defined with -2 m NN. In the sum the required average water depth is 4 m including all sections of the river with river beds lower than -4 m NN.

In addition to the restrictive factor "required depth" existing uses of the river (competitive water uses) reduce the area to deploy the energy converter. In the investigation area, existing uses are mainly the use of the river as a waterway. In addition, uses like roadstead and spoil ground are of importance. The deployments of energy converter in the navigation canal are prohibited, in order to protect the navigation. A permission of hydropower deployment

outside of the navigation canal will be decided individually under consideration of the energy converter and the chosen deployment site.

Areas which are identified by a legal restriction, e.g. protection areas, or other environmental designation will be considered by the *environmentally compliant hydropower potential* (see chapter 3). A large part of the investigation area is defined as natural protected area.

At the latest by the implementation of the Water Framework Directive (WFD) it is not licensable to obstruct the whole river section with anthropogenic water uses. Also within the *environmentally compatible hydropower potential* the impact of uses is considered (see chapter 3). As mentioned above, the operation of the *FSEC* has only a minor effect on the environment. As a result, the use of the environmental friendly converter, like the *FSEC*, is a contribution for the *environmentally compatible hydropower potential.*

It is conceivable to deploy several energy converters in some converter fields. In this case, a distance between the single energy converters is required; especially in order to provide the river continuity, which is a main objective in the WFD. For the following analysis it is assumed that uses of 25 % of the river section is a minor impairment of the water bodies and therefore licensable. To not influence the operation mode and therefore the power output negatively, the distance between the single converters or to other uses and boundary are also important. Rightly this aspect is part of the *technical hydropower potential*.
The lateral distances between energy converters or to other uses/users or any other boundaries is chosen to 2 times of the converter width and is 5 m. In this paper the hydropower potential is only described along cross sections, therefore, the distance between the converter in down or upstream direction is not described.

It is distinguished between the demand of area for the deployment of the *FSEC* and the obstructed area caused by an *FSEC*. The obstructed area includes only width of the *FSEC*. The demanded area includes over more to the width of an *FSEC* the required distance between two successive energy converters, to other uses or to banks. For the calculation of the obstructed areas and for the demanded area the equation (2) and (3) are used, respectively.

Obstruct area: $L_{obstruct} = n \cdot w_{FSEC}$ (2)

Demand of area for deployment: $L_{demand} = n \cdot w_{FSEC} + 2 \cdot (n+1) \cdot w_{FSEC}$ (3)

In the following chapter it is determined how many energy converters like e.g. *FSEC* or other similar converters could be deployed along selected sections.

6.2. Results

The application of the mentioned aspect and the determination of the different hydropower potentials are described exemplarily along cross section 3 and 8 (see chapter 4). The power was determined based on the mean flow velocity and only at sites with water depths greater or equal to 4 m. The determined power and competitive uses along section 3 and section 8 are displayed in Fig. 7 and Fig. 8.

In case of section 3, the waterway utilizes 125 m of the total section of approx. 560 m. An average water depth higher than d = 4 m is available along a 410 m stretch of the section. More upstream of the river *Ems*, almost the total cross section length with a water depth

higher than d = 4 m is used by the waterway (e.g. section 1), therefore a deployment of the *FSEC* is not possible, there. The section 8 has a length of approx. 28,000 m. Thereof, approx. 13,500 m are land areas, for example the island *Borkum*. Only along approx. 7,000 m of the section length the average water depth is higher than 4 m. In addition, approx. 4,400 m of the remaining approx. 7,000 m are already in use or are protected areas. Along both sections possible deployment sites for the *FSEC* are remained (green lines in Fig. 7 and Fig. 8).

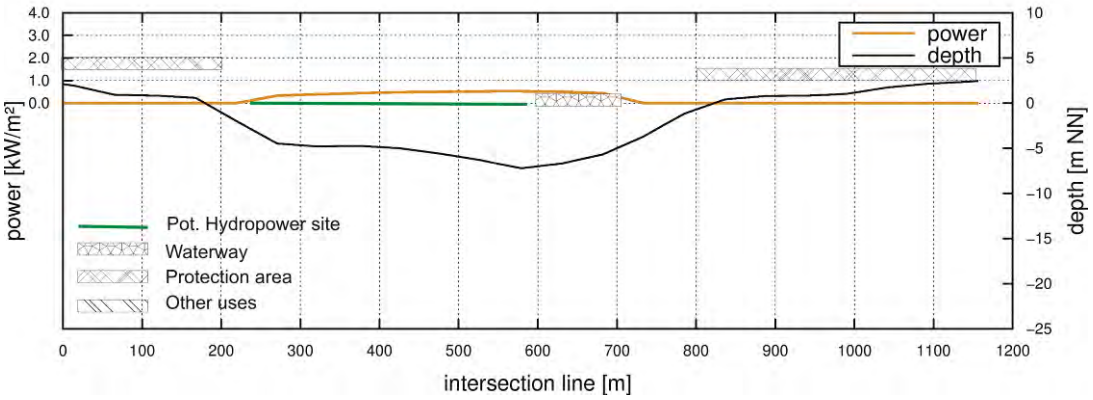

Fig. 7: Potential sites for hydropower uses and competitive uses, section 3 (power based on mean flow velocities)

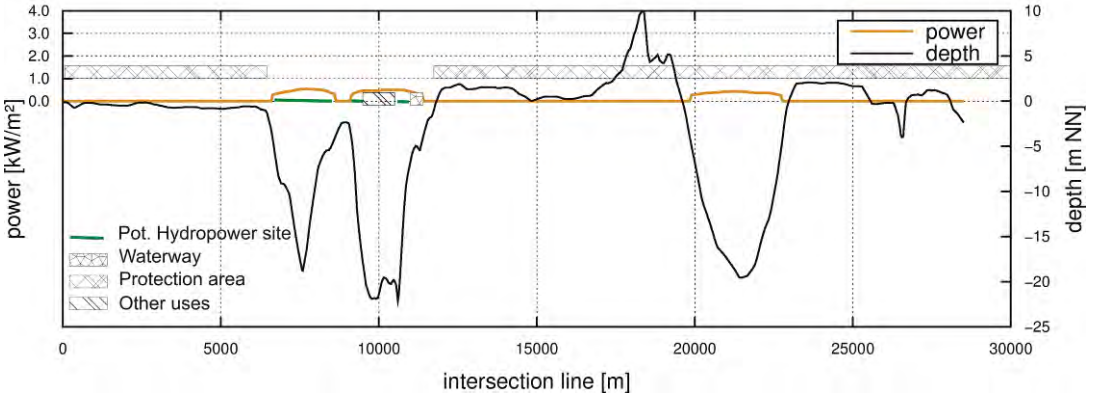

Fig. 8: Potential sites for hydropower uses and competitive uses, section 8 (power based on mean flow velocities)

Tab. 1: Properties of the sections

	Section 1	Section 8
Length of river cross section, only water areas (m)	560	16,590
Length of river cross section with existing uses/ protections area (m)	125	4,424
Length of river cross section d > 4 m (m)	411	7,003
25 % of river cross section length (m)	141	4,147

In Tab. 1 and Tab. 2 the properties and the *environmentally compatible potential* for the selected sections are presented. Along section 3 approx. 300 m and in the section 8 approx. 2,600 m could be used for the deployment of hydropower converters like the *FSEC*. Along all sections the obstructions of the river because of already existing uses are only minimal and therefore neglected. These results, that converter fields of possible 37 energy converters along section 3 and possible 343 energy converters along section 8 could be deployed. Accordingly, 16% of the river cross section 3 and 5% of the river cross section 8 would be obstructed.
For these possible energy converters fields the *environmentally compatible hydropower potential* is estimated with equation (1) on the basis of the assumptions that: all possible number of energy converter are installed, the average flow velocity v = 1 m, the flow through

area A_{FSEC} = 1.2 m² and the efficiency factor η = 0.3. If all 37 energy converters along section 3 and all 343 energy converters along section 8 could be installed, the potential is estimated with 7 kW and 62 kW (see Tab. 2). The operation period depends mainly on maintenance periods and weather conditions. With a realistic 5000 ope rating hours per year, the *environmentally compatible hydropower potential* is estimated with 33 MW/y for section 3 and 308 MW/y for section 8.

Tab. 2: useable resources of sections

	Section 1	Section 8
Length of river cross section d > 4 m minus length of other uses/ protections area (m)	287	2,579
25 % of river cross section length minus length of other obstructing uses (m)	141	4,147
Possible number of energy converters	37	343
Ratio: obstructed length / river cross section length (%)	16	5
Potential based on v_m = 1 m/s, A_{FSEC} = 1,2 m², η = 0.3 (kW)	7	62

7. Conclusion

The *realistic hydropower potential* will be lower than the afore-determined *environmentally compatible hydropower potential*. Furthermore the economical aspect was not considered in the paper. After the optimization procedure, the investigation costs will be calculated and put in relation with the expected power output. The estimated yearly performance per *FSEC* of approx. 890 kW/y is - compared to conventional energy converters - relatively low, but the advantage of *FSEC* is, that it has only small influences on the environment. The river *Ems* is an appropriate area for the deployment of the *FSEC*, because energy converters could be deployed in many sites and the flow conditions are continuous over the year. For example the discharge in rivers without tidal impact is seasonally different and depends of precipitation. In several rivers the flow velocity or the water depth are too low.

Acknowledgments

The research leading to these results has received funding from the EuropeanCommunity's Seventh Framework Program [FP7/2007-2013] under grant agreement° 212423.

References / Data sources

[1] Mueller G. and Senior J. (2007): The hydrostatic pressure machine with free surface – a novel energy converter for very low head differences. In: Zehntes Internationales Anwenderforum Kleinwasserkraftwerke 2007, Regensburg

[2] Landy, M. (2008): A methodology to quantify the environmentally compatible potentials of selected renewable energy technologies. ETC/ACC Technical Paper 2008/16, Harwell.

[3] BAW - Waterways Engineering and Research Institute (2004). Technical Report, Mathematical Model UnTRIM, Validation Document, Version June 2004 (1.0), http://www.baw.de/vip/abteilungen/wbk/Methoden/hnm/untrim/PDF/vd-untrim-2004.pdf.

[4] Hydrodynamic data for the river Ems: results of the “Mathematical Model UnTRIM”, Federal Waterways Engineering and Research Institute

Investigation on Effect of Aged Pumped-Storaged Component Replacement on Economic Profits Considering Reliability and Economic Efficiency

Jong Sung Kim[1,*]

[1] *Sunchon National University, Suncheon, Republic of Korea*
** Corresponding author. Tel: +82 617503537, Fax: +82 617503530, E-mail:kimjsbat@sunchon.ac.kr*

Abstract: Recently, availability decrease due to increase of midnight electric power demand has risen necessities to improve economic efficiency of the pumped-storage power plants in South Korea. The necessities cause to extend a preventative maintenance cycle, especially an overhaul cycle. But, unconditional extension cannot be implemented because it may generate unanticipated failures due to insufficient maintenance. So, first, in this study, possibility of extension of the preventative maintenance cycle is identified via investigation on preventative maintenance situation of overseas and domestic hydropower plants. Second, a methodology to optimize the preventative maintenance cycle considering both reliability and economic efficiency is presented via review of the previous reliability studies and considering characteristics of the pumped-storage power plant. The methodology consists of the eight parts including selection of principal components and subcomponents, identification of damage mechanisms in the principal components/subcomponents, FMEA(failure mode effect analysis), derivation of replacement and repair time of the principal components/subcomponents, design of preventative maintenance cycle plan, reliability analysis, economic assessment, and derivation of the optimized preventative maintenance cycle. Also, as a result of application of the methodology to an aged pumped-storage power plant in South Korea, the overhaul cycle has been extended from 4 years to 7.5years. Last, effect of replacement of some aged principal subcomponents such as rotor runner and generator stator on economic profits is investigated via application of the methodology to the aged pumped-storage power plant.

Keywords: *Pumped-Storage Power Plants, Replacement, Preventative Maintenance, Reliability, Economic Efficiency*

1. Introduction

Recently, it has been reported that availability of pumped-storage power plants decreases due to increase of midnight electric power demand in South Korea[1]. This low availability has been risen necessities to improve economic efficiency of the pumped-storage power plants. The necessities cause to extend a preventative maintenance cycle, especially an overhaul cycle. But, unconditional extension cannot be implemented because it may generate unanticipated failures due to insufficient maintenance.

All over the world, some studies has been performed about life extension, modernization and preventative maintenance of hydro and pumped-storage power plants[2-12]. In South Korea, life extension and modernization methodology for hydro power plants was established and applied to the aged hydro power plants several years ago but the methodology to optimize systematically an overhaul cycle wasn't developed[2]. The previous studies didn't investigate effect of aged pumped-storaged component replacement on economic profits considering reliability and economic efficiency.

Therefore, first, in this study, possibility of extension of the preventative maintenance (overhaul) cycle is identified via investigation on preventative maintenance situation of overseas and domestic hydropower plants[3-8]. Second, a methodology to optimize the preventative maintenance cycle considering both reliability and economic efficiency is presented via review of the previous reliability studies[6, 9-12] and considering characteristics of the pumped-storage power plant. Also, the optimized overhaul cycle is derived via application of the methodology to an aged pumped-storage power plant in South Korea. Last, effect of replacement of some aged principal subcomponents such as rotor runner and

generator stator on economic profits is investigated via application of the methodology to the aged pumped-storage power plant.

2. Investigation of Preventative Maintenance Situation

Table 1 presents the preventative maintenance cycles of hydro or pumped-storage power plants in some countries[3-8]. A class means complete overhaul for all components and B class means partial overhaul for some components. From the table, it is found that the preventative maintenance cycles of pumped-storage power plant in South Korea are shorter than those of other countries. It is identified that the A class preventative maintenance cycles of TEPCO and J-POWER have been gradually increased from 6years and will be 15years in the future by interview with working staff of TEPCO and J-POWER[7]. Also, It is confirmed that the recent availability of pumped-storage power plants in Japan is less than 10% similarly with South Korea. In some cases, Japan industries have taken and repaired the damaged principal components such as turbine runner, guide vane and generator rotor at maker's fabrication shops out of the site during A class overhaul period in order to improve their reliability to level of new products, but South Korea industries have repaired all the damaged principal components at the site.

As a result of this investigation, it is possible to extend the A class preventative maintenance cycle of pumped-storage power plants in South Korea like Japan. But, it is necessary to review in more detail and extend sequentially the cycle in order to extend to 10~15 years because there is difference in preventative maintenance method between South Korea and Japan.

Table 1. Preventative maintenance cycles of South Korea and overseas pumped-storage power plants.

Classification			A Class Preventative Maintenance Cycle (years)	Standard Period (days)	
South Korea/other countries	Company	Power Plant		A	B
South Korea : pumped-storage[3]	A	L	4 (A-B-A)	80	18
	B	M	4 (A-B-B-A)	76	12
	C	N	5 (A-B-A)	80	18
	D	O	4~6 (A-B-B-B-A)	80	16
	E	P	4 (A-B-A)	80	18
South Korea : hydro	KHNP[4]	-	4 (A-B-A)	-	-
	K-Water[5]	-	5 (A-B-A) or 6 (A-B-B-A)	-	-
Japan : hydro including pumped-storage[6]	-	-	9~15 or depends on equipment condition	-	-
Japan : pumped-storage[7]	TEPCO	Tamhara	12~18 (20,000hours)	150~180	21~28
	J-Power	Okki	15	125	8~10
USA : pumped-storage[8]	-	-	Average 10 (5~16)	75~150	-

3. Review of the Previous Studies about Reliability Assessment

Fig. 1 shows an optimization result of Snowy Mountains Hydro-electric Authority[9] for the complete overhaul cycle of hydro power plants by using the commercial program, RCM Turbo[13]. As shown in the figure, cost of unplanned maintenance increases drastically due to increase of breakdown probability with time span between planned activity while cost of

planned maintenance decreases continuously with the time span. So, sum of two costs has minimum value and the time corresponding to the value is an optimum overhaul cycle. However, this methodology cannot consider reliability reduction according to operation time beyond unit preventative maintenance cycle.

Japan Electricity Association presented a methodology to determine economic maintenance cycle of hydro-electric power equipments[6]. The methodology uses the same concept with Fig. 1.

Fig. 2 presents Vasilevski et al.'s methodology to investigate change of reliability with preventative maintenance cycle in order to determine optimal overhaul cycle and re-construction time[10]. As shown in Fig. 2, reliability reduction trend vs. operation time is changed with overhaul cycle, re-construction should be carried forward before reliability reaches critical value, and it mean that the overhaul cycle has to be adjusted as late as possible to be re-constructed. But, this study didn't present the method to set up critical failure probability and didn't consider economic efficiency so has practical problem.

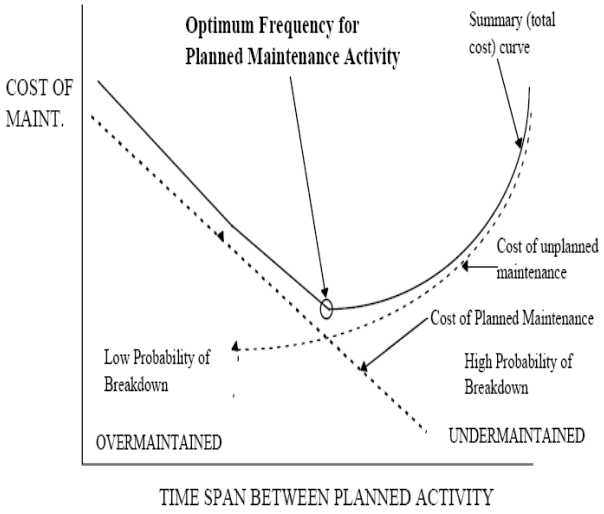

Fig.1 Maintenance cost optimization curve of Snowy Mountains Hydro-electric Authority[9].

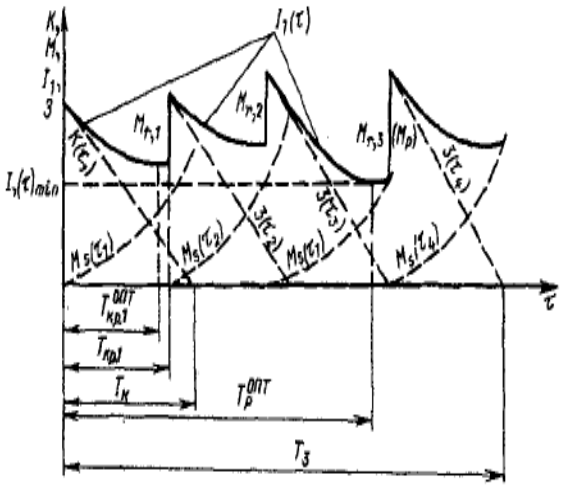

Fig.2 Vasilevski's methodology to determine optimal overhaul cycle and re-construction time[10].

EPRI TR-111488 presented outline of SRCM(streamlined reliability-centered maintenance) program for hydroelectric power plants instead of RCM(reliability-centered maintenance) that requires huge amounts of data and information[11]. EPRI TR-114160[12], which is a follow-up report of EPRI TR-1114888, presented three key factors(sound/cost-effective SRCM process, a software tool to manage consistently/effectively SRCM data and project management/working culture change) to succeed in performing SRCM and explained requirements for three key factors. However, purpose of the EPRI studies[11, 12] isn't optimization of overhaul cycle but deduction of preventative maintenance tasks for reliability improvement.

4. Methodology to Optimize Overhaul Cycle

Based on the review results of previous studies, this paper presents a methodology to optimize overhaul cycle considering both reliability and economic efficiency. Basic assumptions are used to develop the methodology as follows:

- Reliabilities of component and system should be drastically increased by A class preventative maintenance(overhaul).
- In cases of subcomponents or components applied only to B class preventative maintenance, effect of B class preventative maintenance on reliabilities of component/ system is insignificant.

Fig. 3 depicts overall flow chart of process to optimize overhaul cycle of pumped-storage power equipments. As depicted in the figure, item "task selection and comparison" of the RCM/SRCM methodology is removed because purpose of the methodology is to determine optimal overhaul cycle. Also, FFA(functional failure analysis) is performed including in FMEA(failure modes and effects analysis). Overall process consists of selection of target subcomponents/components, derivation of aging related damage mechanisms for the target subcomponent/components FMEA, calculation of repair/ replacement years, planning of preventative maintenance scenario, reliability analysis, economic efficiency analysis, and derivation of optimal overhaul cycle.

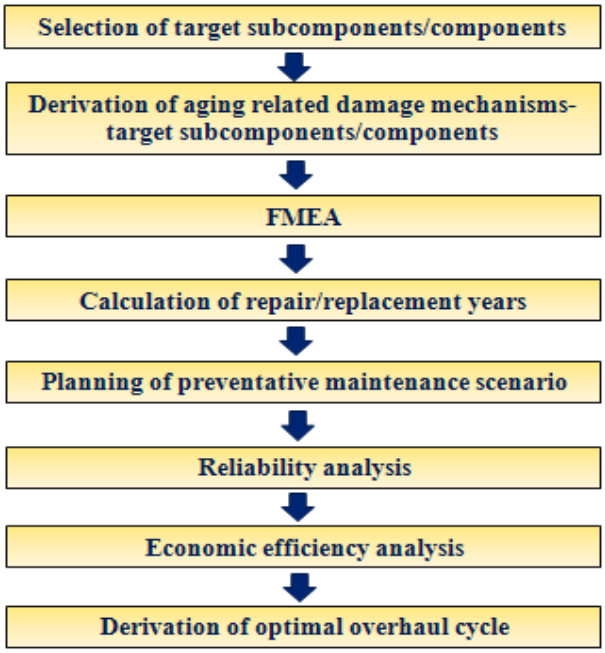

Fig.3 Overall flow chart of process to optimize overhaul cycle of pumped-storage power equipments.

Fig. 4 presents flow chart to select the target subcomponent and components. As presented in the figure, the subcomponents and components subject only to B class preventative maintenance are exclude from target in accordance with the basic assumption about effect of B class preventative maintenance on reliability. Fig. 5 shows flow chart to derive the aging related damage mechanisms for the target subcomponent and components.

Fig. 6 depicts flow chart of FMEA process. First, effect of each damage mechanism on intended function (e.g. structural integrity or performance) of subcomponent is evaluated. Second, based on the evaluation results, effect of the damage occurred on subcomponent on

component/system is evaluated. Third, next step, check whether subcomponents or components can be repaired or replaced during B class preventative maintenance or not. Last, if repair or replacement is impossible during B class preventative maintenance, draw up a final list of the relevant aging damage mechanisms for the target subcomponents/components.

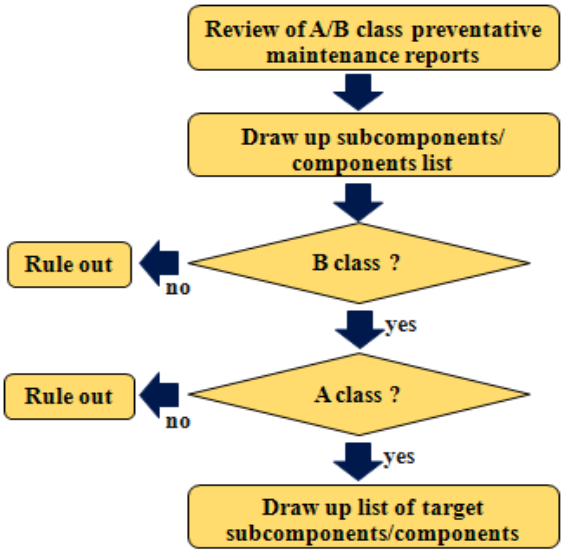

Fig. 4 Flow chart to select target subcomponents and components.

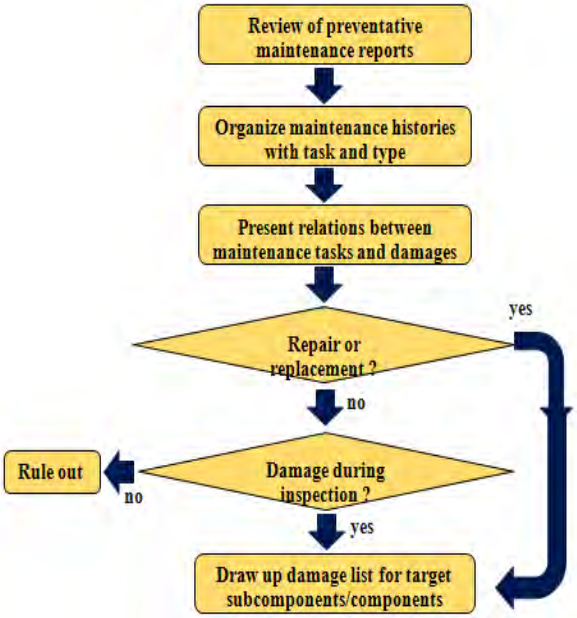

Fig. 5 Flow chart to derive the aging related damage mechanisms for the target sub-components/components.

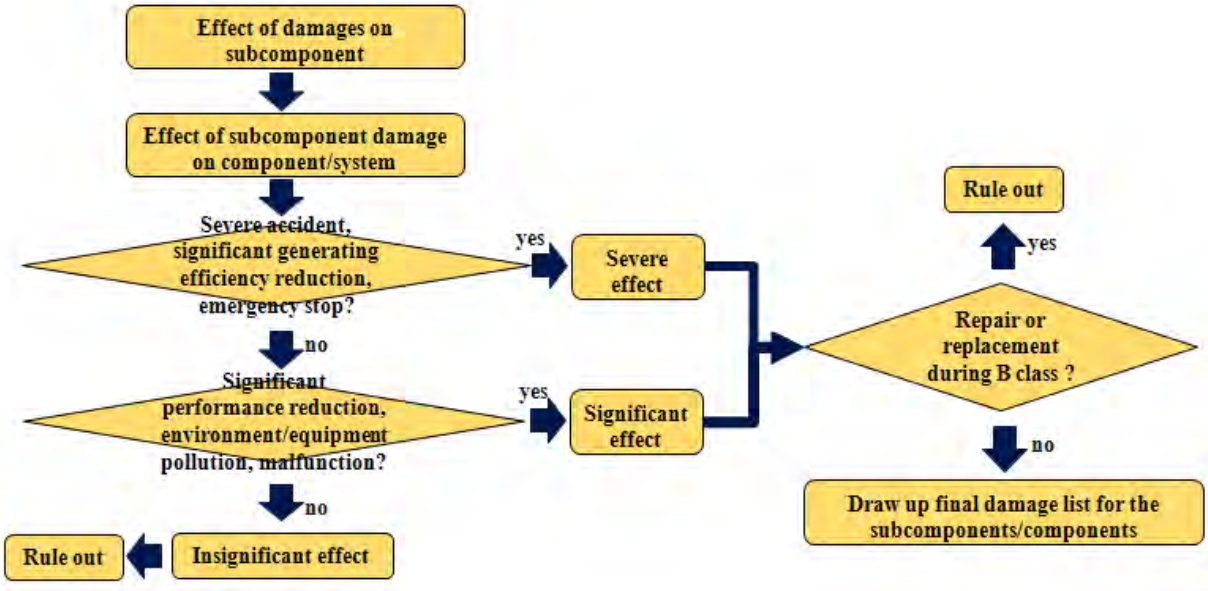

Fig. 6 Flow chart of FMEA.

Analyzing A and B class preventative maintenance histories for the final list derived via the process presented in Fig. 6, real repair/replacement cycles(minimum/mean) for the subcomponent-damage mechanism are derived. These repair and replacement cycles are used as an input for derivation of CHRF(cumulative hazard rate function) coefficients.

A preventative maintenance scenario has to be prepared because reliability has variation with order of maintenance class and number within unit cycle. For example, A-B-A, A-B-B-A, A-B-B-B-A, etc.
Fig. 7 shows flow chart of reliability analysis. If repair and replacement data are enough to evaluate, CHRF coefficients of equation (1) are directly derived via the numerical analysis using the repair and replacement cycles.

$$H(t) = a_0 + a_1 t + a_2 t^2 \quad (1)$$

$$R(t) = exp(-H(t)) \quad (2)$$

$$F(t) = 1-R(t) \quad (3)$$

where $H(t)$ is CHRF, $R(t)$ is reliability function, $F(t)$ is CDF(cumulative damage function) for failure time. If repair and replacement data are not enough to evaluate, CHRF coefficients are derived by using real repair/replacement data, reference reliability curve[14] or database[15], and Bayesian updating technique.

Finally, the overhaul cycle to derive minimum CPUT(cost per operating unit time) value at the target period is determined as an optimal overhaul cycle. CPUT for each preventative maintenance scenario is calculated by equation (4).

$$CPUT(t) = \frac{t_p[C_P R_{min} + C_U(1-R_{min})]}{t\int_0^{t_p} R(s)\,ds} \quad (4)$$

where C_p is preventative maintenance cost, C_u is post-accident preservation cost, t_p is unit cycle time, t is target period of scenario, R_{min} is minimum reliability within unit cycle.

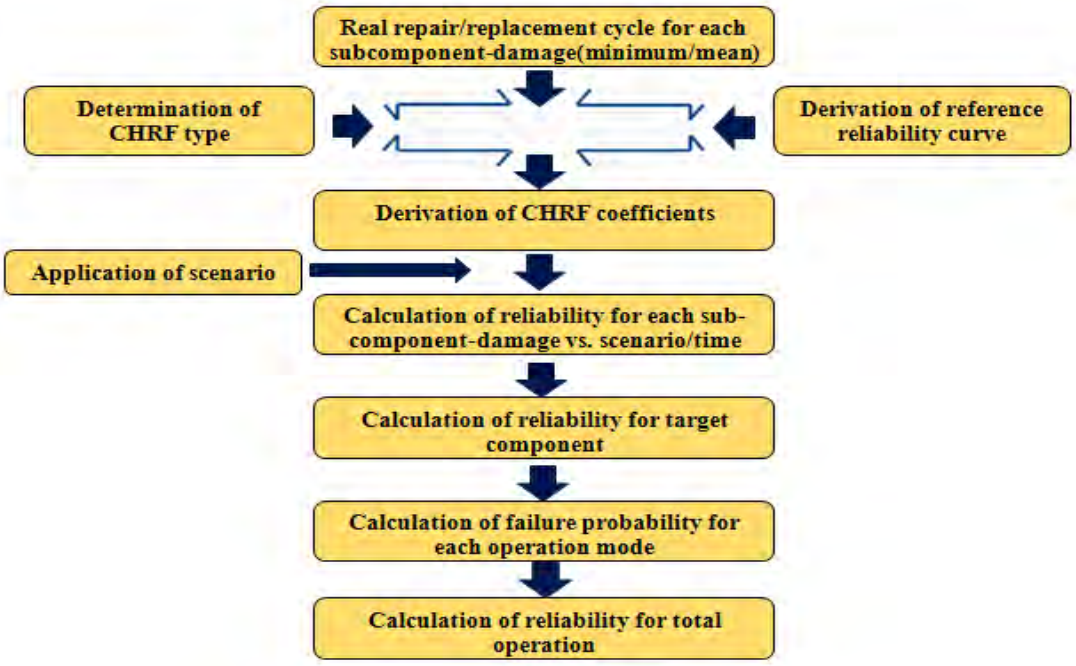

Fig. 7 Flow chart of reliability analysis.

5. Application Results

Table 2 presents overview of a pumped-storage power plant for application of the developed optimization methodology.

Table 2 Overview of a pumped-storage power plant for application of the methodology.

Items		Unit	Generation	Pumping
Operating time		years	24	
Capacity		MW	300×2	370×2
Pump turbine	Type	-	Francis	
	Max./min. head	m	345/288	355/310
	Max. output	kW	310,000	370,000
Generator/ Motor	Type	-	Vertical Inductive	
	Output	kVA	335,555	294,752
	Voltage/current	kV/A	18/10,763	18/10,763
Pony motor	Type	-	-	Vertical Inductive
	Output	kW	-	12,000
	Revolution speed	rpm	-	300
	Voltage/current	V/A	-	6,600/1,712

Fig. 8 depicts variation of reliability vs. time for various overhaul cycles of scenario 1(A-B-B-A). As depicted in the figure, reliability decreases continuously with time but increases after B or A class preventative maintenance. It is identified that improvement of A class is greater than B class in the viewpoint of reliability. Also, the overhaul cycle becomes longer, reduction degree of reliability is greater.

Fig. 9 shows CPUT variation vs. target operating time after the first overhaul completion for various overhaul cycles of scenario 1. As shown in the figure, the target operating time increases, CPUT value decreases irrelevantly to overhaul cycle. It is identified that CPUT has a minimum value at overhaul cycle, 7.5years when the target operating time for scenario 1 is more than 10 years. In other words, if the target operating time for scenario 1 is more than 10 years, optimal overhaul cycle is 7.5years. As a result of application of the methodology to an aged pumped-storage power plant in South Korea, the overhaul cycle has been extended from 4 years to 7.5years.

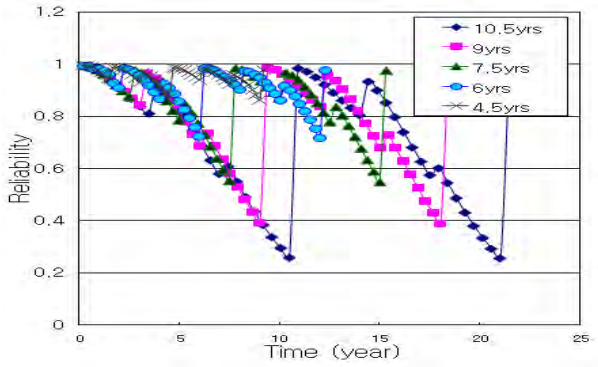

Fig. 8 Reliability of unit vs. time according to various overhaul of scenario 1.

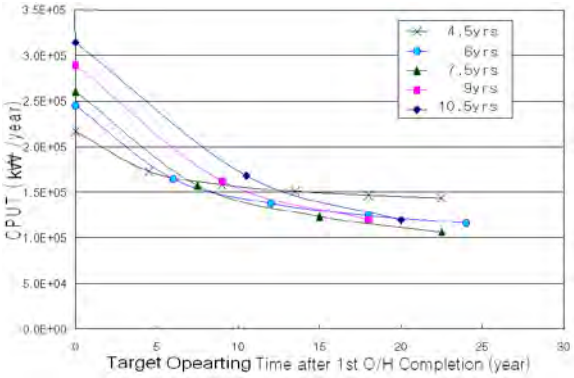

Fig. 9 CPU of unit vs. target time according to various overhaul cycles of scenario 1.

Table 3 presents CPUT variation according to replacement of principal components such as runner and generator. From the table, it is found that generator replacement has greater effect than runner replacement. When replaced with the runner and the generator to bring more economic benefits.

Table 3 CPUT variation according to replacement of runner and generator.

Component	Nothing	Runner	Generator	Runner & Generator
CPUT(kW/year)	1.2349×10^5	1.1611×10^5	1.1352×10^5	1.0491×10^5

Note) Scenario 1, Overhaul cycle: 7.5years, Target operating time: 15years

6. Conclusions

From the study to optimize overhaul cycle of pumped-storage power plants, the following findings are derived:

- As a result of this investigation, it is possible to extend the A class preventative maintenance cycle of pumped-storage power plants in South Korea.
- A methodology to optimize the preventative maintenance cycle based on the reliability and economic efficiency is presented, which can investigate variation of reliability and economic efficiency of generating unit vs. overhaul cycle.
- As a result of application of the methodology to an aged pumped-storage power plant in South Korea, the overhaul cycle has been extended from 4 years to 7.5years.
- When replaced with the runner and the generator to bring more economic benefits.

Acknowledgments

This work has been supported by KESRI-09310, which is funded by Korea Western Power Co. Ltd. and KHNP(Korea Hydro and Nuclear Power) Co., Ltd.

References

[1] http://news.naver.com/main/read.nhn?mode=LSD&mid=sec&sid1=0000070659.

[2] J.S. Kim, et al., Transaction of KSME, A, Vol.33, No.10, pp.1171-1176.

[3] Korea Western Power Co., Ltd., 2009, Planning Report to Optimize Preventative Maintenance of Pumped-Storage Power Plant.

[4] Korea Hydro & Nuclear Co., Ltd., 1976~2006, Electricity Generation Chronicles.

[5] K-Water, 2008~2010, Electricity Generation Chronicles.

[6] Japan Electricity Association, 2004, Investigation on Diagnosis Methods and Measures for Aging of Hydro Turbine.

[7] J.S. Kim, 2009, Overseas Business Trip Report for Investigation on Preventative Maintenance Situation of Japan Pumped-Storage Power Plant.

[8] EPRI, 1991, EPRI GS-7325.

[9] http://www.strategicorp.com/news%20case%20studies / rcm01.pdf.

[10] A.G. Vasilevski, et al., 1995, Power Technology and Engineering, Vol.29, No.1.

[11] EPRI, 1998, EPRI TR-111488.

[12] EPRI, 1999, Guidelines for RCM in the Hydro Power Industry, EPRI TR-114160.

[13] http://www.pinnaclesystems.us/solutions/manuf-reliability-mro-solutions/rcm-turbo.

[14] USACE, 1998, IWR Report 98-R-6.

[15] IEEE, 1984, IEEE Standard Reliability Data for Pump and Drives, Valve Actuators, and Valves, ANSI/IEEE Std 500-1984 P&V.

Risk assessment of river-type hydropower plants by using fuzzy logic approach

S.Kucukali[1,*]

[1] *Cankaya University, Department of Civil Engineering, Balgat, 06530 Ankara, Turkey*
** Corresponding author. E-mail: kucukali78@hotmail.com*

Abstract: In this paper, a fuzzy rating tool has been developed for river-type hydropower plant projects risk assessment and expert judgments have been used instead of probabilistic reasoning. The methodology is a multi-criteria decision analysis which provides a flexible and easily understood way to analyze project risks. The external risks, which are partly under the control of companies, have been considered in the model. The eleven classes of risk factors were determined based on the expert interviews, field studies and literature review as follows: site geology, land use, environmental issues, grid connection, social acceptance, financial, natural hazards, political/regulatory changes, terrorism, access to infrastructure and revenue. The relative importance (impact) of risk factors was determined from the survey results. The survey was conducted with the experts that have experience in river-type hydropower projects. The survey results revealed that the site geology and environmental issues were considered as the most important risks. The new risk assessment method enabled a Risk Index (R) value to be calculated, establishing a 4-grade evaluation system: low risk having R values between 1.2 and 1.6; medium risk, between 1.6 and 2; high risk, between 2 and 2.4; extreme risk, between 2.4 and 2.8. Applicability of the proposed methodology was tested on a real case hydropower project namely Kulp IV which was constructed on Dicle River in East Anatolia in Turkey. The proposed risk analysis will give investors a more rational basis on which to make decisions and it can prevent cost and schedule overruns.

Keywords: *Hydropower, Risk Analysis, Fuzzy Logic.*

1. Introduction

Renewable energy projects life cycle is full of various risks which will cause cost and schedule overrun or project failure. The surveys conducted by Gronbrekk et al. [1] and Komendantova et al. [2] identified the highest risk as political and regulatory changes for renewable energy projects in developing countries. Similarly, Ernst and Young [3] identified the most important business risk for 2010 as regulation and compliance.

Construction of river-type hydropower plants involves uncertainties because of various external factors such as site geology, grid connection, and environmental issues. These factors increase the construction costs and duration. For example, in one of the river-type hydropower plant in Turkey, namely Kulp IV, the cost of civil works increased by a factor of two because of unpredicted geologic structure at the tunneling site. In another example, the judges have ruled against hydroelectric power plants in 33 completed cases in Turkey, issuing a stay of execution decision or canceling the construction altogether because of the environmental issues.

In the literature there are several studies considering the risk analysis in construction projects [4] but risk analysis in renewable energy projects, especially for hydropower plants is very limited. In classical project risk analysis techniques, risk rating values are calculated by multiplying impact and probability values and direct analysis of these linguistic factors is often neglected [5]. Most existing risk analysis models, such as Monte Carlo simulation and tornado chart, are based on quantitative techniques which require numerical data. Kangari and Riggs [6] note that probabilistic models suffer from detailed quantitative information which is not normally available in the real construction world. However, much of the information related to risk analysis is not numerical [7]. Rather, this information is expressed as words or

sentences in a natural language. These conceptual factors can be expressed in linguistic terms that are, so called fuzzy information [8]. Uncertainty factors such as "poor geology" or "unstable policy" fall into this category. The aim of this paper is to introduce a new approach for hydropower projects risk assessment through the fuzzy set concepts.

2. Methodology

The eleven classes of risk factors were determined based on the expert interviews, field studies and literature review. The risk factors and their evaluation criteria are listed in Table 1. The risk factors are: site geology (geotechnical properties of the construction site), land use (right to use of the land for the construction of hydropower scheme), environmental issues (impact on ecosystem), grid connection (connection to the power system), social acceptance (impact on local community who use the river or the surrounding lands), financial (the status of the inflation and interest rate), natural hazards (earthquake, flooding and landslide), political/regulatory changes (level of political stability), terrorism (human-made disasters), access to infrastructure (road, electricity and water), revenue (cash flow). It should be noted that the financial, political/regulatory changes and terrorism were regarded as risks related to country conditions and their evaluation were done based on [9], [10].

In order to determine the relative importance (impact) of the risk factors, a survey was conducted with the experts from the banks and companies that have experience in the construction of river-type hydropower schemes. 14 experts were participated to the survey. The participants were asked to grade the importance of the risk factors regarding their importance and seriousness of concern. They graded the risk factors using a scale between 1-4, where 1 represents "low" and 4 "very high". The experts ranked site geology and environmental issues as the most important risks for river-type hydropower plants (Fig.1).

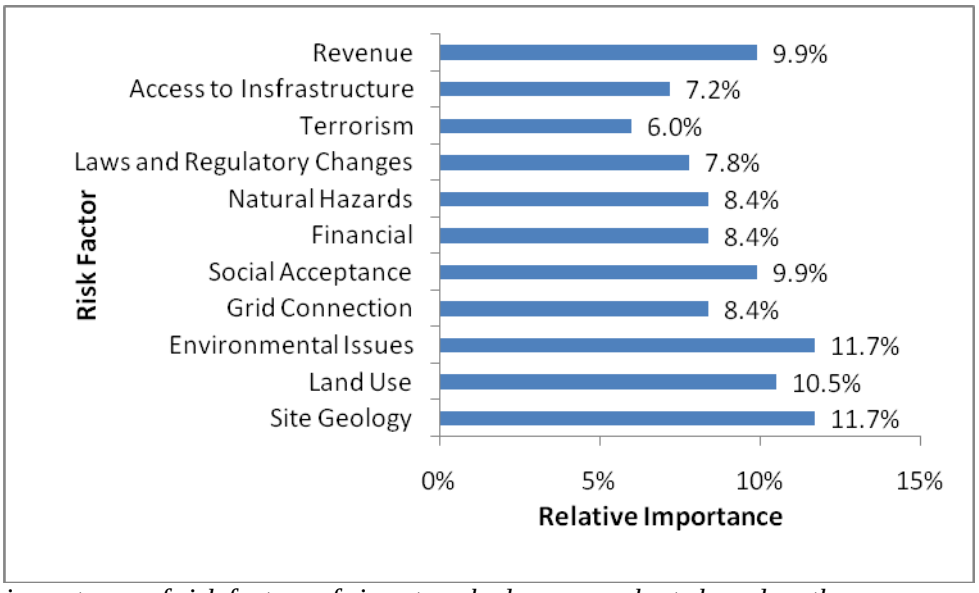

Fig.1 The importance of risk factors of river-type hydropower plants based on the survey results

Table 1. Evaluation criteria of risk factors in river type hydropower plants

Risk Factor	Score (1)	Score (2)	Score (3)	Score (4)
Site Geology	Rock mass quality is very good-good: RQD=%60-100	Rock mass quality is fair: RQD=%40-60	Rock mass quality is poor-very poor: RQD=%0-50	Soil with high ground water level
Land use	Property of Treasury	Forest	Private property: Agricultural land	Private property: Residential area
Environmental Issues	Project has detailed Environmental Impact Report	Project has Environmental Impact Report	Project has no Environmental Impact Report	Project is in an ecological sensitive area.
Grid Connection	Close to power system	Near to power system	Far to power system	Connection to the power system has some limitations
Social Acceptance	Project has detailed Social Impact Report	Project has Social Impact Report	Project has no Social Impact Report	Local community benefit from the river or the surrounding lands
Financial[a]	Economic performance of country is very high	Economic performance of country is high	Economic performance of country is medium	Economic performance of country is low
Natural Hazards	Low risk	Medium risk	High risk	Very high risk
Change in Laws and Regulations[a]	Political risk of country is low	Political risk of country is medium	Political risk of country is high	Political risk of country is very high
Terrorism[b]	Terror risk index of country is low	Terror risk index of country is medium	Terror risk index of country is high	Terror risk index of country is extreme
Access to Infrastructure	Very easy	Easy	Difficult	Very difficult
Revenue	Design discharge is high reliable	Design discharge is medium reliable	Design discharge is low reliable	Design discharge is unreliable

[a] country related risk and its evaluation is based on [9], [b] terrorism risk index is based on [10]

For each 11 parameter, an 1x4 input matrix was developed, each column corresponding scores 1- 4. If the score for a parameter is 3 and the input matrix (*I*) for the parameter is:

$$I = \begin{bmatrix} 0 & 0 & 1 & 0 \end{bmatrix} \quad (1)$$

Each parameter has an identical membership grading matrix. The fuzzy grading matrices were developed considering the degree of error a scoring observer may cause due to subjectivity and bias in the assessment process [11], [12]. Eq. (2) shows the fuzzy grading matrix (*FG*) used in this study:

$$FG = Score \begin{matrix} 1 \\ 2 \\ 3 \\ 4 \end{matrix} \begin{bmatrix} 1 & 0.4 & 0 & 0 \\ 0.2 & 1 & 0.2 & 0 \\ 0 & 0.2 & 1 & 0.2 \\ 0 & 0 & 0.4 & 1 \end{bmatrix} \quad (2)$$

The fuzzy assessment matrix (*FA*) was obtained by multiplying input matrices (*I*) with fuzzy grading matrix (*FG*) of the parameter,

$$FA_j = I_j \times FG_j \quad (j = 1\,to\,11) \quad (3)$$

where, j is the row number of the fuzzy assessment matrices. The membership degree matrix (*MD*) was obtained by multiplying weight of parameters (*w*) with fuzzy assessment matrix (*FA*) and summing the columns resulting in a one row matrix;

$$MD = w \times FA \quad (4)$$

A decision parameter computation was agreed upon f rom several scenarios considering membership degree versus attributes curves and formulation of Risk Index (R) was given as

$$R = \frac{1 \times A_{12} + 2 \times A_{23} + 3 \times A_{34}}{A_T} \quad (5)$$

where the area under the curve between the attributes i and j is named A_{ij} with: i =1,2, 3, and j = 2, 3, 4, . The total area under the curve is A_T. This enabled a R isk Index (*R*) value to be calculated, establishing a 4-grade evaluation system: Low risk having R values between 1.2 and 1.6; medium risk, between 1.6 and 2; high risk, between 2 and 2.4; extreme risk, between 2.4 and 2.8. The risk scale index represents the minimum and maximum values calculated by Eq.(5).

3. Investment Costs of Hydropower Schemes

Hydro power is the backbone of carbon dioxide free energy generation, about 22% of the world's electricity production comes from hydropower installations [13]. Hydropower plants can be classified into two categories: storage and river-type. In storage type hydropower plants, dams are used to retain river flow in a reservoir. A river-type hydropower plant diverts a portion of river through a channel or tunnel (Fig.2). River-type hydro power plants are dependent on the prevailing flow rate and can present problems of reliability if the flow varies greatly with time of the year or the weather [14]. Small hydropower (SHP) plants are mostly included in this category.

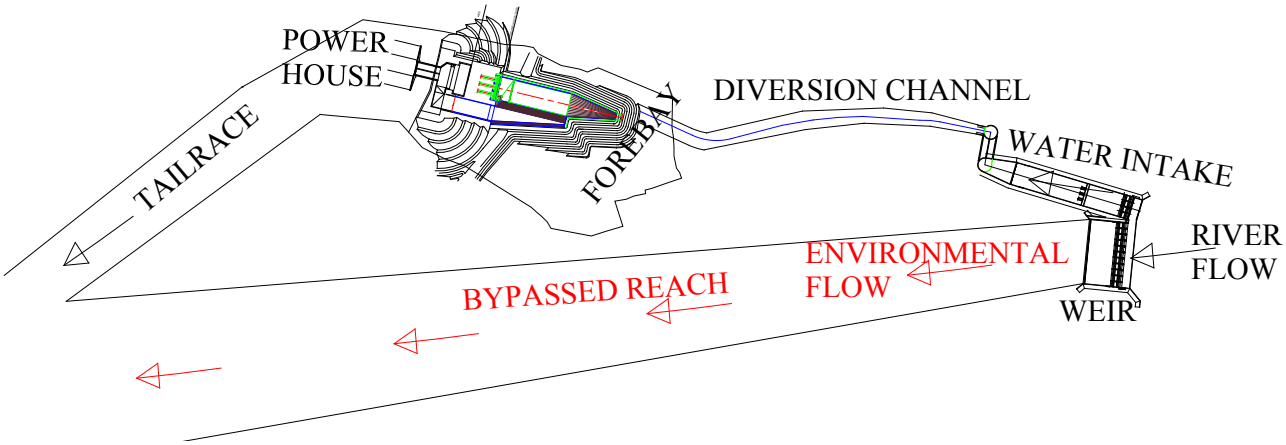

Fig.2 Site plan and components of a river-type hydropower plant

Hall et al. [15] determined the specific investment cost (total investment cost of the project divided by the installed capacity) of river-type hydropower plant in USA in the range of 2000-4000 $/kW. Also, they reported that the civil works account for 65-75% of capital cost. Each hydropower project is site specific that can explain the wide range of investment costs. Gordon [16] identified the main factors which can lead to cost overrun as the rate of inflation and site geology. The specific investment cost (SC) of a hydro power plant is the function of the net head (H) and installed capacity (P). It is well known from the literature that the SC increases as the head and installed capacity decreases [17], [18]. The investment cost a hydropower plant can be classified as follows: project design, land use and permits, financial, civil works, electro and hydro mechanical equipment, and grid connection (Table 3).

4. An Application of the Proposed Methodology

The developed risk assessment technique was applied to a real-time hydropower project namely Kulp IV which was constructed on Dicle River in Diyarbakır in East Anatolia. The characteristics of the project are as follows: Gross head=77 m, discharge=20 m^3/s, output=12.68 MW, energy=36.64 GWh/year, tunnel length=1885 m. Table 3 presents the investment cost analysis of Kulp IV hydropower plant. Actual cost of civil works and grid connection increased by a factor of two because of the poor geology and the technical demands by TEIAS, respectively. Table 4 shows the application of the risk assessment to the hydropower project. In the assessment fuzzy grading matrix provides more room for the justification of relationships between variables on the basis of fuzzy words. The project risk evaluation was done based on the criteria presented in Table 1. For example, Turkey has been ranked as extreme for Terrorism Risk Index by Maplecroft [9]. Therefore the risk factor of terrorism has a score of 4 for the project. Yet, project has no Environmental impact report, which yields the score of environmental issues as 4. By applying this method to other risk factors, the Kulp IV hydropower project Risk index was calculated as 2.26 which means project involves high risk.

Table 3. Analysis of the investment cost of Kulp IV hydropower plant (P=12.7 MW)

Description	Estimated Cost ($)	Actual Cost ($)	Rate of Increase	Share of Total Cost	Reason
Project design	1,090,000	1,180,000	8.3%	2.2%	Additional project designs
Civil works	12,500,000	25,700,000	105.6%	48.6%	Poor geology (serpentine) at the tunneling site
EME[a]	6,790,000	7,490,000	10.3%	14.2%	Under estimated costs of Technical equipment demand
HME[b]	8,900,000	4,800,000	-46.1%	9.1%	The prices of DSI are very high compared to the market.
Grid connection	2,600,000	5,400,000	107.7%	10.2%	Technical demands by TEIAS and length of the power supply line was increased
Land Use and Permits	2,200,000	2,600,000	18.2%	4.9%	The cost of the forest usage permit was not taken into account
Financial	3,100,000	5,700,000	83.9%	10.8%	Increase in interest rates because of the financial crisis

[a] Electro mechanical equipment, [b] Hydro mechanical equipment

Table 4. Fuzzy risk assessment rating tool application for Kulp IV Hydropower Plant

Risk Assessment																	
No	Risk Factor	Score	Relative Importance (W)	Input Matrix (*I*)				Fuzzy Logic Evaluation									
									Fuzzy Grading Matrix (*FG*)					Fuzzy Assessment Matrix (*FA*)			
														Membership Degree			
														1	2	3	4
1	Geology	3	0.117	0	0	1	0	*FG=f(I)*	0.00	**0.20**	**1.00**	**0.20**	*FA=FG*W*	0.000	**0.023**	**0.117**	**0.023**
2	Land Rent	3	0.105	0	0	1	0		0.00	**0.20**	**1.00**	**0.20**		0.000	**0.021**	**0.105**	**0.021**
3	Environment	3	0.117	0	0	1	0		0.00	**0.20**	**1.00**	**0.20**		0.000	**0.023**	**0.117**	**0.023**
4	Grid Connection	3	0.084	0	0	1	0		0.00	**0.20**	**1.00**	**0.20**		0.000	**0.017**	**0.084**	**0.017**
5	Social Acceptance	2	0.099	0	1	0	0		**0.20**	**1.00**	**0.20**	0.00		**0.020**	**0.099**	**0.020**	0.000
6	Financial	3	0.084	0	0	1	0		0.00	**0.20**	**1.00**	**0.20**		0.000	**0.017**	**0.084**	**0.017**
7	Natural Hazard	2	0.084	0	1	0	0		**0.20**	**1.00**	**0.20**	0.00		**0.017**	**0.084**	**0.017**	0.000
8	Political Changes	3	0.078	0	0	1	0		0.00	**0.20**	**1.00**	**0.20**		0.000	**0.016**	**0.078**	**0.016**
9	Terorism	4	0.060	0	0	0	1		0.00	0.00	**0.40**	**1.00**		0.000	0.000	**0.024**	**0.060**
10	Access to Insfrastructure	3	0.072	0	0	1	0		0.00	**0.20**	**1.00**	**0.20**		0.000	**0.014**	**0.072**	**0.014**
11	Revenue	3	0.099	0	0	1	0		0.00	**0.20**	**1.00**	**0.20**		0.000	**0.020**	**0.099**	**0.020**
Membership Degree Matrix (MD)														**0.037**	**0.335**	**0.817**	**0.211**
														0.19	**0.58**	**0.51**	**1.28**
														A_{12}	**A_{23}**	**A_{34}**	**A_T**
Decision Parameter (R)														**R = 2.26**		**High Risk**	

5. Conclusions

In this research, a new methodology is proposed for risk rating of river-type hydropower plant projects. The relative importance of the risk factors was determined from the expert judgments. The survey results showed that the most concerned risks are site geology and environmental issues. These results are in agreement with the Gordon [16].

Applicability of the proposed methodology has been tested on a real case. Findings of the case study demonstrate that the proposed methodology can be easily applied by the professionals to quantify risk ratings. The advantage of the proposed methodology is it will give investors a more rational basis on which to make decisions and it can prevent cost and schedule overruns. Forecasting the measure of risk of a river-type hydropower plant can be made by any decision maker with the help of the fuzzy rating tool described in this paper.

References

[1] Gronbrekk, W., Barton, H., and Khoury, R.H., International sustainability tools for hydropower role, relevance and industry reporting trends. Proc., Hydro 2010 C onf., Lisbon, Portugal, 2010.

[2] Komendantova, N., Patt, A., Barras, K. and Battaglini, A., Perception of risks in renewable energy projects: The case of concentrated solar power in North Africa, Energy Policy, 2011**,** In press.

[3] Ernst and Young, Business Risk Report, 2010. (www.maplecroft.com)

[4] Zavadskas, E.K., Turskis, Z., Tamosaitiene, J., Risk assessment of construction projects, J. Civil Engineering and Management, 16, 2010, 33-46

[5] Dikmen, I., Birgonul, M.T., Han, S., Using fuzzy risk assessment to rate cost overrun risk in international construction projects, Int J Project Management, 25, 2007, 494-505.

[6] Kangari, R. and Riggs, L.S., Construction risk assessment by linguistics, IEEE Transactions on Engineering Management, 36, 1989, 126-131.

[7] Mustafa, M.A., and Al-Bahar, J.F., Project risk assessment using the analytic hierarchy process, IEEE Transactions on Engineering Management, 38, 1991, 46-52.

[8] Kucukali, S., Baris, K., Turkey's short-term gross electricity demand forecast by fuzzy logic approach, Energy Policy, 38(5), 2010, 2438-2445.

[9] ECR-Euro Money Country Risk, 2010. (www.euromoney.com)

[10] Maplecroft , Terrorism Risk Index, 2010. (www.maplecroft.com)

[11] Karakaya, S.T., Coastal Scenic Evaluation by Application of Fuzzy Logic Mathematics, Msc. Thesis, METU,The Graduate School of Natural and Applied Sciences, Dept.of Civil Eng., Ankara, Turkey, 2004.

[12] Sahin, F., Scenic Evaluation of the Western Black Sea Coasts Using Fuzzy Logic, Msc. Thesis, ZKU, Graduate Sc. Of Natural and App. Sci., Dept. of Civil Eng., Zonguldak, Turkey, 2008 (inTurkish).

[13] Boyle, G., Renewable Energy: Power for a Sustainable Future. Oxford University Press, 2004.

[14] Kucukali, S. and Baris, K., Assessment of small hydropower (SHP) development in Turkey: Laws, regulations and EU policy perspective, Energy Policy, 37, 2009**,** 3872-3879.

[15] Hall, D.G., Hunt, R.T., Reeves, K.S. and Carroll, G.R., Estimation of Economic Parameters of U.S. Hydropower Resources, Idaho National Engineering and Environmental Laboratory, 2003.

[16] Gordon, J.L., Hydropower costs estimates, J Water Power Dam Constr, 35, 1983, 30-37.

[17] Gordon, J.L. and Noel, C.R., The economic limits of small and low-head hydro, J Water Power Dam Constr, 38, 1986, 23-26.

[18] Aggidis, G.A., Luchinskaya, E., Rothschhild, R. and Howard, D.C., The costs of small-scale hydropower production: Impact on t he development of existing potential, Renewable Energy, 35, 2010, 2632-2638.

Pump as turbine: dynamic effects in small hydro

Pedro A. Morgado[1,*], Helena M. Ramos[2,**]

[1, 2] *Civil Engineering Department and CEHIDRO, Instituto Superior Técnico, Technical University of Lisbon, Portugal.*
** Av. Rovisco Pais, 1049-001, Lisbon, Portugal , E-mail: plmorgado@gmail.com*
*** Av. Rovisco Pais, 1049-001, Lisbon, Portugal , E-mail: helena.ramos@civil.ist.utl.pt*

Abstract: This work focuses on the hydraulic aspects of a Pump as Turbine (PAT) when subjected to different working conditions, including accidental situations. This will provide useful information for the choice of the most adequate solution and will ensure a correct design and safe operation of the installed equipments. This work is supported by experimental data obtained in a series of tests performed at the university's laboratory and by calibrated computational modelling. The obtained data was used to perform a sensitivity analysis on the relation between discharge variation, runaway time and rotational speed and make inferences about the expected peak overpressure in an accidental situation. Based on the results, the hydropower system may be characterized by a relevant set of calculated parameters that are of extreme utility in the construction and calibration of a computational model capable of accurately predicting different scenarios and alternatives.

Keywords: *Dynamic effects; Reversible hydro; Safety solutions; Hydraulic transients.*

1. Introduction

In the operation of hydropower systems it is inevitable the occurrence of variations in the flow, being true either in routine manoeuvres, either in accidental or exceptional unforeseen events. To ensure the safety and reliability throughout the system life, it is very important that these dynamic effects and the associated risk factor are considered in the early stages of each design and the overpressures are accurately estimated [1, 2]. A detailed analysis for each operating situation is vital for understanding the dynamic behavior of hydro-mechanical equipment and their interaction with the flow and hydraulic circuit. This study is based on a parametric characterization of the different components of a hydro system as a support for a CFD modeling.

2. Methodology

2.1. Simulation-based modelling

2.1.1. Method of Characteristics

The quantitative analysis of unsteady flow through long conveyance systems is based on the fundamental hydrodynamic principles described by the dynamic (Eq. (1)) and continuity (Eq. (2)) equations [3]:

$$\frac{\partial V}{\partial t} + g\frac{\partial H}{\partial x} + \frac{fV|V|}{2D} = 0 \qquad (1)$$

$$\frac{\partial H}{\partial t} + V\frac{\partial H}{\partial x} + \frac{c^2}{g}\frac{\partial V}{\partial x} = 0 \qquad (2)$$

The previous equations can be used given the following conditions: the fluid in the pipe is homogeneous and mono-phase; the flow is mainly one-dimensional and the velocity profile is considered uniform through the cross-section of the pipe; the pipe axis remains static; the fluid and the pipe walls have physical linear elastic properties. For each calculation time step,

each pipe will be divided in a finite number of stretches bounded by the calculation sections building the rectangular mesh presented in Figure 1.

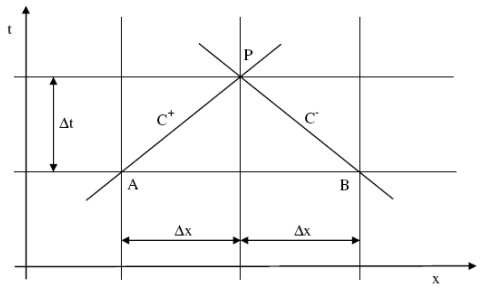

Figure 1 - Method of characteristics calculation grid.

The positive and negative characteristic equations can be written as follows:

$$Q_P = C_P - C_a H_P \tag{3}$$

$$Q_P = C_n + C_a H_P \tag{4}$$

in which:

$$C_P = Q_A \frac{gA}{c} H_A - \frac{f\Delta t}{c} Q_A |Q_A| \tag{5}$$

$$C_n = Q_B \frac{gA}{c} H_B - \frac{f\Delta t}{c} Q_B |Q_B| \tag{6}$$

and:

$$C_a = \frac{gA}{c} \tag{7}$$

Eq. (3) and Eq. (4) are only valid along the positive and negative characteristic lines, respectively. The values of C_P and C_n are known for each time step, although for the interior points of the mesh there are two unknowns, Q_P and H_P. These values can be determined by solving simultaneously Eq. (3) and Eq. (4):

$$Q_P = 0.5(C_P + C_n) \tag{8}$$

At both ends of each pipe it is only possible to define one characteristic line, so in order solve the system another equation is needed. This additional information may be obtained through the introduction of a boundary condition. Depending on the simulated system this boundary may be another pipe (with different characteristics), a reservoir, a turbine, a pump, a valve, a protection device or any other component analytically describable.

2.1.2. Turbine

The functioning of a turbogenerator can be characterized by a specific valve-type with adapted characteristics associated to customized closure maneuvers. Even though this solution may roughly simulate the vast majority of systems and situations, it does not consider the

specific parameters of the turbine, nor does it consider the overspeed of the turbine wheel and its complex interaction with the conveyance system. On this matter an innovative formulation was proposed for the simulation of the dynamic behavior of a turbogenerator based on a set of significant parameters that characterize a turbogenerator, allowing the evaluation of overspeed induced extreme upsurges and its propagation along the hydraulic circuit [4, 5, 6, 7, 8, 9] . This methodology simulates the turbine as a hydraulic resistive element, where the head lost by the flow is characterized by the basic formula of a hydraulic orifice equipped with dynamic discharge and rotational speed coefficients:

$$Q_P = C_g Q_R \left[1 + \frac{\alpha_R - 1}{\beta_R - 1} \left(\frac{N}{N_R} \sqrt{\frac{H_R}{H_u}} - 1 \right) \right] \sqrt{\frac{H_u}{H_R}} \tag{9}$$

in which q_P and h_P are respectively the relative flow through the orifice and available head at a certain time step. The factor C_g is the gate opening coefficient that defines the maximum discharge for a given head and rotational speed, as a function of the gate opening. The factor C_S accounts for the runner's rotational speed, adjusting the flow in each time step accordingly with the following formulation:

$$C_S = 1 + \frac{\alpha_R - 1}{\beta_R - 1} \left(\frac{n}{\sqrt{h}} - 1 \right) \tag{10}$$

where n stands for the dimensionless value of the rotational speed. The parameters $\alpha_R = \frac{Q_E}{Q_0}$ and $\beta_R = \frac{N_E}{N_0}$ are established for each turbomachine and represent the relation between the runaway situation and rated conditions, respectively for the flow and rotational speed. These values may be obtained from the manufacturers of the turbo equipments. The variation of the rotational speed for each time step depends on the inertia of the rotating masses, I, and the equilibrium between the hidraulic torque, T_H, and the magnetic torque, T_M. This relation may be expressed through the rotating mass equation:

$$\frac{d\omega}{dt} = \frac{60}{2\pi} \left(T_H - T_M \right) \tag{11}$$

in which ω is the angular speed (rpm). From Eq. (11), it is possible to conclude that for T_M = 0, the acceleration of the runner depends only on the hydraulic torque (T_H) and the inertia of the rotating masses, I. The hydraulic torque actuating in the rated operating conditions is given by the following equation:

$$B_{H,0} = \left(\frac{60}{2\pi} \right) \frac{\gamma \eta_0 Q_0 H_0}{N_0} \tag{12}$$

in wich η_0 = rated efficiency; Q_0 = rated flow; H_0 = rated net head; N_0 = rated runner speed. Assuming a linear variation of the discharge with the rotating speed under runaway conditions, the hydraulic torque at each timestep may obtained by multiplying the initial torque by a corrective factor, b, given by the following equation where $e = \frac{\eta}{\eta_0}$:

$$b = \frac{B_H}{B_{H,0}} = h^{3/2} C_g \frac{e}{n}\left[1 - \frac{\frac{n}{\sqrt{h}} - 1}{\beta_R - 1}\right] \tag{13}$$

The evaluation of the efficiency is a complex matter that depends on a vast set of parameters. This value may be considered to vary accordingly to the following approximate equations [4, 9].

$$\begin{cases} \eta_0 \dfrac{N}{N_0} & \text{for } N<N_0 \\ C_g\left(\dfrac{N_E}{N_E - N_0} - \dfrac{N}{N_E - N_0}\right)\eta_0 & \text{for } N>N_0 \end{cases} \tag{14}$$

2.1.3. Pumping system

The pump operation may be accurately simulated using the method of characteristics incorporating specific boundary conditions. Pump manufacturers generally provide the characteristic curves for their pumps as a function of the wheel diameter. These curves relate flow, manometric head, efficiency and power for a specific rotational speed and can be approximately represented in the first quadrant of operation (H,Q) by a second degree polynomial (Eq. (15)) [10]. Should this methodology be applied, a check valve should be installed at the downstream pump section to avoid reverse flow.

$$H_0 = AN^2 + BNQ - CQ^2 \tag{15}$$

The values A, B and C are constants and can be estimated from three known pairs of values (*Q, H*) of the pump characteristic curve. If correct data is available, a higher degree polynomial may be considered to enable a multi operating zone simulation. Although pump characteristic curves in the pumping zone operation are usually easy to obtain, the same is not true for the remaining zones. Figure 2 presents a schematic of a pump with the upstream and downstream connecting pipes and hydraulic grade line.

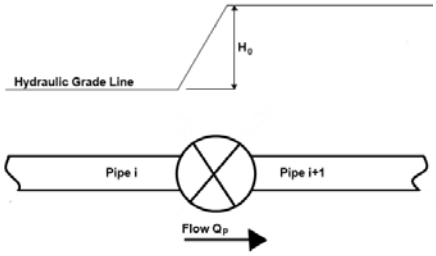

Figure 2 - Schematic drawing of a pump.

Referring to Figure 2 and considering the continuity equation, the relation, $Q_{P,i} = Q_{P,i+1}$, can be written. If the losses at the junctions are neglected, Eq. (16) gives the relation between head and discharge, in which *N* is the rotational speed:

$$H_{P,i+1} - H_{P,i} = AN^2 + BNQ - CQ^2 \tag{16}$$

when $A_i = A_{i+1}$, substituting Eqs. (3) and (4) into Eq. (16) the following polynomial is obtained, which can be solved for Q_P.

$$CC_a Q_P^2 + (BNC_a - 2)Q_P + \left(AC_a N^2 + C_n + C_P\right) = 0 \quad (17)$$

Once the flow Q_P is known, the heads $H_{P,i}$ and $H_{P,i+1}$ can be calculated for each time step. The total or partial shutdown of the pump as the cause of severe transient regimes may also be simulated. In this case the variation of the runner speed is given by Eq. (11) in which the hydraulic torque can be calculated based on efficiency data provided by the manufacturer.

2.1.4. Valve

Valves are installed in hydro systems to regulate the flow (or the pressure) by opening, closing or partially obstructing the pipe section. They can also be utilized to isolate system components in order to enable maintenance procedures or even their replacement. Figure 3 presents the schematic of a valve in hydraulic ciruit.

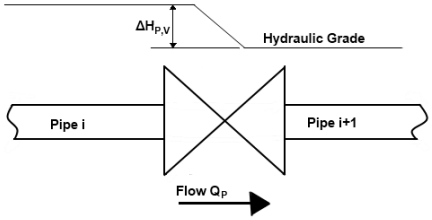

Figure 3 - Schematic of a generic valve.

The boundary condition for a valve can be written based on steady state head loss equation. The flow through the valve, Q_P, remains constant and the head loss can be written as the difference between the head at upstream and downstream valve section:

$$\Delta H_{P,V} = H_{P,i} - H_{P,i+1} = K_V \frac{Q_P^2}{2Ag} \quad (18)$$

in which K_V is a head loss coefficient obtained experimentally that depends on the Reynolds number, the type of valve and its opening at each time step. Substituting Eq. (3) or (4) in Eq. (18) a second degree polynomial equation is obtained:

$$\frac{K_V C_a}{2gA^2} Q_P^2 + 2Q_P - \left(C_P + C_n\right) = 0 \quad (19)$$

Solving for Q_P, the flow through the valve is obtained for each instant of simulation and subsequently the upstream and downstream head. For the situation where the valve is fully open, the head loss may be neglected and the flow can be determined by solving Eq. (8) or a fixed value should be considered. For the determination of the parameter K_V, a set of empirical results for each type of valve is presented in [11].

2.2. Model validation

Some supporting experimental tests were carried out in the Hydraulic lab of DECivil/IST, in order to analyze the behaviour of a reaction type turbomachine in different operation conditions. The hydraulic circuit is composed by a pipe of High-density polyethylene (HDPE), with an internal diameter of *0.043 m* and a length of *100 m*, which connects the pressurized vessel to the turbomachine. At the downstream end the water is discharged into a free surface tank. Both the air vessel and the free surface reservoir are responsible for

imposing a constant head respectively on t he upstream and downstream section. An intercalated pump is responsible for setting a recirculated constant flow. The turbomachine is a horizontal, single-stage pump-as-turbine, PAT*, KSB model Etanorm 32-125*. The generator was connected to the national grid via a l arge electrical transformer. Figure 4 presents a comparison between experimental pressure head variation and the corresponding simulation in the event of a full load rejection followed by a valve actuation.

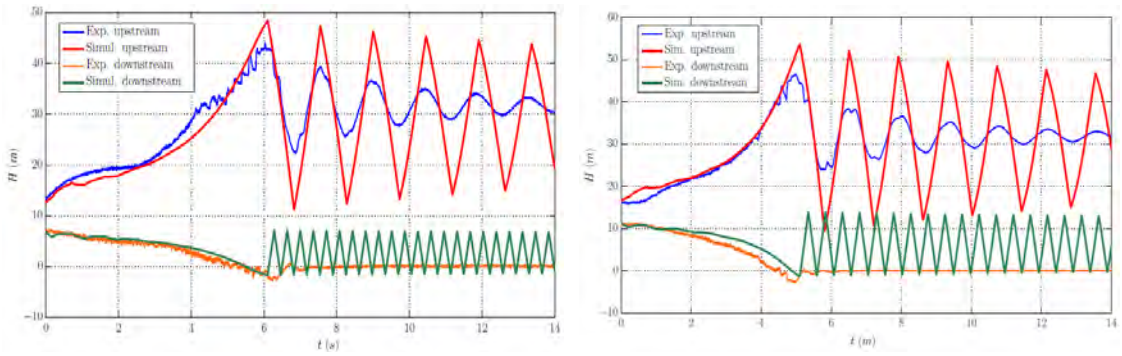

Figure 4 - Comparison between simulation and experimental results for Q = 4.2 l/s and Q=3.9l/s

3. Overspeed and dynamic effects

Based on a general hydropower system, a detailed analysis of the runaway effect without the interference of the closure of the flow control shutter (e.g. guidevane) or any special protection device was established. This was done in order to fully isolate and better understand the phenomenon under analysis. Under these conditions several independent computer simulations were carried out for a broad set of pairs of values of inertia, I, and specific speed, n_S. Figure 5 shows the upsurge on the upstream section of a turbine for the different combinations of parameters. For the lower values of n_S, the overspeed results in a flow reduction, causing an upsurge in the hydraulic system. On the other hand, turbines with high specific speeds are associated to an increase in flow when a load rejection occurs, resulting in sub-atmospheric pressures in the pipeline.

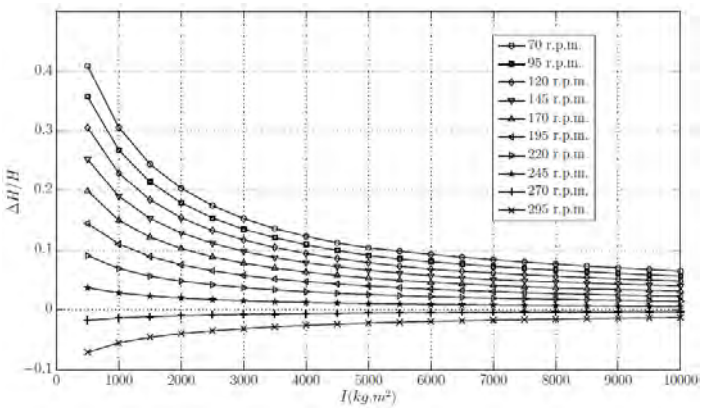

Figure 5 - Extreme relative pressure head as a function of I and n_S.

4. Load rejection and closure of flow control device

From the different emergency operations a hydropower system endures throughout its service life, the full load rejection followed by the actuation of a discharge shutter may stand among the most severe situations. Considering the same turbomachine used in the paragraph 3, the influence of the length, L, of the pipeline and its interaction with the safety valve closure time, t_C, was studied. For this purpose, a set of simulations were carried out in order to

calculate the maximum upsurge for different combinations of values, obtaining the results presented in Figure 6.

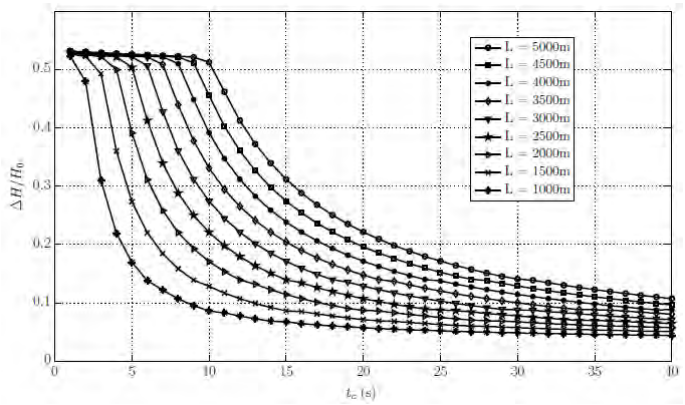

Figure 6 - Maximum relative overpressure for different combinations of L and t_C.

For all pipeline lengths, when approaching the elastic time constant, T_E, the maximum values of ΔH rise very quickly. It should be noted that below a certain value of t_C, for each different penstock length, all the curves tend to a common maximum value. This is the domain of what is called a fast manoeuvre, $t_C < T_E$, in which the transient peak overpressure depends only on the celerity of the elastic waves, c, and the mean flow velocity, U_0, given by the Frisel-Joukowsky formula.

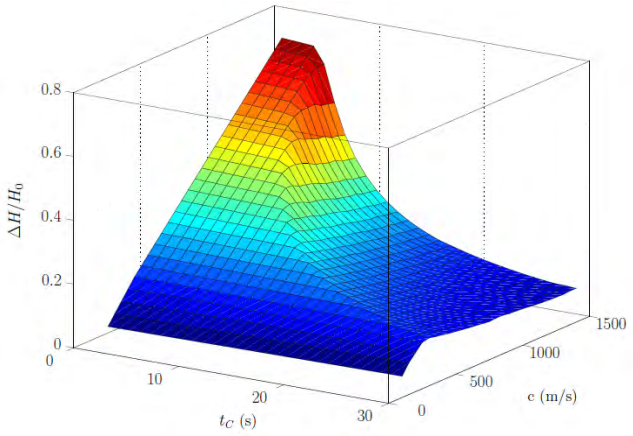

Figure 7 - Maximum relative overpressure for different combinations of c and t_C

Figure 7 was generated by utilizing the developed computational model, to show the maximum overpressure reached for different combinations of values of the celerity, c, and closure durations, t_C, for a fixed penstock length $L = 4000m$. When observing closely, it becomes evident that the classification of a closure manoeuvre as fast ($t_C < T_E$) or slow ($t_C > T_E$) is a relative concept that depends on the celerity of the elastic waves, thus on the pipe properties. In fact, the lower the value of c, the bigger the value of t_C must be in order to perform a slow closure manoeuvre. For a slow manoeuvre, the maximum pressure head depends essentially on the mean fluid velocity and on the flow control valve closure time. The maximum value can be estimated based on the by Michaud formula. Unlike what happens in a fast manoeuvre, the maximum overpressure is independent from the wave speed celerity.

5. Results

Both the experimental and the simulation results demonstrate the turbine load variation, in particular the runaway condition has a relevant impact on the discharge and, given the right circumstances, can be the sole cause of severe transients in hydropower systems. This is

especially evident for certain combinations of values of n_S and I that can result in a significant flow reduction during a short time interval. The comparison between the developed model and the experimental test results suggests a good estimation for the maximum transient overpressures, presenting conservative values valid for hydro and pumping design. This formulation based on modular linkable components proved to be flexible enough to allow the easy setup of a v ast set of different scenarios that are able to simulate the majority of situations. This methodology has the ability of predicting the runner overspeed of turbogenerators, as well as pumping stoppage and its effect on the flow along the pipe system.

References

[1] Ramos, H., Guidelines for Design of Small Hydropower Plants. Book published by WREAN (Western Regional Energy Agency and Network) and DED (Department of Economic Development - Energy Division). Número de páginas: 205. Belfast, North Ireland. ISBN 972-96346-4-5, 2000.

[2] Morgado, P.; Ramos, H., "Renewable Energy Production Integrated in Water Supply Systems: Dynamic Effects Analysis*" in Seminario Iberoamericano sobre Planificación, Proyecto y Operación de Sistemas de Abastecimiento de Agua,* Valência (Espanha), 24-27 de Novembro de 2009 (in Portuguese).

[3] Streeter, VL e Wylie, EB, *Hydraulic Transients*. New York, McGraw-Hill Book Co., 1967.

[4] Ramos, H., Simulation and Control of Hydraulic Transients in Small Hydro. Modelling and Analysis of Induced Effects by Turbogenerator Overspeed (in Portuguese). Ph. D. Dissertation in Civil Engineering. Portugal, Instituto Superior Técnico, 1995.

[5] Ramos, H.; Almeida A.B, *Experimental and C omputational Analysis of Hydraulic Transients Induced by Small Reaction Turbomachines* (in Portuguese). APRH, LNEC. Lisboa, 2001.

[6] Ramos, H., Unconventional Dynamic Effects in Pressurized Hydraulic System (in Portuguese). Support document for the subject Transients in Elevation and Hydroelectric Systems from the PhD in Hydraulics and Water Resources. IST, DECivil, 2004.

[7] Ramos, H. and Almeida, A. B., Parametric Analysis of Waterhammer Effects in Small Hydropower Schemes. HY/1999/021354. ASCE - Journal of Hydraulic Engineering. Volume 128, 7, pp. 689-697, ISSN 0733-9429, 2002.

[8] Ramos, H; Almeida, A. B., Dynamic orifice model on waterhammer analysis of high and medium heads of small hydropower schemes. Journal of Hydraulic Research, IAHR, Vol. 39 (4), pp. 429-436, ISSN-0022-1686, 2001.

[9] Morgado, P.; Ramos, H., "Dynamic Effects Analysis in Hydropower Systems" (in Portuguese), 10º Congresso da Água (Portugal), 2010

[10] Ramos, H., Support document for the subject Elevation and Hydroelectric Systems Subject of the Hydraulic and Water Resource Msc. IST, DECivil, 2003.

[11] Lencastre, A. – General Hydraulic (in Portuguese). Hidroprojecto, 1983.

Acoustic impact of an urban micro hydro scheme

Neil Johnson[*1], Jian Kang[1], Steve Sharples[1], Abigail Hathway[2], Papatya Dökmeci[1]

[1] *School of Architecture, University of Sheffield, Sheffield, UK*
[2] *School of Civil and Structural Engineering, University of Sheffield, Sheffield, UK*
** Corresponding author. Tel: +44 7534916870, E-mail: arq09nj@sheffield.ac.uk*

Abstract: Micro hydro systems can be regarded as a renewable energy source resulting from the natural hydrological cycle, it is by some considered sustainable due to the lack of impoundment of water and assumed negligible environmental impact. Experience with wind energy has highlighted that as the uptake of renewable energy technologies increases so government policies need to keep pace if public complaints and rejection of these technologies is to be averted. Studies on micro hydropower, particularly in an urban setting where propagation of noise is a planning issue, have been very limited. This paper focuses on the acoustic environmental impacts of micro hydropower considering a Reverse Archimedean Screw (RAS). Acoustic samples were taken directly above the RAS, and on a 5m interval along a transect and then at, 30m and 60m along another transect. Two further transects were considered and sampling was made at 30m and 60m. Initial results indicate that during normal operation at 25kW the screw would be barely perceptible beyond 60m; the weir provides significant masking of the turbine noise. It also shows that the noise generated is directional in nature at this site.

Keywords: *Micro hydro, Acoustics, Noise, Renewable energy, Environmental impact.*

1. Introduction

It is widely recognised that worldwide energy demand and use is continuing on an apparent, unceasingly ascending trend as, rapid population growth, economic development and therefore inherent demand for fuel increases [1, 2]. The world energy mix is depicted by the International Energy Agency (IEA). According to their *World Energy Outlook* (2008) [3]; renewables accounted for around 13% of global energy in 2006. This figure is predicted to rise to around 14% in the IEA 2030 reference scenario; and 24% in the IEA 450 (2030) policy scenario (based on policies under consideration). Oil and gas shares are predicted to be around 50% in both 2030 scenarios whilst coal lost some of its market share to an increase in the use of renewables (including biomass and waste), and nuclear energies.

The role of hydropower as a renewable resource varies dependent on the scale of the installation. As discussed by Frey and Linke [5], many legislative organisations do not consider large-scale hydro power to be a renewable resource when determining eligibility for government support. However, as argued in the paper, this is not a question of renewability but of sustainability. Although micro and pico hydro systems are assumed to be more environmentally friendly due to the lack of impoundment of water and assumed negligible environmental impact [4-6] emerging literature indicates that detrimental environmental impacts can be caused by smaller scale schemes [4].

Paish (2002) [4] indicates that small scale hydro developments in Europe will be the main area for hydro development in the future as the majority of large scale sites have already been exploited and micro hydro schemes seem to be growing in development and government support in the UK [2, 6]. In the urban setting, the issue of noise generation from visible systems can be a significant factor in the viability of the scheme, and the time period over which it is run. As part of a wider on-going research on the above issues, this paper will focus on initial results from a study of the impacts of a hydro scheme on the acoustic environment.

As there is recognised potential for hydro schemes in cities due to existing infrastructure, it would appear that there is need for such a study.

Three sites (semi-rural) within the UK using a Reverse Archimedean screws (RAS) to generate electrical power have already been identified as causing a noise nuisance. However, this tends to be associated with poor installation/design faults rather than general noise nuisance during normal operation. Any noise nuisance, whether design faults or operational, may be escalated within a densely populated and built-up urban setting. If micro-hydro is to penetrate into our cities then noise evaluation will become a key issue in the planning and design of such schemes. An extensive but not exhaustive literature search has demonstrated that this type of research has yet to be undertaken. Government policies may need to change to support these technologies and make them more viable; however, evidence is required to enable the government to establish the true impact on the environment of such technologies.

It is known that hydropower sites are most efficient at a particular speed, head and flow [4]. However, the relationship between the power output, river flow and sound power levels is not known. The following study will present measurements taken in the field to evaluate the sound generated from a RAS scheme in New Mills, running at a power output of 25kW, with a total head of 3+ metres, and in comparison to the existing sound produced by water flowing over a weir.

2. Methodology

Acoustic measurements were carried out around a 2.6 x 11m tri-blade RAS, with a fixed rotation of 28.03min^{-1} generating at 25kW and a river flow of around 2.17cumecs, located in a parkland setting, within an urban environment. *Figures 1 and 2* show plans, and photos of the site respectively. There do not appear to be any standards, or current methods for acoustic sampling of micro hydro turbines in the field in the UK possibly the world. It was therefore prudent to utilize BS 7445 and BS 4142 and the field site's complex geography to design a sampling strategy. Acoustic samples were taken along transects shown in *figure 1*. All samples were taken at 1.4m above the ground surface and where possible over 3m away from any facades. Acoustic samples were also taken directly above the RAS to enable the sound power level to be derived. On transects (a), (b) and (c) samples were taken at 30m and 60m from the RAS. Transects (b) and (c) also included a sample at 90m. Samples were then taken at 5m intervals along transect (d). Sampling directly to the side of the RAS was deemed unsuitable due to the presence of a wall. *Figure 2* is a photo of the site taken from above; the right hand image shows the bridge from which it was taken

After numerous visits, it was determined that the site's acoustic characteristics do not alter significantly over time. However, a sample of the acoustic environment was carried out using WinMLS (Windows Maximum Length Sequence), at a fast sampling rate to determine the required acoustic sampling time at each sampling instance. Two minute samples were deemed sufficient for this study.

In addition to the acoustic sampling, *figure 1 also,* shows the location of two pressure gauge sensors, which have been installed to allow future work on river flows, efficiency and acoustic impacts of the turbine at this site.

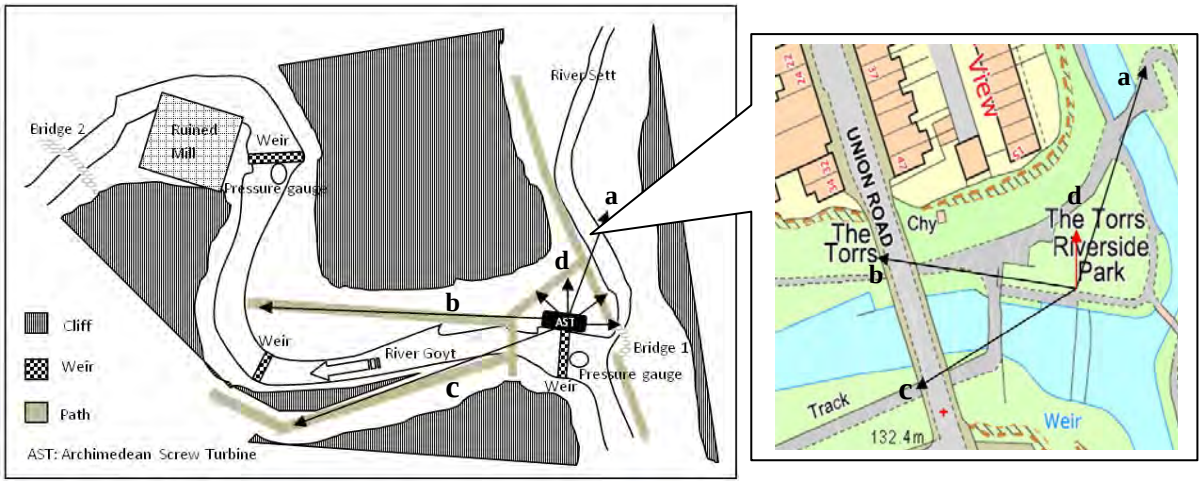

Figure 1. Location of the RAS studied, including the positions of the sampling transects (arrows) a, b and c, short red arrow is transect d. also shown is the positions of the pressure gauge sensors (for future work), and the location of the injection (Bridge 1), and sampling points (Bridge 2)

Figure 2. (Left) plan view photo of the RAS at New Mills and (right) a photo looking across the top of the weir to the angled transect (left-hand arch) and same axis (second arch in from right) NB: the bridge is indicative of the stone cliff heights around the site.

Sound Pressure Level (SPL) samples were taken (unweighted Leq) at each point along the transects using Class 1, MP231 microphones and WinMLS 2008. This was repeated when the RAS was running, and when all the water was diverted over the weir and the fish pass. A laser range finder and tape measure were used to give accurate distance of the sampling points from the weir and RAS for accurate sound propagation calculations and soundscape analysis. Processing of the acoustic samples was undertaken in the lab using WinMLS 2008. The main acoustic assumption is that the background soundscape is the same as when the screw is operational.

3. Results & Discussion

It is noted that in this paper, only limited results available are presented, and further measurements are being made. However, the results are of interest as there is no known data published for the sound propagation from RASs in the literature.

At a distance of 90m, the effects of other weirs downstream from the site were found to mask the sound from the RAS. Therefore, data from the 90m samples are not analysed further. *Figure 3* shows the SPL at increasing distances from the RAS along transect (d). As expected,

higher frequencies attenuate at a greater rate, see *figure 3*. The attenuation along distance is significant, and at a typical frequency, 500Hz, the SPL attenuation is about 10dB.

Observations of 1/3 octave plots and signals, *figures 4, 5 and 6* and recordings from the near field, transect (d); indicate a near white noise soundscape environment. By this, it is meant that the sound environment sounds like white noise. This near white noise is generated mainly by the water falling over the broad crest weir. Further to this a noticeable drop in amplitude in the signal can be observed with distance and between on and off, though less so. The spectrum plots of zero metres from screw, *figure 4*, indicate that there is a 3dBA difference between the screw being off and on which in acoustic terms contributes a barely legible amount [7].

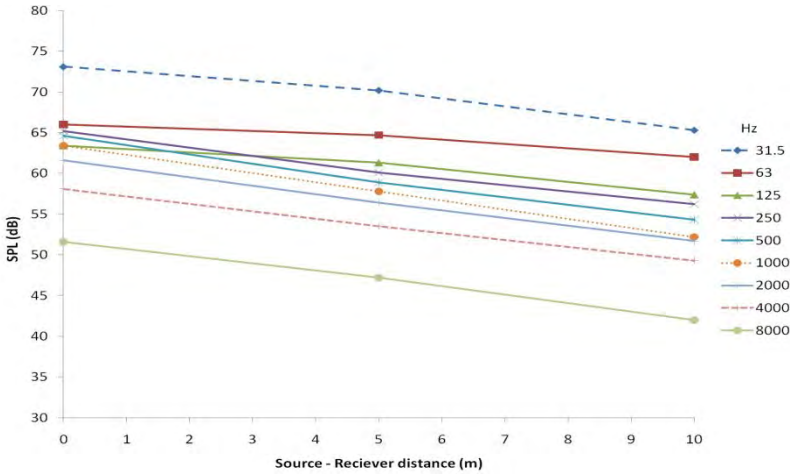

Figure 3. Background SPL when the flow is diverted from the RAS over the weir. Measurements taken along transect d (red arrow, figure 1) of SPL at a range of frequencies with increasing source - receiver distance.

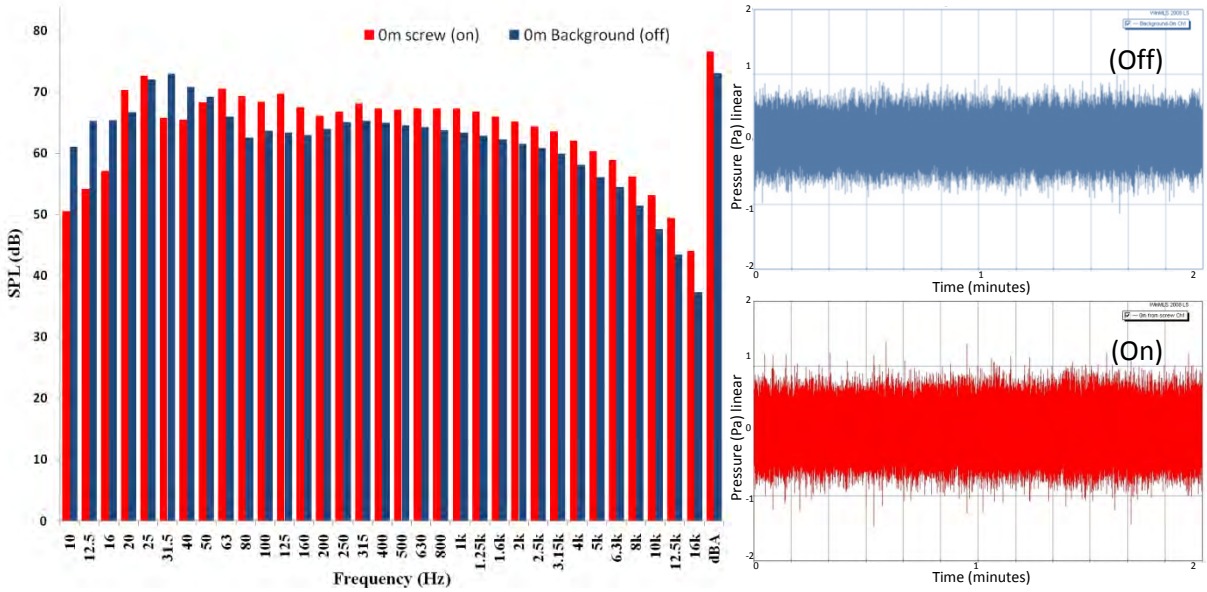

Figure 4. 1/3 octave spectrum plots of the SPL with 2 minute signal, when the RAS is operational at 25kW (red) and when the RAS is off, flow is diverted over the weir (blue) taken from directly above the RAS zero metres from screw.

At lower frequencies, the SPL with the RAS being off is 7-10dB higher. This might be due to the reduced volume of water falling over the weir when the RAS is running at 25kW,

reducing the low frequency component as less water falls into the weir pool. This may also explain the increase in SPL in the mid ranges. A similar pattern can be observed in the plots of samples taken 5m from the RAS, *figure 5*; and again at 10m, *figure 6*. However, there is less of a difference between the dBA results; with a difference of around 1dB and the mid to high frequency ranges being of a similar nature. However, lower frequencies are higher in amplitude during the background sampling than when the screw is operational, which may also be due to reflections from surrounding walls or being more exposed to the weir through an opening in the wall next to the screw and a function of directivity. *Figures 4-6* show a decrease in signal amplitude with distance.

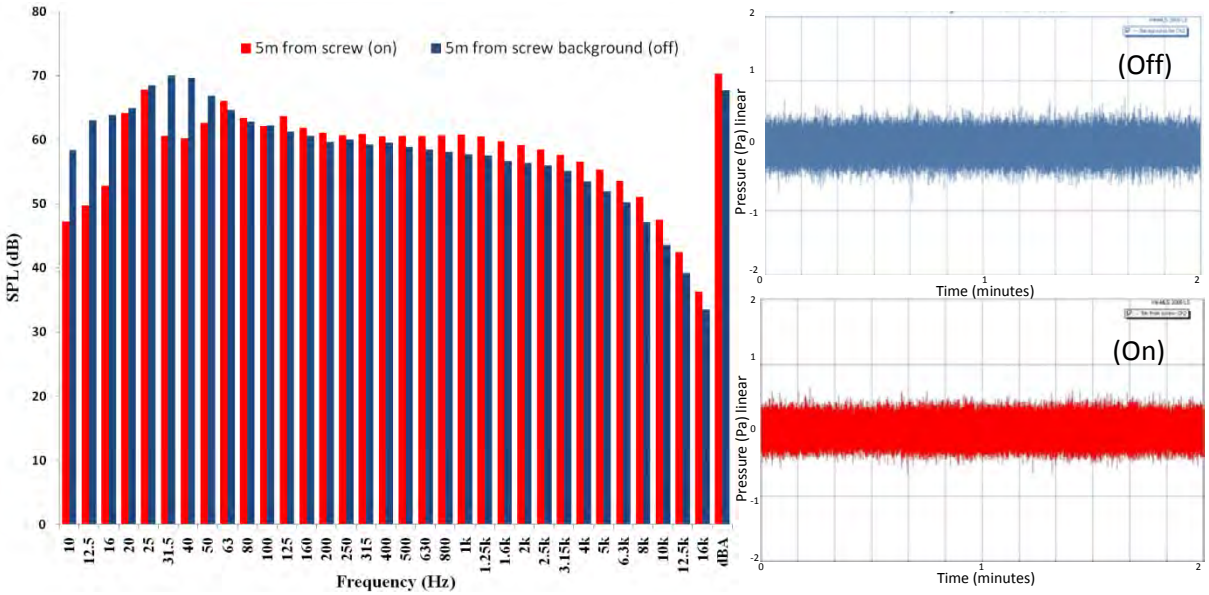

Figure 5. 1/3 octave spectrum plots of the SPL and 2 minute signal, when the RAS is operational at 25kW (red) and when the RAS is off, flow is diverted over the weir (blue) at 5m from screw.

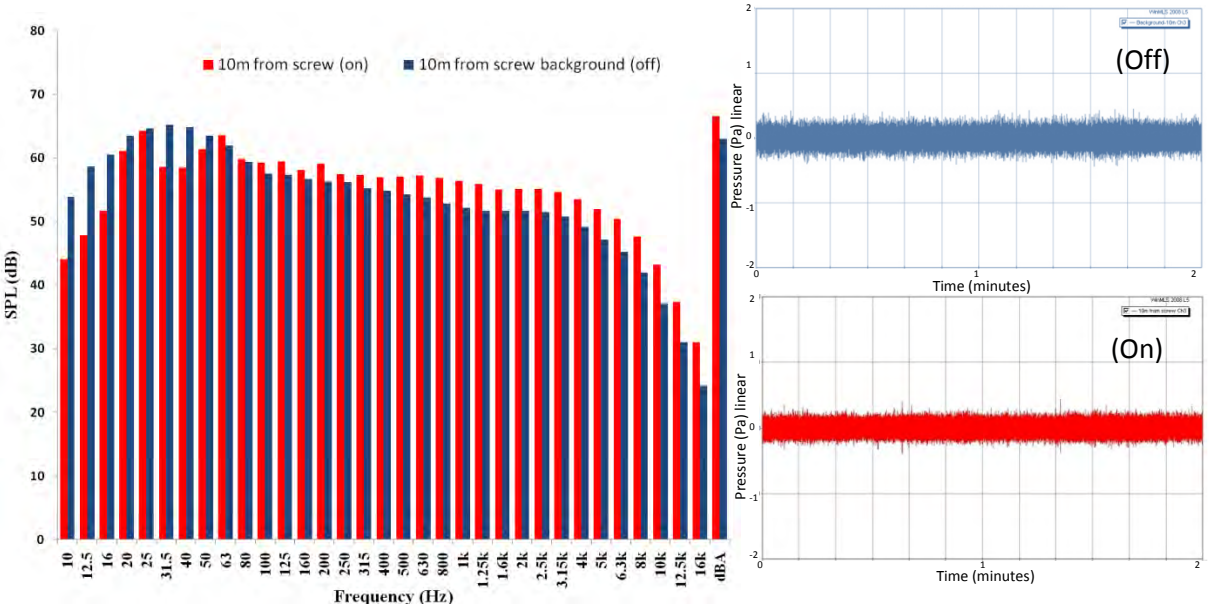

Figure 6. 1/3 octave spectrum plots of the SPL and 2 minute signal when the RAS is operational at 25kW (red) and when the RAS is off, flow is diverted over the weir (blue) at 10m from screw.

Table 1 and figure 7 show the SPL with increasing distance from the RAS along the three different transects a - c when the flow is diverted over the weir and the RAS is off. The

amplitudes are higher along transect (c) than (a) or (b), however this transect is located 10m from a stone cliff and road bridge, and it was noted on site that reflections were audible. The background data was all collected within a 40 minute period.

Table 1. Sample of background full octaves, SPL (dB) by frequency and transect distance figure 7, includes the frequencies not shown in this table.

Frequency [Hz]	SPL (dB) transect a 30 m	SPL (dB) transect b 30 m	SPL (dB) transect c 30 m	SPL (dB) transect a 60 m	SPL (dB) transect b 60 m	SPL (dB) transect c 60 m
250	51.8	55.0	61.4	44.3	53.1	55.3
1000	49.9	53.3	57.7	47.5	52.3	55.0
4000	46.1	49.7	53.6	40.7	45.5	50.5
dBA	60.3	63.6	68.1	56.5	61.5	64.6

At 30m on transect (b); there is a swash noise from water flowing over irregular rocks in the river next to the sample point. There are similar geographical features at this sample point to transect (c), which may increase the reflections in the area, including the large stone bridge, ruined walls and stone cliffs, though these cliffs are situated further away, and the ground is generally softer and grass covered between. There is an increase at 125Hz between the 30m and 60m sampling points on this axis (b). This may be related to other sound sources in the area, such as weirs present further downstream, or reflections in the area. It should also be noted that the large stone bridge near to the sampling point (*Figure 2*), is a road traffic bridge and this may explain the greater SPL low frequency results.

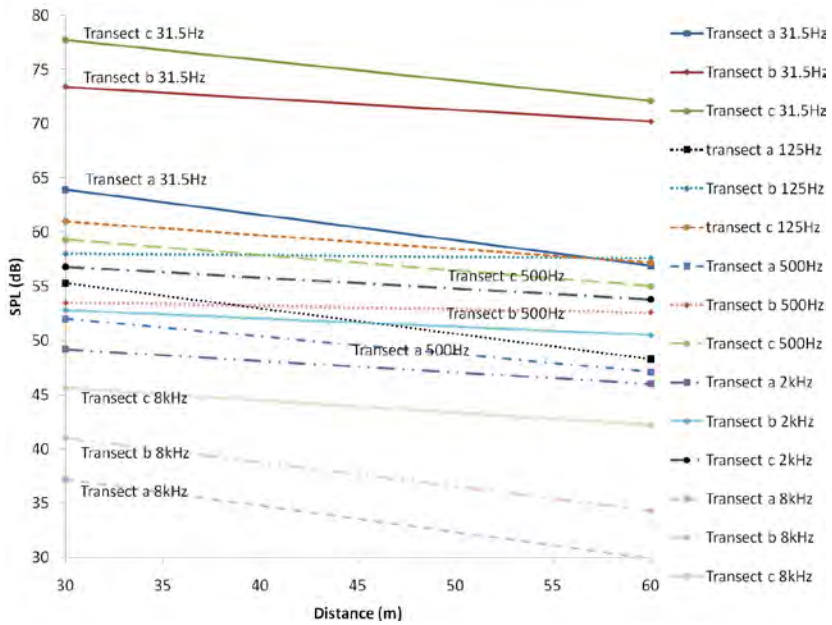

Along transect (a), running perpendicular to the RAS, the results taken at 30m and 60m sample points are noticeably lower in amplitude than (b) and (c) see *figure 7 and table 1*. As with the previous background plots *figures 3, 7 & 8*, the SPL of 31.5Hz is higher than that with the screw operational, see *figure 9*. *Figures 8* and *9* compare the SPL measured along transect (d) when the RAS is both on and off.

Figure 7. Example frequencies of the observed attenuation and SPL along transect a, b and c while the turbine is off. Lines between points are for demonstration purposes only and to aid pattern identification. The standard equation for attenuation of a line source with distance [11] was performed at 45m and it was found that deviation from the theoretical values is -1.6 to +2.1dB.

With a doubling of distance between 30 and 60m, in free-field conditions attenuation would be 3dB. Half the frequencies measured have higher attenuation levels than the 3dB whilst the other frequencies attenuate at a lower rate. It is thought that these differences are a function of the sampling environment as no corrections were added to the data, e.g. surface roughness differences or directivity. The variation in SPL differs depending on the frequency from

0.1dB to 9.1 dB, with an average difference between background frequencies and operational frequencies of 4.5dB at 0m, 3.3dB at 5m and 1.6dB at 10m. At 31.5Hz the SPL when the RAS is not operational is greater than when it is. These results are for a period when river flow enables the RAS to produce 25kW; further research is required to understand the generation of noise at a range of flows and electrical power outputs, and to validate the results presented.

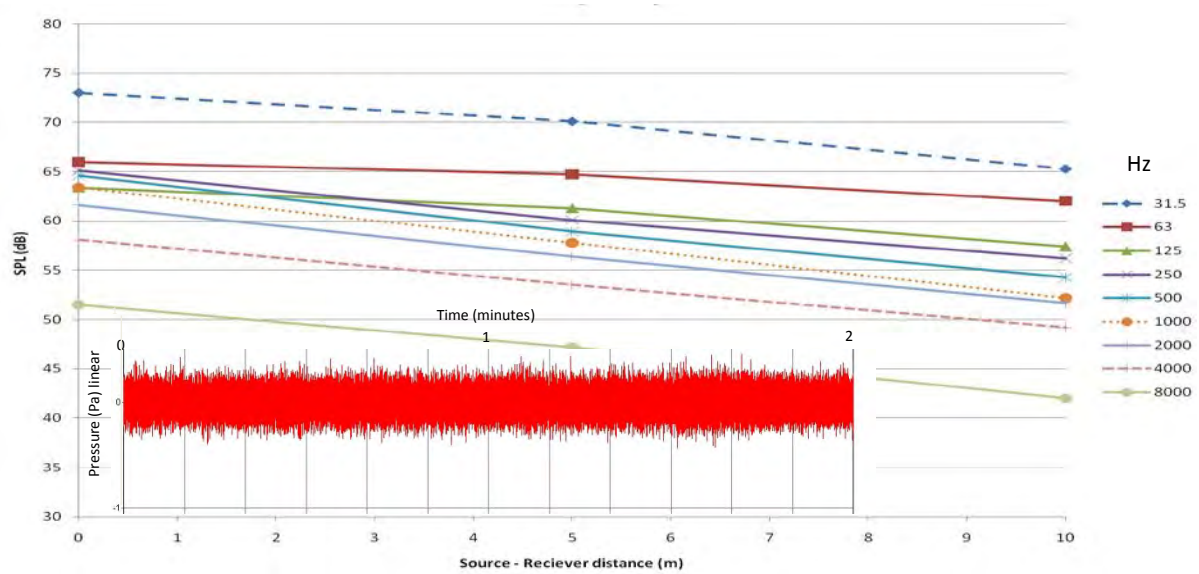

Figure 8. SPL by frequency from 0-10 whilst the turbine is off along transect a, where the insert is the 2 minute sample of the signal measured at 0m.

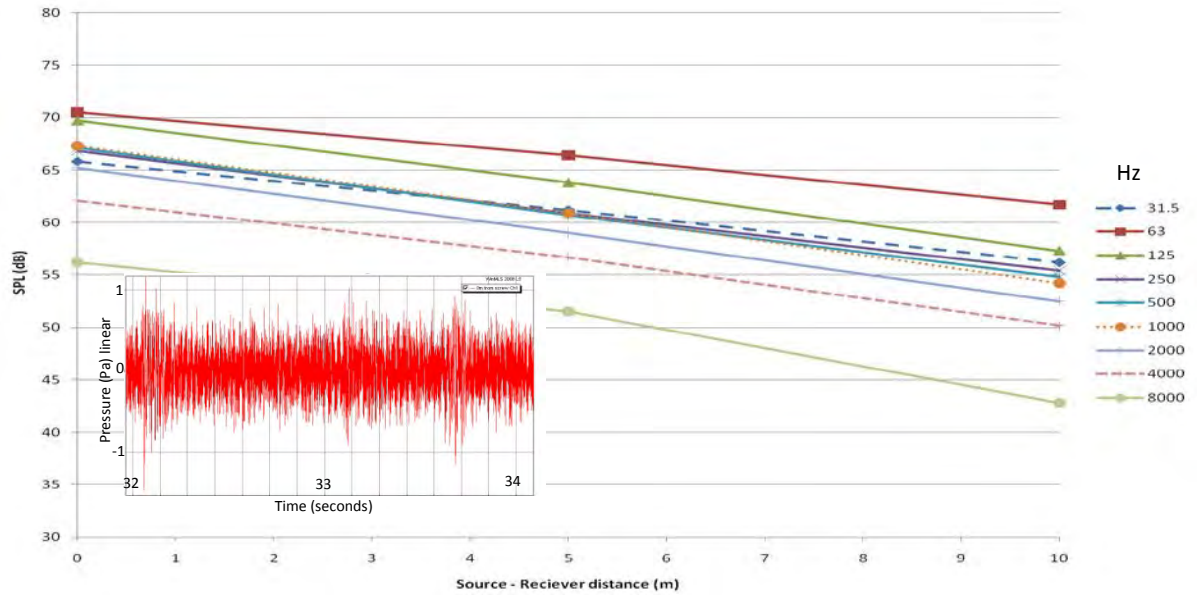

Figure 9. SPL by frequency from 0-10m whilst the turbine is switched on along transect a, where the insert is a 2 second sample of the signal measured at 10m between 32 and 34 seconds. A cyclic impulse can be seen within the signal plotted less than 2 seconds apart. This fits with the tri-blade rotational speed of the RAS which would include the blades entering/exiting the water.

4. Conclusions & Future Work

Initial results indicate that during normal operation at 25kW the screw would be barely perceptible beyond 60m, and adds just 3dB to the background environment and thus in many cases have negligible urban environmental impact running at 25kW. The weir has a significant masking effect on the RAS sound output. Further to this, the results indicate a directional aspect to the sound propagation from a RAS. However, whether this is a feature of the site or a feature of the RAS design is yet to be determined.

The RAS is not operational below 20kW, and therefore this study demonstrates the noise propagation at low flows. Future work will consider a range of flows from this increasing to the RAS design capacity of 53kW. Future work will also include a more detailed study of the RAS at New Mills with greater near field sampling and over shorter sampling periods to limit any extraneous noise sources from the results. Evaluation of other RAS sites will be carried to enable modeling and validation of the sound propagation. This will be used to assess the effect of various interventions in reducing noise nuisance from a RAS in an urban setting. Some further results will be presented at the conference.

References

[1] Driscoll, H.J.R., Micro-hydro power in Dorset: A re-assessment of potential installed capacity. Earth & E-nvironment, 2008. 3: p. 52-114.

[2] Lior, N., Energy resources and use: The present (2008) situation and possible sustainable paths to the future. Energy, 2009. 35: p. 2631-2638.

[3] International Energy Agency, World Energy Outlook 2008. IEA 2008.

[4] Paish, O., Small hydro power: technology and current status. Renewable & Sustainable Energy Reviews, 2002. 6(6): p. 537-556.

[5] Frey, G.W. and Linke, D.M., Hydropower as a renewable and sustainable energy resource meeting global energy challenges in a reasonable way. Energy Policy, 2002. 30(14): p. 1261-1265.

[6] Yi, C.-S., Lee, J.-H. and Shim, M.-P., Site location analysis for small hydropower using geo-spatial information system. Renewable Energy, 2010. 35(4): p. 852-861.

[7] Watson, R. and Downey, O., The Little Red Book of Acoustics: A Practical Guide. 2nd ed. 2008: Blue Tree Acoustics.

A Piezoelectric Energy Harvester Based on Pressure Fluctuations in Kármán Vortex Street

Dung-An Wang[1,*], Huy-Tuan Pham[1], Chia-Wei Chao[1], Jerry M. Chen[2]

[1] *Graduate Institute of Precision Engineering, National Chung Hsing University, Taichung 40227, Taiwan, ROC*
[2] *Department of Mechanical Engineering, National Chung Hsing University, Taichung 40227, Taiwan, ROC*
** Corresponding author. Tel: +886 422840531, Fax: +886 422858362, E-mail: daw@dragon.nchu.edu.tw*

Abstract: We have developed a new energy harvester for harnessing energy from the Kármán vortex street behind a bluff body in a water flow. It converts flow energy into electrical energy through oscillation of a piezoelectric film. Oscillation of the piezoelectric film is induced by pressure fluctuation in the Kármán vortex street. Prototypes of the energy harvester are fabricated and tested. Experimental results show that an open circuit output voltage of 0.12 V_{pp} and an instantaneous output power of 0.7 nW are generated when the pressure oscillates with an amplitude of ~0.3 kPa and a frequency of ~52 Hz. This approach has the potential of converting hydraulic energy into electricity for powering wireless devices. The low output power of the device can be improved by an optimization design procedure or by adopting a piezoelectric material with higher piezoelectric constants. An array of these devices with multiple resonant frequencies may be considered for energy harvesting from ambient flow sources.

Keywords: *Energy Harvester, Piezoelectric, Kármán vortex street*

1. Introduction

Recent development of wireless sensor networks allowing real-time industrial process monitoring, machine health monitoring, environment monitoring, healthcare applications, and traffic control demands an economical source of energy not requiring fuel or replacement of finite power stores. Considerable effort is focused on use of renewable energy coming from natural resources such as flowing water, rain, tides, wind, sunlight, geothermal heat and biomass. Renewable energy from small-scale hydro, modern biomass, wind, solar, geothermal and biofuels accounted for 2.7% of global final energy consumption in 2008 and is growing very rapidly [1].

Small hydro systems using turbines/wheels can be used to convert mechanical energy from water flow into electricity. Krähenbühl et al. [2] designed an electromagnetic harvester based on a turbine driven by water pressure drop in throttling valves and turbo expanders in plants that outputs 150 W power with a rotation speed of 490000 rpm. Their device comprises a turbine and a permanent generator. A detailed electromagnetic machine design, rotor dynamics analysis and a thermal design were required to construct their energy harvester. Holmes et al. [3] reported an electromagnetic generator integrated with a microfabricated axial-flow microturbine. The power output of the fabricated microdevice can be as high as 1.1 mW per stator when operated at a rotation speed of 30000 rpm, but the fabrication processes for their prototype involve deep reactive ion etching, multilevel electroplating, SU8 processing and laser micromachining. Herrault et al. [4] presented a rotary electromagnetic generator to harvest the mechanical energy of an air-driven turbine. The fabrication of their device requires electroforming, magnet demagnetization and laser machining. A maximum output power of 6.6 mW is attained when their device is driven at a rotation speed of 392000 rpm by an air turbine. The devices of Krähenbühl et al. [2], Holmes et al. [3] and Herrault et al. [4] require elaborate techniques for fabrication of their stator-rotor subcomponents and high rotation speeds for efficient energy harvesting. A device with simpler structure design

and ease of application may be needed to extract energy from fluid motion for microsensor and communications applications.

Installations with miniaturized pipe-line systems may provide an alterntive for harvesting small scale water flow energy. Sanchez-Sanz et al. [5] assessed the feasibility of using the unsteady forces generated by the Kármán street around a micro-prism in the laminar flow regime for energy harvesting. They presented design guidelines for their devices, but fabrication and demonstration of the proposed device are not shown in their work. Allen and Smits [6] used a piezoelectric membrane placed behind the Kármán vortex street formed behind a bluff body to harvest energy from fluid motion. They examined the response of the membrane to vortex shedding. The power output of the membrane is not presented. Taylor et al. [7] developed an eel structure of piezoelectric polymer to convert mechanical flow energy to electrical power. They have focused on characterization and optimization of the individual subsystems of the eel system with a generation and storage units in a wave tank. Design and deployment of the eel system need further investigation. Tang et al. [8] designed a flutter-mill to generate electricity by extracting energy from fluid flow. Their structure is similar to the eel systems of Allen and Smits [6] and Taylor et al. [7]. They investigate the energy transfer between the structure and the fluid flow through an analytical approach. These authors utilized the flow-induced vibrations of fluid-structure interaction system to extract energy from the surrounding fluid flow [9]. The eel structures of Allen and Smits [6], Taylor et al. [7] and Tang et al. [8] have the potential to generate power from milli-watts to many watts depending on system size and flow velocity, but a power-generating eel has not been demonstrated.

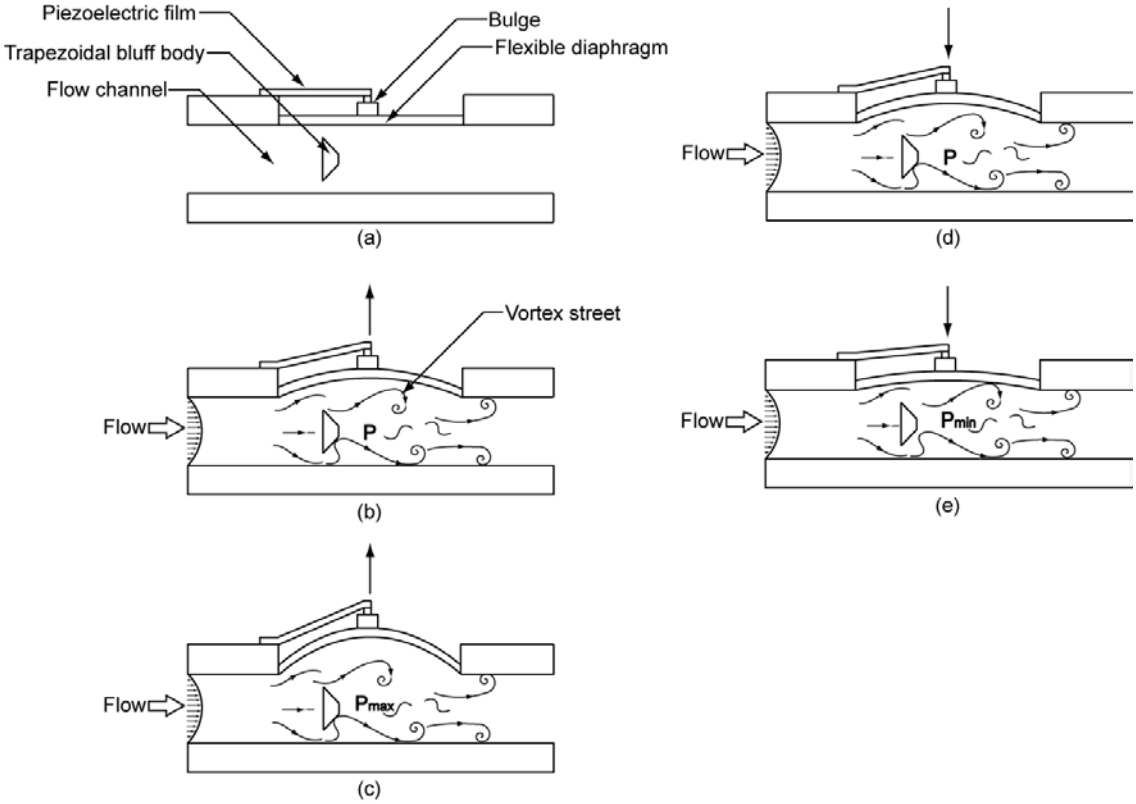

Fig. 1. Operation of a piezoelectric energy harvester.

In this report, we demonstrate a new device for energy harvesting from pressure fluctuations in the Kármán vortex street, where a piezoelectric film is placed on top of a flexible

diaphragm, which is located in the wake of a bluff body. The piezoelectric film oscillates on a flexible diaphragm due to the vortices shed from the bluff body in a water flow. As illustrated in Fig. 1(a), a flow channel with a flexible diaphragm is connected to a flow source. A piezoelectric film of a cantilever type is glued to a bulge affixed to the top surface of the flexible diaphragm. A bluff body is placed in the flow channel. Pressure in the flow channel behind the bluff body may fluctuate with the same frequency as the pressure variation caused by the Kármán vortex street. Fig. 1(b) shows that the pressure in the channel causes the diaphragm and the piezoelectric film to deflect in the upward direction. As the pressure increases to the maximum, the diaphragm reaches its highest position (Fig. 1(c)). When the pressure drops, the diaphragm and the piezoelectric film deflect downward (Fig. 1(d)). As the pressure decreases to the minimum, the diaphragm reaches its lowest position (Fig. 1(e)). Thus, by placing the energy harvester in a flow source, the oscillating movement of the diaphragm with the cantilever piezoelectric film attached to it makes the energy harvesting possible.

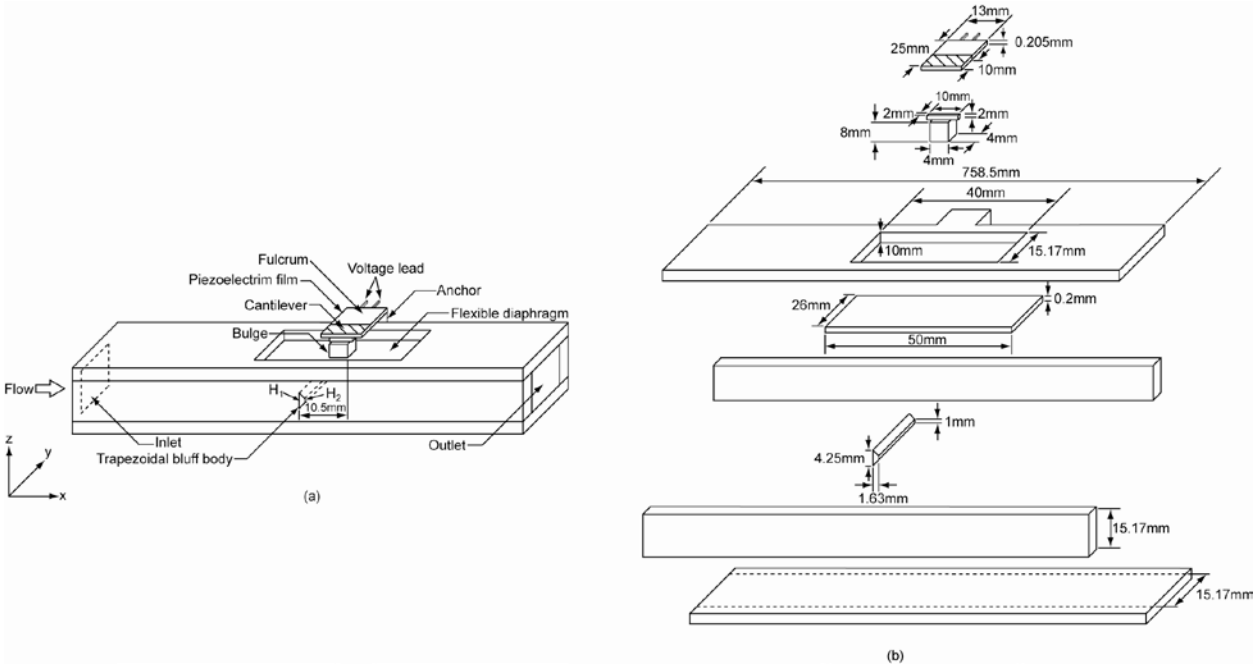

Fig. 2. (a) An assembled energy harvester. (b) Components of the energy harvester..

2. Methodology

2.1. Operational principle

A piezoelectric energy harvester considered in this investigation is shown in Fig. 2(a). Fig. 2(b) is an exploded view of the energy harvester. The dimensions of the energy harvester are indicated in Fig. 2(b). It consists of a flow channel, a bluff body, a polydimethylsiloxane (PDMS) diaphragm bonded to the channel, and a piezoelectric film attached to the PDMS diaphragm through a bulge made of acrylic blocks. Flow past a bluff body creates an unstable wake in the form of alternating vortices and induces periodic pressure variation [10]. The frequency at which the vortices are shed from the bluff body is given by the Strouhal number, St, $St = \omega \ell / U_\infty$ [11], where ω is the frequency of oscillating flow, ℓ is the characteristic length, and U_∞ is the free-stream velocity. Vortex shedding from a circular cylinder immersed in a steady flow occurs in the range $10 < Re < 10^5$, where Re is the Reynolds number, with an average Strouhal number $\omega d / 2\pi U_\infty \approx 0.2$ [12]. For a trapezoidal bluff

body, the Strouhal number is given as $S = \omega H_1 / U_\infty$ [13], where H_1 is the height of the front side of the trapezoidal cylinder. The front height H_1 and rear height H_2 of the trapezoidal cylinder are denoted in Fig. 2(a).

The piezoelectric film (LDT0-028K/L, Measurement Specialties, Inc., US) is a laminate including a polyvinylidene fluoride (PVDF) film, two silver electrode layers and a polyester (PE) layer. The PDMS flexible diaphragm has a thickness of 200 μm. The electrode layers with a thickness of 28 μm are attached to the top and bottom surfaces of the PVDF film of 24 μm. A 125 μm PE layer is laminated to the top surface of the top electrode layer. The values of d_{31} and d_{33} of the PVDF are 23 and -33 $pm \cdot V^{-1}$, respectively. The capacitance of the PVDF film is 380 $pF \cdot cm^{-2}$. The Young's modulus and Poisson's ratio of the PVDF are 3 GPa and 0.35, respectively. When used in a bending mode, the laminated piezoelectric film develops much higher voltage output when flexed than a non-laminated film. The neutral axis is in the PE layer instead of in the PVDF film so the film is strained more when flexed.

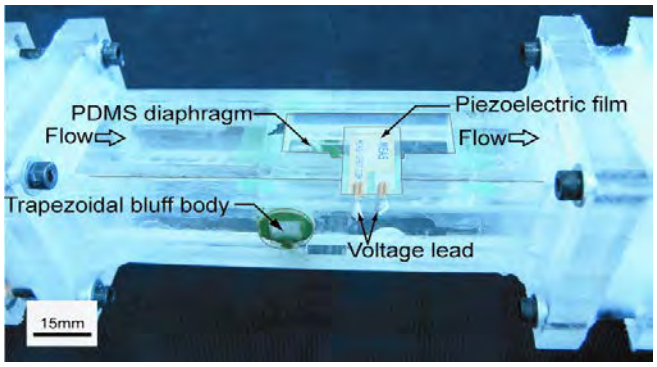

Fig. 3. Assembled energy harvester.

2.2. Fabrication and Experiments

In order to verify the effectiveness of the proposed energy harvesting device, prototypes of the energy harvester were fabricated. Fig. 3 is a photo of an assembled energy harvester. Its dimensions are indicated in Fig. 2(b). Fig. 4 is a photo of the experimental apparatus for testing of the fabricated device. The energy harvester is placed on an optical table for vibration isolation. From the bottom of a storage tank, an inlet pipe is run down to the inlet of the energy harvester. The water level in the storage tank is kept constant for a steady water flow at the inlet of the flow channel. Using gravity, water is forced into the inlet of the energy harvester. Tap water is pumped into the storage tank through a pump located in a recycle tank. An outlet pipe extending between the outlet of the energy harvester and the recycle tank provides a continuous supply of water. The oscillating deflection of the piezoelectric film is measured by a fiberoptic displacement sensor (MTI-2000, MTI Instruments Inc., US). The generated voltage of the piezoelectric film is recorded and analyzed by a data acquisition unit (PCI-5114, National Instruments Co., US). The pressure in the pressure chamber is measured with a subminiature pressure sensor (PS-05KC, Kyowa Electronic Instruments Co. Ltd., Japan) embedded in the bottom plate of the flow channel. The pressure sensor is connected to a data acquisition unit (DBU-120A, Kyowa Electronic Instruments Co. Ltd., Japan).

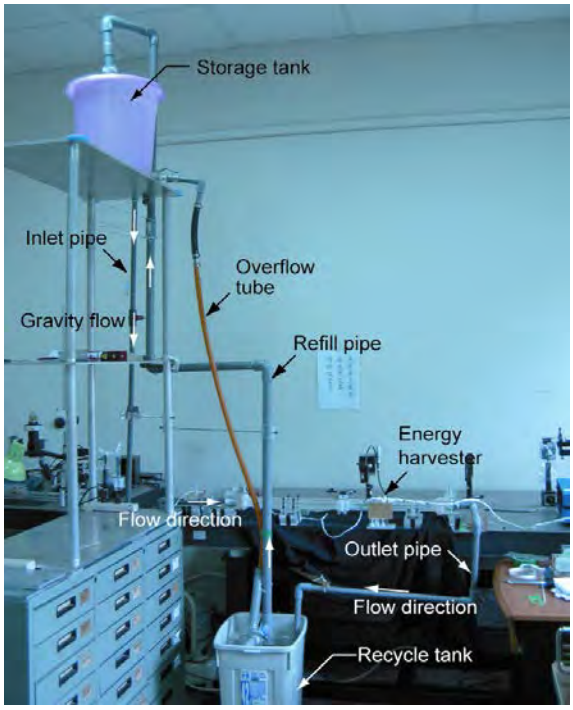

Fig. 4. A photo of the experimental setup.

3. Results

The experimental results are shown in Fig. 5. Fig. 5(a) shows the pressure history in the flow channel behind the bluff body, where the pressure oscillates with an amplitude of nearly 0.3 kPa and a frequency of 52 Hz. The measured deflection history of the free end of the piezoelectric film is shown in Fig. 5(b). The film oscillates with an amplitude of about 20 μm. The measured open circuit voltage generated by the piezoelectric film is shown in Fig. 5(c). The output peak-to-peak voltage is nearly 120 $\mathrm{mV_{pp}}$. The results shown in Figs. 5(a-c) are typical of those obtained over 20 seconds of measurements. Figs. 5(d-f) are the power spectral density corresponding to Figs. 5(a-c), respectively, but are based on all 20 seconds of measurements. Fast Fourier transform is used to compute the power spectral density. It can be seen from Figs. 5(d-f) that there is one obvious peak value of 52 Hz, caused by the pressure fluctuation in the flow channel. The low-frequency noise, below 20 Hz, observed in Figs. 5(d-f) can be attributed to the fact that flows in the experimental setup are always contaminated by ambient noise sources, and the geometry of the bluff body and the walls of the flow channel are not perfectly symmetric and smooth.

The average free-stream velocity U_∞ measured in the experiments is 1.083 m/sec. The Reynolds number Re of the flow can be determined by $\mathrm{Re} = \rho U_\infty D_h / \mu$, where μ is the dynamic viscosity of the water, 1.002×10^{-3} Pa·sec, and D_h is the hydraulic diameter, which is 15.17 mm for the flow channel considered. The calculated Re is 1.64×10^4, which is turbulent. The frequency of the pressure fluctuation is nearly 52 Hz (Fig. 5(d)), which is the rate at which the vortices are shed from the bluff body. Using the equation $\mathrm{St} = \omega H_1 / U_\infty$, the corresponding value of St is estimated as 0.204. White [12] reported an average St about 0.21 for the shedding from a circular cylinder immersed in a steady flow occurring in the range $10^2 < \mathrm{Re} < 10^3$. The estimated value of St for a trapezoidal bluff body of the experiments is reasonable compared with the value 0.21 reported by White [12]. The experimental values of

St for trapezoidal cylinders with the height ratio, H_2/H_1, ranging from 0.3 to 1.0 and the Re values of 100, 150, and 200, have a range from approximately 0.135 to approximately 0.155 [13]. Based on the work of Norberg [14] for a circular cylinder, the variations in St are within the limit 0.1 9 2 0.0 1 for the Re ranging from 250 t o 3×10^5. Ho and Huerre [15] commented that the values of St changes from 0.016 for a laminar flow to 0.022-0.024 for turbulent flow. Based on the reported experimental data [12-15], the estimated value of St, 0.204, based on the experiments carried out in this investigation could be acceptable.

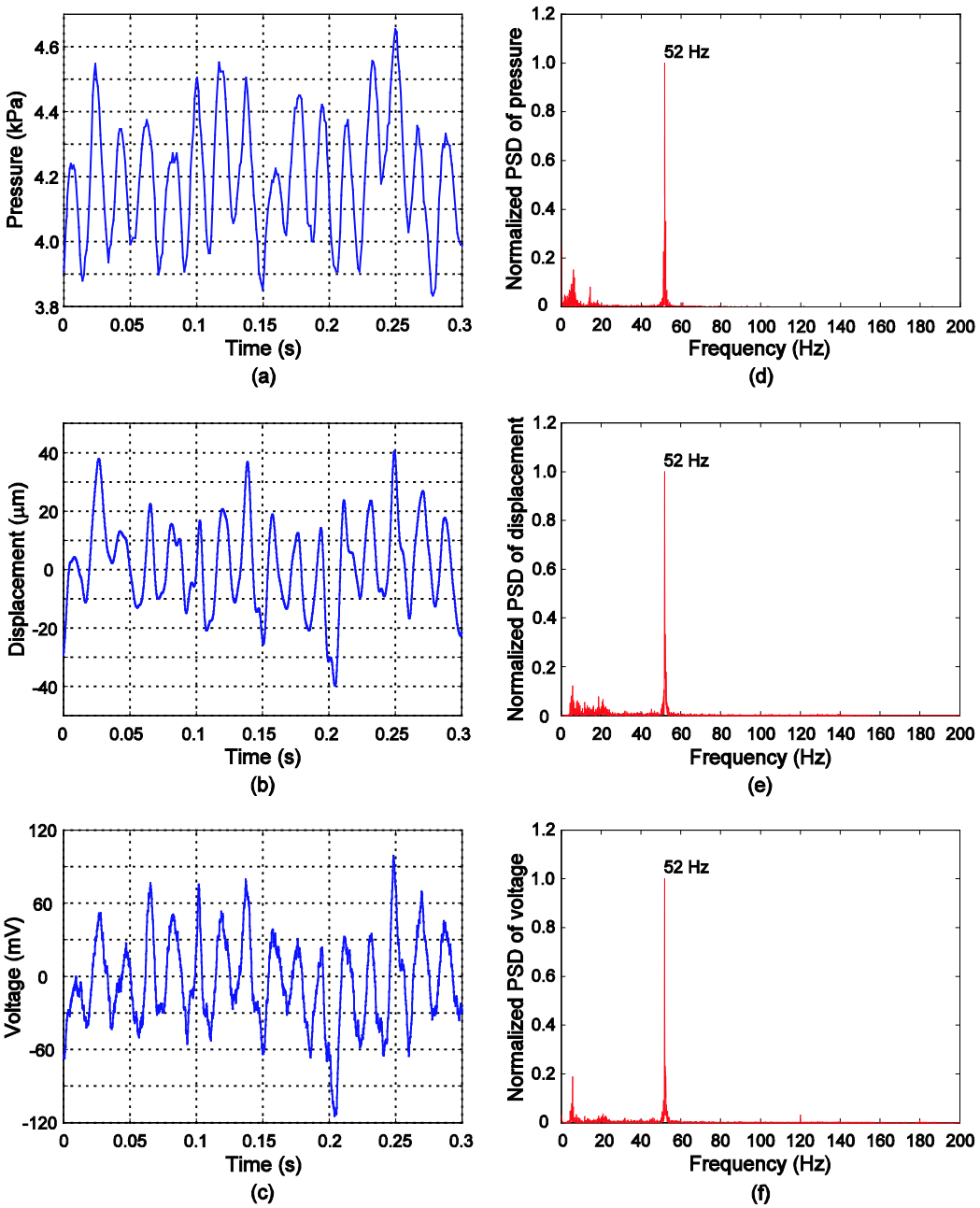

Fig. 5. Experimental results. (a) Pressure variation in the pressure chamber. (b) Deflection of the free end of the cantilever piezoelectric film. (c) Output voltage of the piezoelectric film. (d-f) Power spectral density corresponding to (a-c).

A matched load can be connected to the device to evaluate the power output of the device. The internal electrical resistance of the device is measured by a LCR meter (WK 4235,

Wayne Kerr Electronics, Ltd., UK). The instantaneous power can be expressed as $P = (\sqrt{2}\widetilde{V})^2 / R$, where R is the resistance value of the matched load and $\widetilde{V}$ is the root-mean-square value of the voltage drop across the matched load. By connecting the matched load of 655 kΩ to the device and detecting the voltage drop across the matched load, 14.89 mV_{rms}, the instantaneous power is determined as 0.7 nW.

4. Discussions

The output power of the device is relatively low, given the structure design of the flow channel, the bluff body and the cantilever piezoelectric film. In order to obtain a higher output power of the piezoelectric energy harvester, the dimensions and structure of the device can be optimized, and a piezoelectric material with higher piezoelectric constants can be adopted. In this investigation, the device is not operated at its resonance frequency. Most energy harvesting device based on piezoelectric effects have focused on single-frequency ambient energy, i.e. resonance-based energy harvesting [16]. The resonance frequency of the energy harvesting device can be tailored to the shedding frequency of the Kármán vortex street in order to increase the output power of the device. For random and broadband ambient flow sources, such a device may not be robust. A structure with multiple resonant frequencies may also be considered for energy harvesting from random vibrations with multiple resonant peaks, for example a segmented composite beam with embedded piezoelectric layers [17].

In order to generate the pressure fluctuation of the Kármán vortex street in the channel, a flow source assisted by gravity is used to force tap water into the flow channel in the laboratory environment. Energy can be harvested from pipe flows, blood flow in arteries [18,19], or air flow in tire cavities. The proposed device can be deployed on slopes to provide electricity for wireless sensor networks for detection of landslides. Landslides are usually preceded by heavy rainfalls, and the device can harvest the energy of the water flow along slopes due to rainfall. Energy harvesting from regular, periodic shedding can be integrated into tire pressure monitoring systems to harness the energy of air flow in tire cavities, or self-powering implantable and wireless devices in human bodies to convert the hydraulic energy of flow of body fluid.

References

[1] REN21, Renewables 2010 Global Status Report, 2010, pp. 15-16.

[2] D. Krähenbühl, C. Zwyssig, H. Weser, J.W. Kolar, Theoretical and experimental results of a mesoscale electric power generation system from pressurized gas flow, Journal of Micromechanics and Microengineering 19, 2009, 094009.

[3] A.S. Holmes, G. Hong, K.P. Pullen, Axial-flux permanent magnet machines for micropower generation, Journal of Microelectromechanical Systems 14, 2005, pp. 54-62.

[4] F. Herrault, C.-H. Ji, M. G. Allen, Ultraminiaturized high-speed permanent-magnet generators for milliwatt-level power generation, Journal of Microelectromechanical Systems 17, 2008, pp. 1376-1387.

[5] M. Sanchez-Sanz, B. Fernandez, A. Velazquez, Energy-harvesting microresonator based on the forces generated by the Kammon street around a rectangular prism, Journal of Microelectromechanical Systems 18, 2009, pp. 449-457.

[6] J.J. Allen, A.J. Smits, Energy harvesting eel, Journal of Fluid and Structures 15, 2001, pp. 629-640.

[7] G.W. Taylor, J.R. Burns, S.M. Kammann, W. B. Powers and T. R. Welsh, The energy harvesting eel: A small subsurface ocean/river power generator, IEEE Journal of Oceanic Engineering 26, 2001, pp. 539-547.

[8] L. Tang, M.P. Païdoussis, J. Jiang, Cantilevered flexible plates in axial flow: Energy transfer and the concept of flutter-mill, Journal of Sound and Vibration 326, 2009, pp. 263-276.

[9] R.D. Blevins, Flow-induced vibration, Van Nostrand Reinhold, ed. 2, 1990.

[10] R. Violette, E. de Langre, J. Szydlowski, Computation of vortex-induced vibrations of long structures using a wake oscillator model: Comparison with DNS and experiments, Computers and Structures 85, 2007, pp. 1134-1141.

[11] D.F. Young, B.R. Munson, T.H. Okiishi, A brief introduction to fluid mechanics, John Wiley & Sons, 2001.

[12] F.M. White, Fluid Mechanics, McGraw-Hill, 1986.

[13] Y.J. Chung, S.-H. Kang, Laminar vortex shedding from a trapezoidal cylinder with different height ratios, Physics of Fluids 12, 2000, pp. 1251-1254.

[14] C. Norberg, An experimental investigation of the flow around a circular cylinder: influence of aspect ratio, Journal of Fluid Mechanics 258, 1994, pp. 287-316.

[15] C.M. Ho, P. Huerre, Perturbed free shear layers, Annual Review of Fluid Mechanics 16, 1984, pp. 365-422.

[16] S. Adhikari, M.I. Friswell, D.J. Inman, Piezoelectric energy harvesting from broadband random vibrations, Smart Materials and Structures 18, 2009, 115005.

[17] S. Lee, B.D. Youn, B.C. Jung, Robust segment-type energy harvester and its application to a wireless sensor, Smart Materials and Structures 18, 2009, 095021.

[18] C. Mo, L.J. Radziemski, W.W. Clark, Experimental validation of energy harvesting performance for pressure-loaded piezoelectric circular diaphragms, Smart Materials and Structures 19, 2010, 075010.

[19] Z.L. Wang, J. Song, Piezoelectric nanogenerators based on zinc oxide nanowire arrays, Science 312, 2006, pp. 242-246.

Low head hydropower – its design and economic potential

Jana Hadler[1,*], Klaus Broekel[1]

[1] *University of Rostock, Institute of Engineering Design, Rostock, Germany*
** Corresponding author. Tel: +49 381 4989181, Fax: +49 381 4989172, E-mail: jana.hadler@uni-rostock.de*

Abstract: The large scale model of a Free Stream Energy Converter (FSEC) is built, and can be installed in protected as well as in tidal areas. This is one of the determined objectives of the EU-Project HYLOW, funded by the FP7. First field tests with rope winch and towing boat were done; further, in a protected area near Rostock, and the installation in the River Ems under tidal conditions and ship traffic, are planned for the first half of 2011. Besides, the permanent design control for the FSEC is as necessary as the monitoring of the behaviour of the model positioned in all the sites. If design changes or modifications are necessary, these can be done directly on site, respectively in the Steel Construction Company nearby. Whether it is suited for practice, however, is still dependent on other factors. The investigations are primarily limited on technical and ecological level. It is now necessary to look at the cost-sided development, too. Starting with considerations for the financing and economic efficiencies about expressive cost-benefit analyses up to design and material costs, the European need should be determined in hydropower for low potentials. Realization of hydropower plans takes a long period.

Keywords: *Low head differences, Free Stream Energy Converter, EU-Project, Hylow, Cost-benefit analysis.*

1. Introduction

One reason for the Hylow project is the rising demand for energy. Another one is the necessity to implement renewable energies, because of undeniable importance in view of declining natural resources. Small hydropower is a possible substitute for fossil fuels which are already limited. The European committee has fixed specific targets with a view to initiating change towards renewable energy. In order to achieve these objectives, energy generating systems, which were economically unattractive, are given greater priority.
The Hylow project focuses on the development of a mobile energy converter for low head differences – a topic which is usually neglected, because of missing significant results.

2. Motivation for hydropower

Compared to wind power and photovoltaic, small hydropower is often undervalued - at least in the public perception. In theory the worldwide demand for energy could be covered by hydropower. But it will not be economically practical, because of the uneven distribution of water resources on world territory.

2.1. Strong arguments

The power source “hydropower” offers many advantages.
Minimal emissions occur just in the installation period and in the first running period, when converters have to be stabled. A running energy converter does not need a great number of additional materials or energy. In sum there are low CO_2 emissions during operating time.

Hydropower requires no primary energy – therewith the respective countries relieve their own energy bills as well as they increase the security of energy supply. Furthermore, hydropower depends neither on the natural rhythm of the sun nor on the strength of the wind. This allows a permanent and continuous electricity generation.

There is a significant potential for hydropower in the EU and worldwide. However, the availability of use is limited by specific features of energy supply, such as localization, use of sites, power supply and current collection.

2.2. Background of Hylow

Small hydropower plants are close to nature; their design is often environmentally compatible. This applies to Hylow also. The floating Large Scale Model (LSM) of the FSEC is nearly 7,800 mm in length, 2,400 mm in width, and 3,500 mm in height. The wheel diameter is 3,200 mm and 1,100 mm in width (see Figure 1).

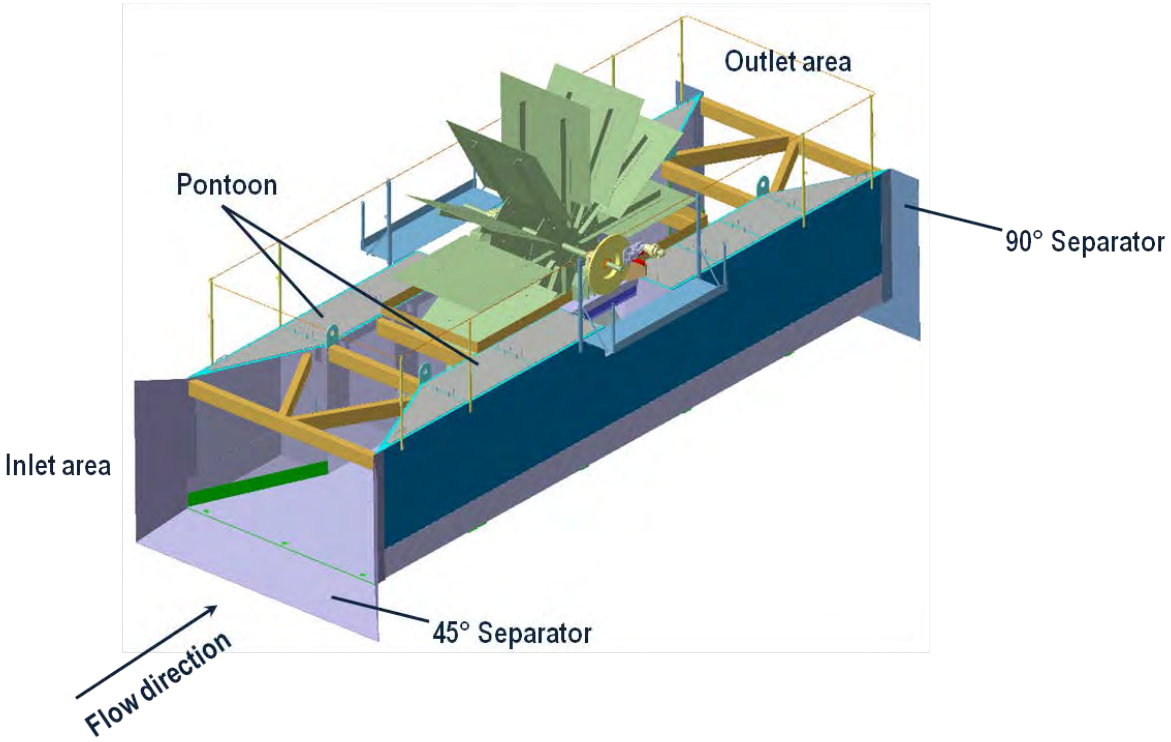

Fig. 1. The CAD model of the LSM, separators included.

The LSM will be placed in running waters with flow velocities of up to 1.5 m/s. The model is dimensioned for exceptional situations, in which the velocity rises, such as floodwaters or strong winds. To realize test runs with the LSM in protected areas no lubricants or other persistent products will be used. The power take-off is envisaged as a friction-type brake, and works without any liquids, so that even in the average case the environment takes no damage. For later applications and for deployment in developing countries to energy production, the brake system will be substituted with a generator solution which is adapted in ecological respects. [1]

3. Product development

Essential for product development activities, besides the idea, are calculations. These start with the power output to be expected. In addition, all forces, which appear, are to be taken into consideration.

3.1. Free Stream Energy Converter

The first geometry of the pontoon was given by calculations and basis tests done with simplified and down scaled configurations. The outline geometry consists of two hulls which

are connected via a base. The hulls in the inlet area are v-shaped, so that the channel will get narrowed, and the flow velocity accelerates. This procedure corresponds to the Venturi principle. [1]

Fig. 2. The LSM on the first deployment – the naval base in Rostock.

During the whole project three field tests with the LSM at different locations (with expected flow velocities between 0.4 and 1.5 m/s) are planned. The first deployment site was envisaged for towing tests; these tests have been successfully completed in autumn, 2010 (see Figure 2). The second and third test sites are in a protected area near Rostock, and in the River Ems in Northern Germany.

Initial towing tests were meant to demonstrate the model behaviour during operational conditions. In addition, the floating behaviour of the model with different velocities and geometries (additional separators) should be tested. The LSM delivered an electric power output up to 500 W.

The towing tests show that something has to be changed concerning the geometry of the LSM. The best results in the first deployment site were achieved with separators at both ends of the LSM. In the inlet area works the separator as a scoop with an angle of 45°, and in the outlet it has 90°. In order to limit the costs several models have to be analysed with the computational fluid dynamics (CFD) software FLOW-3D [3]. See first results in Figure 3.

The FLOW-3D tests are useful for the fine adjustment of length, arrangement and angular size of the separators. Moreover, the trim angle of the FSEC can be adjusted according to the waterline (horizontal alignment in the flow). Figure 3 shows three situations in FLOW-3D with different arrangements of the separators. The set velocity is determined with 1 m/s, and it changes as expected in several areas of the flow pattern – in narrowed parts of the channel are higher velocities than in the widened areas. The simulations are ongoing; final results are expected in spring, 2011.

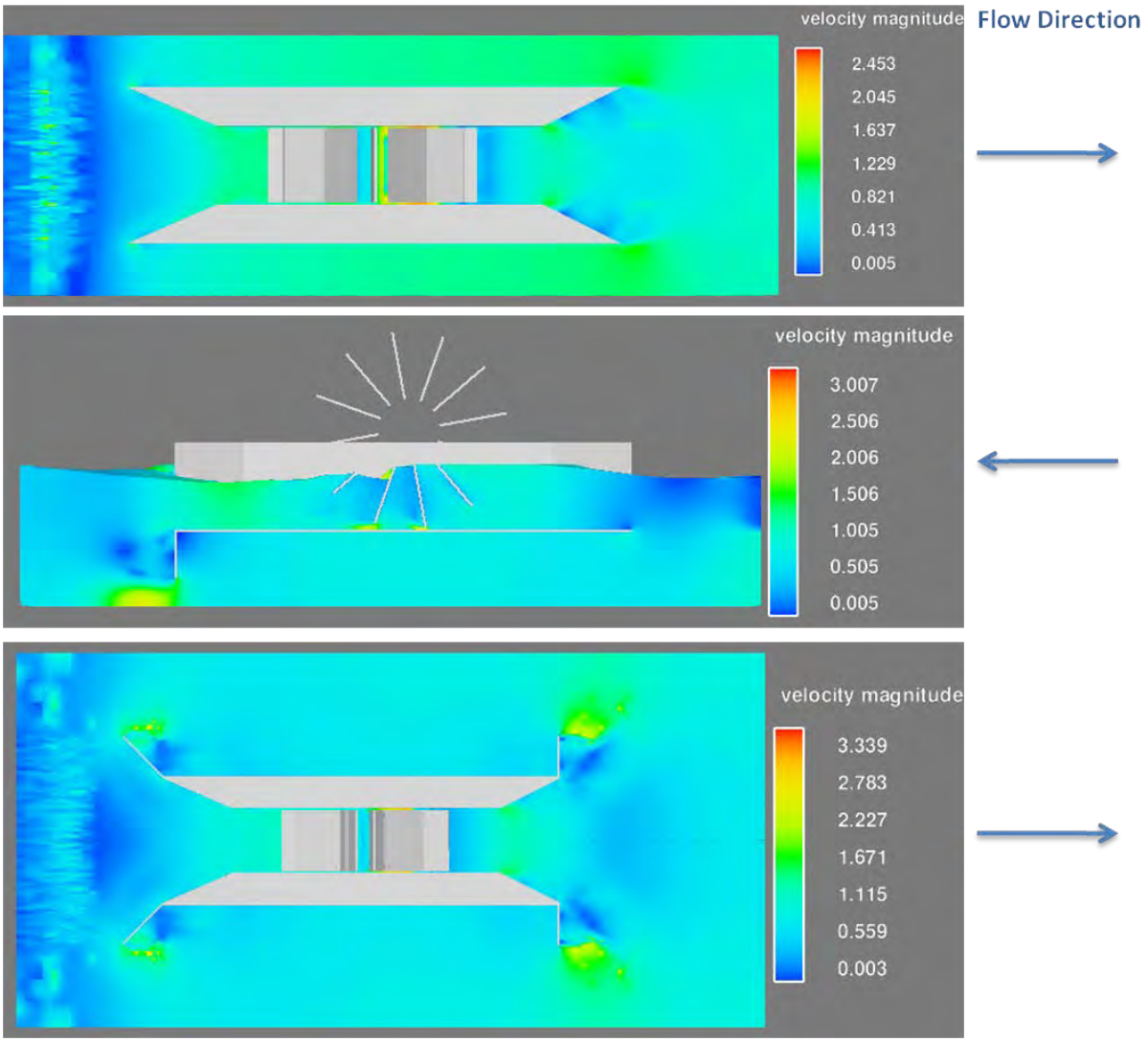

Fig. 3. Geometry tests with FLOW-3D.

3.2. Cost report of the FSEC prototype

To check the efficiency of the FSEC the annual costs are compared with the benefit. The benefit will be calculated from the sale of electricity to the energy companies. Thus, the investment can determine the annual profit, as the difference between the yields and costs. For the considerations, the average values of all costs and yields are used.

The total costs of the energy converter arise from different cost types. A calculation basis of these are the given production costs of the prototype which consist as follows (table 1):

Table 1. Production costs for prototype.

Cost type	**Total** [€]
Personnel costs	30,491.00
Material, standard parts & consumables	24,750.00
Indirect costs (20 % of direct costs)	11,048.20
Manufacturing costs	66,289.20

In these costs no costs for research and development included. Because of the prototype, no values of experience have still integrated into the production procedure. Moreover, detailed

values of wear behaviour are neglected, because there are no empirical values for this special case exist.

4. An FSEC in Europe – where conditions are most favorable

The benefit of the FSEC consists in the production of electrical energy using the potential of flowing water. For the feed in existing electrical grids there are fixed feed-in tariffs which mostly have a limited duration. In addition, a purchase obligation by the energy groups exists in several European countries.

4.1. Feed-in tariffs

Table 2 shows height and duration of the feed-in tariffs for selected European countries. To calculate the annual yield the payment must be multiplied by the energy generated in the year. It is assumed that the FSEC works continually without interruption 8,760 hours per year. The electrical energy is the product of the expected average electric power (assumption = 3 kW) and the annual power consumption in hours.

In case of permanent consumption the electrical energy for 3 kW power output will be 26,280 kWh. The resulting annual yields are given in the right column of table 2 [3]. The countries are sorted according to the amount of feed-in tariffs, starting with the highest.

Table 2. Feed-in tariffs and their time limits in Europe.

European country	**Amount of feed-in tariff**	**Duration of feed-in tariff***	**Annual yield**
	[€/kWh]	[years]	[€]
Great Britain	0.23	-	6044.40
Italy	0.22	15	5781.60
Germany	0.1267	20	3329.68
Netherlands	0.125	15	3285.00
Latvia	0.11	10	2890.80
Slovenia	0.105	15	2759.40
Czechia	0.081	30	2128.68
Denmark	0.0803	10	2110.28
Luxembourg	0.079	15	2076.12
Spain	0.077	25	2023.56
Portugal	0.075	20	1971.00
Ireland	0.072	15	1892.16
Greece	0.07	10	1839.60
Lithuania	0.07	-	1839.60
Slovakia	0.066	15	1734.48
France	0.06	20	1576.80
Estonia	0.051	12	1340.28
Belgium	0.05	-	1314.00
Bulgaria	0.045	15	1182.60
Austria	0.0378	13	993.38
Hungary	0.029	payoff time	762.12

* Some values are not known; duration is unlimited.

The European countries of the first rows have a good chance to invest in the small hydropower market. Therefore the use of the energy converter is determined as a value size. Now as a comparison the costs are considered.

4.2. Overview to cost covering

Thus, the production costs fall with renewed individual manufacture on 70%, because the development is concluded and is possible for a shorter manufacturing time by experience-guided, structured work.

With a small batch production of five energy converters, a cost reduction on 60% (according to the manufacturer) is to be achieved. With these estimates the manufacturing costs change as follows (table 3):

Table 3. Types of production series.

Manufacturing costs for	**Price per unit** [€]
Prototype	66,289.20
Individual production	46,402.44
Batch production (5 pieces)	39,773.52

It is assumed that steady wear behaviour during utilisation exists. The amount of annual depreciation may be calculated according to the linear method. Thereby in every period the same depreciations are created. If the lifespan is 20 years, than the following results can be represented (table 4):

Table 4. Cost structure for all considered production series.

	Prototype **100%**	**Individual production** **70%**	**Small batch production** **60%**
	[€]	[€]	[€]
Personnel costs	30,491.00		
Direct costs	24,750.00		
Indirect costs	11,048.20		
Total manufacturing costs*	***66,289.20***	***46,402.44***	***39,773.52***
Imputed depreciations**	3,314.46	2,320,12	1,988.68
Imputed interests***	1,756.66	1,229.66	1,054.00
Imputed costs of capital	***5,071.12***	***3,549.78***	***3,042.68***
Leasing costs	200.00	200.00	200.00
Maintenance costs	253.56	177.49	152.13
Insurance, taxes, administration	530.31	371.22	318.19
Annual costs	***6,054.99***	***4,298.49***	***3,713.00***

* Total manufacturing costs = A_0
** A_0 / lifespan
*** A_0 / 2 * 5.3% (discount rate of German Central Bank) [4]

The imputed costs of capital are divided into imputed depreciation and imputed interests. The imputed depreciations are the costs for losses in value. Whereas the imputed interests are the interests due on the amount of money lent over the maturity of the operation period.
The amount of the leasing costs depends on the plant size and the location. It varies from country to country, therefore it was assumed that the leasing costs are 200 € per year (average value in Germany). The maintenance costs are 5% of the imputed costs of the capital. The costs for insurance, taxes and administration are 0.8% of the total manufacturing costs.

Concluding, the following table 5 gives an overview to the first five European countries and the profit per annum (annual yield minus costs).

Table 5. Profit per annum for all considered production series.

European country	**Prototype 100%**	**Individual production**	**Small batch production**
	[€]	[€]	[€]
Great Britain	-10.59	1,745.91	2,331.40
Italy	-273.39	1,483.11	2,068.60
Germany	-2,725.31	-968.81	-383.32
Netherlands	-2,769.99	-1,013.49	-428.00
Latvia	-3,164.19	-1,407.69	-822.20

The profit table clearly shows that the prototype is not profitable in the next 20 years. With the other production forms the FSEC under described conditions could be a lucrative business.

5. Summary

The FSEC is able to convert the kinetic energy of flowing waters into electricity. By means of low head differences and by applications of separators power outputs of at least 3 kW are expected. To attain this objective a lot of additional research is needed. Initial results of the ongoing FLOW-3D trials show how the design of the FSEC might essentially change.

The presented cost report demonstrates that only in a few European countries the balance between annual costs and benefit can be achieved. The most important criterion is how long the payback period is. The other item to note is that all the assumptions are defined as cases with ideal conditions. It is still uncertain how long an FSEC in this form will work.

In the manufacture of the FSEC prototype, personnel and material costs is the biggest cost block by far. As a result of batch production and growing experience the personnel costs will be reduced. It is to think about moving the production of further plants in countries which have lower production costs to cover the risk of rising material costs, because of the development in the steel market. It is expected that the steel price and in this connection the material costs for the converter will increase. The saving in materials has direct impacts on the operating earnings, especially when using alternative materials such as wood or glass fibre plastics (GRP) [2].

Acknowledgements

The research leading to these results has received funding from the European Community's Seventh Framework Programme [FP7/2007-2013] under grant agreement n° 212423.

References

[1] J. Hadler and K. Broekel, (2010), Development and design of low potential hydropower converters in protected areas, in Proceedings of hidroenergia 2010, Lausanne, June 16 – 19, 2010.

[2] J. Hadler and K. Broekel, (2011), Cost-benefit analysis for low potential hydropower converters, in Proceedings of 34th IAHR World Congress 2011, Brisbane, June 26 – July 1, 2011 (not yet published).

[3] http://www.energy.eu (*20.11.2010*).

[4] http://www.bundesbank.de (*25.11.2010*).

On the Large Scale Assessment of Small Hydroelectric Potential: Application to the Province of New Brunswick (Canada)

Jean-François Cyr, Mathieu Landry, Yves Gagnon*

K.C. Irving Chair in Sustainable Development, Université de Moncton, Moncton (NB), Canada
** Corresponding author. Tel: +1 506 858 4152, Fax: +1 506 863 2110, E-mail: yves.gagnon@umoncton.ca*

Abstract: The mapping of the small hydropower (SHP) resource over a given territory is indispensable to identify suitable sites for the development of SHP renewable energy projects. In this study, a straightforward method to map the SHP potential over a large territory is presented. The methodology uses a synthetic hydro network (SHN) created from digital elevation models (DEM) to ensure precise hydro head estimations. From the SHN, hydro heads are calculated by subtracting the minimum from the maximum elevation of synthetic stream segments. Subsequently, stream segments with low hydro heads over a specified maximum distance are removed. Finally, the method uses regional regression models to estimate the annual baseflow for all drainage areas in the study area. The technical SHP potential can then be estimated as a function of the hydro head and maximum penstock length. An application of the method is made to the province of New Brunswick, Canada, where SHP maps have been developed to promote the development of the SHP energy sector in the province. In terms of the SHP opportunity, it is shown that the province of New Brunswick (71,450 km^2) has a good SHP resource. Using a representative hydro head (10 m) and penstock length (3,000 m) for the region, 696 potential sites have been identified over the territory. Results show that the technical SHP potential for New Brunswick is 368 MW for the conventional hydroelectric reservoir SHP configuration.

Keywords: *Small hydropower (SHP), Resource assessment, Hydroelectric power potential, Mapping*

1. Introduction

The definition of small hydropower (SHP) varies according to jurisdictions; in some instances, hydroelectric generating stations having installed capacities of up to 15 MW are generally characterized as SHP [1], while in Canada, hydroelectric generating facilities with installed capacities of up to 50 MW are considered as SHP [2]. Similarly to other renewable energy sources, such as wind power, the mapping of the SHP resource over a given territory is indispensable to identify suitable sites for the development of SHP renewable energy projects.

Large scale SHP assessments for pre-feasibility studies have been done in the United States [3], where data from hydrological regions were used to estimate the annual average streamflow for ungauged drainage areas; the estimated annual average streamflow was then used in conjunction with digital elevation models (DEM) to determine the hydropower potential for sites situated in ungauged natural streams in the corresponding regions. In Canada, even though the province of British Columbia is the only province to have developed an official map of the SHP resource [4], many Canadian SHP sites have been mapped in the International Small-Hydro Atlas [5]. However, the latter was developed with information from ref. [6-10] which are generally based on a combination of historical data and observations from field research; modern mapping techniques have only been implemented in a few of these studies.

In this paper, a methodology for the large scale assessment of small hydroelectric potential is presented along with an application to the province of New Brunswick, Canada. In the first instance, a method is described to find the available hydro head on the hydrographic network of a study area. Secondly, the annual streamflow is calculated, as a function of the hydro head and maximum penstock length, for each available hydro head sites. The technical

hydropower potential is then calculated and the study results are presented in the form of a SHP map.

2. Hydropower Potential Modeling

At a given site, the hydropower potential, P, can be calculated as

$$P = \rho Q g h \eta \quad (1)$$

where ρ is the density of water (kg/m^3), Q is the volumetric fluid flow rate (m^3/s), g is the gravity constant (9.81 m/s^2), h is the height (m) of the drop (gross hydro head), and η is the efficiency coefficient. In this study, the density of water is assumed constant at 1,000 kg/m^3, the efficiency coefficient is set to 0.8 while the hydro head is defined as the height difference between the intake and the generating station. Thus, with these assumptions, only two remaining parameters, Q and h, are needed to determine the hydropower potential for any site in a given study area. A third indirect parameter, the penstock length, can also be used in the determination of the gross hydro head.

2.1. Hydro head modeling

Assuming that a drainage area generates enough streamflow to be considered as a potential site, the first phase of large scale SHP mapping is to locate every potential hydro head on all stream segments of the hydrographic network. To this end, a synthetic hydro network (SHN) using DEM is created to ensure relatively precise hydro head estimations. This is done because spatial entities in the National Hydro Network (NHN) are based on existing data of different agencies [11] and do not perfectly match with the DEM. Since the SHN perfectly matches the DEM, the interoperability between information layers is assured. GIS software tools such as the TauDem tools [12], along with algorithms based on the previous works [13-15] are used to create the SHN from the DEM. The SHN is then validated with the NHN and all stream segments present in the SHN that does not correspond to a NHN stream segment are excluded. From the SHN, hydro heads are calculated by subtracting the minimum from the maximum elevation of the synthetic stream segment. Subsequently, because the penstock length represents an important capital cost of the total civil work costs for SHP projects, a limit is imposed on the Euclidian distance between the highest and lowest node of a SHN stream segment, which is used to represent the penstock length. In this work, the maximum penstock length is established at 3,000 m and all stream segments up to the maximum penstock length having hydro heads of less than 10 m are removed from the model, due to the altitudinal precision of the DEM (± 5 m, 90 % of the time).

2.2. Streamflow modeling

A regional regression model based on the work of Vogel et al. [16] is used to estimate the annual streamflow for all drainage areas in the study area, namely:

$$Q = e^{C_0} X_1^{C_1} X_2^{C_2} \ldots X_n^{C_n} e^{\varepsilon} \quad (2)$$

where Q is the observed annual streamflow or baseflow in a gauged basin (m^3/s), X_i are the various drainage area characteristics (climatic and physical attributes such as average annual temperature, average annual precipitation, elevation and drainage area), C_i are the ordinary least square regression coefficients and ε is the residual of the model.

In order to evaluate the efficiency of the regional regression model between the estimation results and the observation data, a goodness of fit statistical model, known as the Nash and Sutcliff efficiency index [17], E, is used and is given by:

$$E = 1 - \left[\sum_{t=1}^{T} \left(Q_0^t - Q_m^t \right)^2 / \sum_{t=1}^{T} \left(Q_0^t - \overline{Q_0} \right)^2 \right] \quad (3)$$

where Q_o is the observed streamflow at a given time t and Q_m the modeled streamflow. The Nash and Sutcliff efficiency index ranges from -∞ to 1, where 1 represents a perfect match between the model results and the observed data.

2.3. A case study: Province of New Brunswick, Canada

As an application of the methodology proposed, and in order to promote the development of the small hydropower energy sector in the province, the large scale SHP assessment methodology for the conventional hydroelectric reservoir SHP configurations is applied to the province of New Brunswick (NB), Canada. The province of New Brunswick, one of the smallest of the Canadian provinces, both in size (71,450 km^2) and population (748,319), is part of the Maritime provinces on the eastern coast of Canada. The topography of New Brunswick consists in three major geographic regions. The north-west region is characterized by the Appalachian Mountains, which are dominated by Mount Carleton (820 m above sea level). The center of the province is composed of small rounded hills delineated by river valleys. Finally, the southern part of New Brunswick is composed of small hills sloping down to the Bay of Fundy, with the exception of the south-eastern part of the province which is composed of the Caledonia Highlands. In terms of climate, the province of New Brunswick is located within the Atlantic Ecozone, which is characterized by a continental climate due to eastward moving air masses. Although the moist climate provides an annual runoff varying from 600 to 1,000 mm, the annual runoff is more important in the southern region of the province, near the Bay of Fundy, due to higher precipitation events. The province's hydrographic network is composed of three major rivers: the St. John River, which drains the western part of New Brunswick, takes its source in the state of Maine, U.S.A. and discharges into the Bay of Fundy; the Restigouche River, which discharges into the Baie des Chaleurs, drains the northern part of New Brunswick; finally, the Miramichi River, which drains the eastern part of New Brunswick, discharges into the Gulf of Saint Lawrence.

2.3.1. Hydro head modeling input data

The DEM's used to generate the SHN are retrieved from the Canadian Digital Elevation Data (CDED) [11]. The raster dataset, at a 1:50,000 scale, has a minimum cell resolution of 0.75 arc seconds, which represents approximately 32 m^2 for the province of New Brunswick. The altitudinal precision of the dataset is ±5 m, 90% of the time. Furthermore, because some watershed areas are contiguous to the state of Maine, DEM covering corresponding sections of the state are also used. The dataset used to cover the corresponding watersheds are taken from the National Elevation Dataset (NED) 1 Arc Second of the United States Geological Survey (USGS) [18]. The NED dataset has a resolution of approximately 30 m^2 and is resized to match the CDED resolution. Finally, due to computing limitations, the DEM for the entire region is divided into 9 sub-regions, as shown in Fig. 1. These sub-regions are defined by using aggregates of sub-sub-drainage areas as delimited by the Water Survey of Canada (WSC) dataset [19], thus maintaining the topology of the SHN within each sub-region.

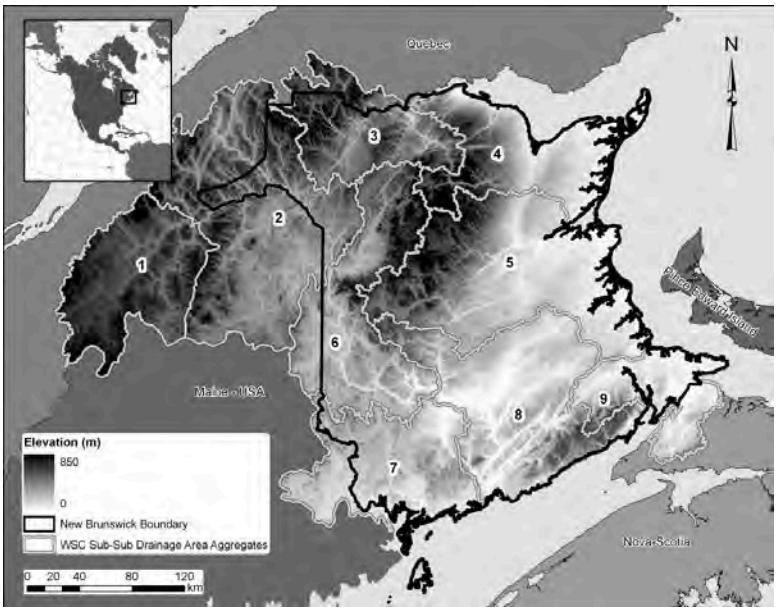

Fig. 1. Study area; sub-regions used for the extraction of the DEM.

2.3.2. Streamflow modeling input data

The climatic attributes such as average annual temperature and average annual precipitation used in several regional regression models tested in this study are taken from ref. [20-21]. In terms of the physical attributes used in the regional regression models, the majority of them, i.e. average slope, average elevation, elevation range, drainage area and eccentricity of the drainage area, are calculated from the DEM.

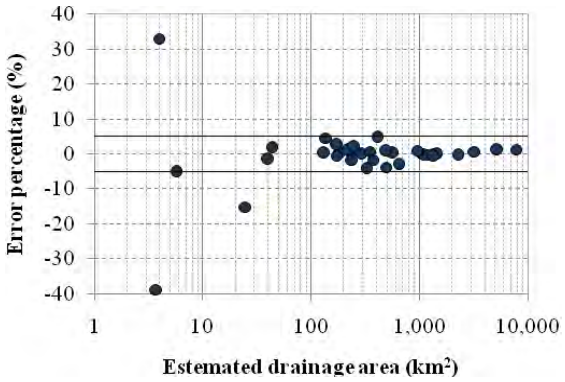

Fig. 2. Relative error between reference basin drainage areas and DEM-based basin drainage area estimation.

Previous research work in regional regression models has shown that the basin drainage areas provide good correlations in such models [16]. As is shown in Fig. 2, by comparing the DEM-based drainage area results for basins having hydrometric stations measuring natural flow to those of the Water Survey Canada as reference, it can be seen that the relative error decreases as the drainage area increases. In this work, a lower limit of 50 km^2 was imposed on drainage basins, such that hydro head having drainage areas with less than the lower limit where not considered. Finally, streamflow data from hydrometric stations [22], located across New Brunswick and having at least 30 years of continuous data, while being situated in basins with drainage areas larger than 50 km^2, are used in the various regional regression models tested.

3. Results

3.1. Hydro head modeling results

Results from the hydro head modeling showed that a total of 696 hydro heads in the province of New Brunswick satisfied the modeling constraints. In general, as in the case of other research in similar topography [23], because the topography is more variable in the upper part of a watershed area, stream segments with high hydro heads were generally located in the upper parts of a watershed area, while sites located in lower parts of a watershed area generally had lower hydro heads. Fig. 3 shows the distributions of hydro head sites by their characteristics.

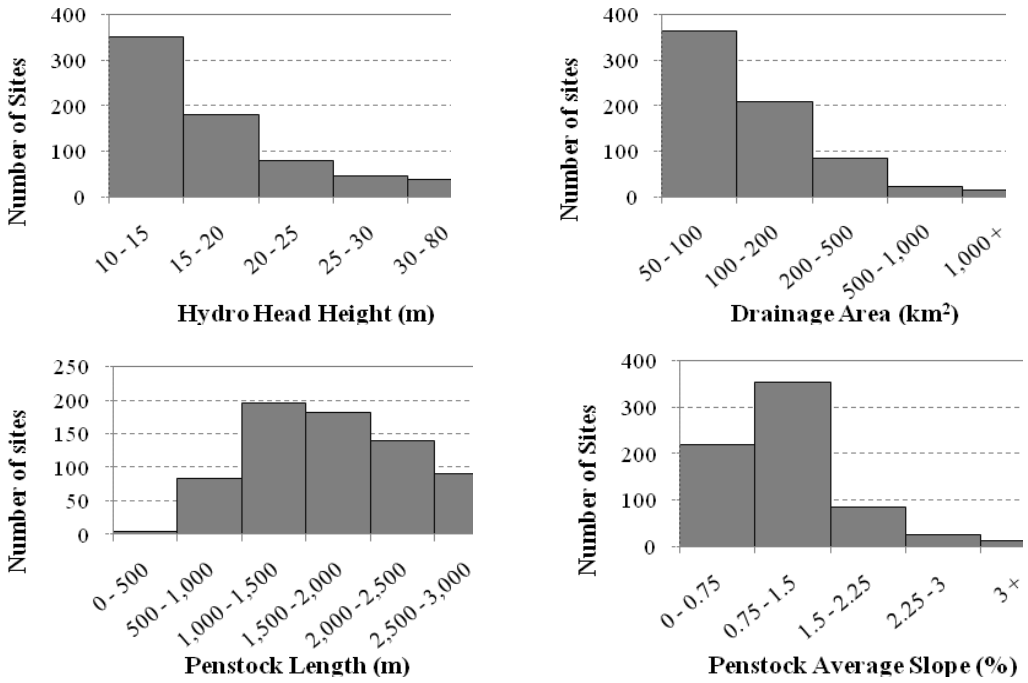

Fig. 3. Distribution of the hydro head sites.

3.2. Streamflow modeling results

In order to estimate the average annual streamflow for all basins in the study region, multiple regional regression models have been attempted in this work; the regional regression model having both the lowest average relative error (6.5%) and the highest Nash and Sutcliffe efficiency index (0.993) was chosen:

$$Q_m = e^{-16.552} A^{0.977} P^{1.733} D^{0.133} \quad (4)$$

where Q_m is the modeled streamflow (m^3/s), A is the drainage area (km^2), P is the average annual precipitation (mm) and D is the average elevation (m) of the drainage area.

3.3. Mapping results

While the methodology described in this paper can be used to estimate the SHP resource potential for both conventional hydroelectric reservoir and run-of-river SHP configurations, only results for the conventional hydroelectric reservoir SHP configuration are presented. Fig. 4 shows the mapping results of the SHP resource potential, for the conventional hydroelectric reservoir SHP configuration, in the province of New Brunswick. For this SHP configuration, the technical SHP potential for New Brunswick is 368 MW. The sites range in

SHP potential from 92 kW to 16.1 MW; the average potential for the 696 sites is 528 kW per site, while the median power potential is 303 kW.

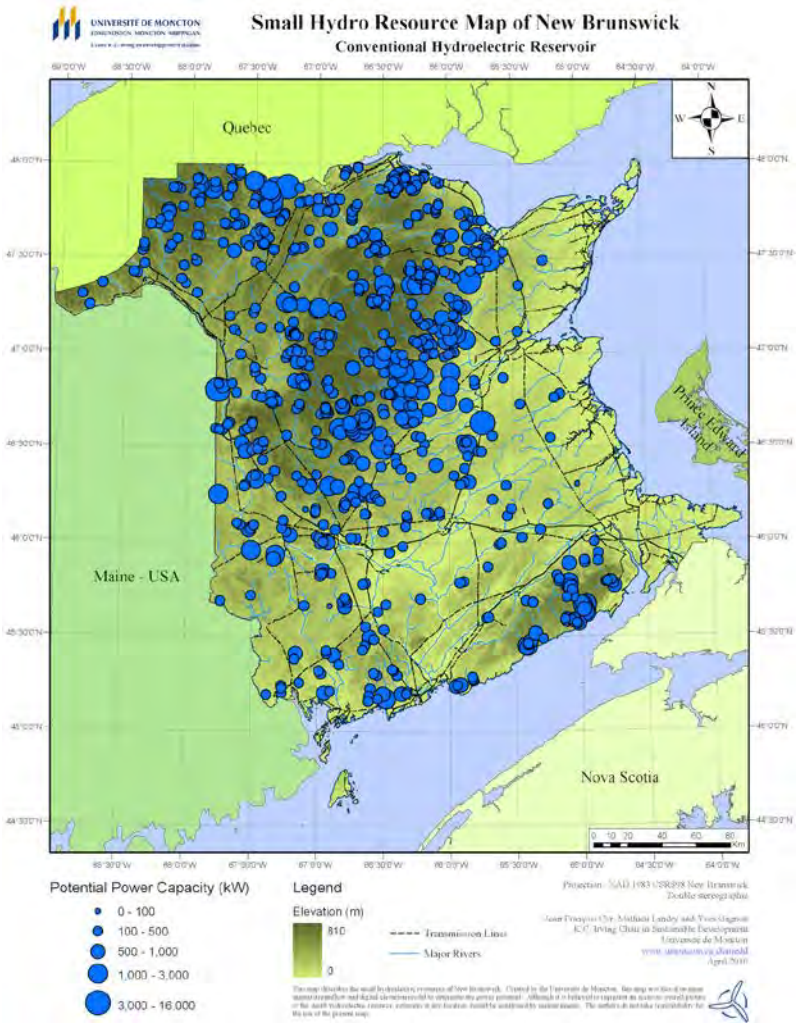

Fig. 4. SHP resource map of New Brunswick for conventional hydroelectric reservoirs.

4. Discussion and Conclusion

In this work, a straightforward method to map the small hydropower (SHP) potential over a large territory was presented. While the methodology presented in this paper is based on previous research work in this field of study, it contains several advantages which are not exclusive to this work but where their combination as a whole represents a significant advancement in this field. First, the methodology is general such that few variables are needed to perform a SHP study. Furthermore, the variables needed in the methodology are readily available at large scale for SHP studies in Canada or in other countries having publicly available GIS data. Secondly, the methodology can simultaneously evaluate and compare the SHP for both conventional and run-of-river configurations over a given area; this point represents a significant advancement in the field of study. Third, the methodology uses the gross hydro head, which significantly reduces the computational efforts of site selection. Fourth, the methodology is extremely fast and cost-effective when implemented using GIS-based software. However, the methodology introduces uncertainties in the estimation of the SHP resource potential which are due to the estimation of the efficiency of the SHP systems, the neglecting of SHP system head losses due to friction, and the use of yearly baseflow data

instead of monthly baseflow data. Finally, field measurements of terrain could be used to increase the accuracy of potential site locations.

An application of the method was made to the province of New Brunswick, Canada, where SHP maps were developed to validate the methodology and to promote the development of the small hydropower energy sector in the province. In terms of the SHP opportunity, it was shown that the province of New Brunswick has a good SHP resource. In comparison to the neighbouring state of Maine[1], a previous study [24] identified that there were over 5,883 sites in the state of Maine having a technical SHP potential capacity of 2,780 MW, thus giving an average SHP of 472 kW/site. In New Brunswick, results from this study have shown that there is a technical SHP potential capacity of 368 MW distributed on 696 sites; thus giving an average SHP of 528 kW/site.

Future work should focus on the elimination of potential sites that are not sustainable economically, environmentally or socially. To this end, potential sites that are located within federal and provincial park boundaries should be notably excluded. In addition, drainage basins having issues such as water supply, tourism, sport fishing, and the presence of species at risk should also be eliminated from the model.

Finally, the New Brunswick SHP map results have shown that the province of New Brunswick has a good small hydropower (SHP) resource which should be developed not only for its environmental benefits and attributes, but also for the social and economic benefits of its residents.

Acknowledgment

This research work was funded by the Natural Sciences and Engineering Research Council (NSERC) of Canada the Department of Energy of New Brunswick and the New Brunswick Innovation Foundation (NBIF).

References

[1] Renewable Energy Policy Network for the 21st Century (REN21), Renewables Global Status 2005 Update, Paris, 2005.

[2] Canada, Department of Natural Resources, Micro-Hydro Systems – A Buyer's Guide, Ottawa, 2004.

[3] United States, Department of Energy, Water Energy Resources of the United States with Emphasis on Low Head/Low Power Resources, Cat. No. DOE/1D-11111, Idaho National Engineering and Environmental Laboratory, 2004.

[4] BC Hydro & Power Authority and Canadian Cartographics Ltd., Energy Resources of British Columbia, Available at: www.canmap.com, 2002.

[5] International Small-Hydro Atlas, Available at: www.smallhydro.com, 2010.

[6] Monenco Limited, Identification of Environmentally Compatible Small Scale Hydroelectric Potential in Atlantic Canada, Phase 1, Vol. 1, Env. Canada, Halifax, 1984.

[7] Sigma Engineering, Small-Hydro Power Resource in the Provincial System, Ministry of Energy, Mines & Petroleum Resources, British Columbia, 1983.

[1] The number are for comparison only, both studies do not use the same methodology, nor the same definition for SHP and were made for different contexts.

[8] Sigma Engineering Ltd., Inventory of Undeveloped Opportunities at Potential Micro Hydro Sites in BC, Vancouver, British Columbia, 2000.

[9] Sigma Engineering Ltd., Green Energy Study for British Columbia Mainland Phase 2, Vancouver, British Columbia, 2002.

[10] Hatch Acres, Evaluation and Assessment of Ontario's Waterpower Potential, Ministry of Environmental Resources, Ontario, 2005.

[11] Geobase, National Hydro Network, Available at: www.geobase.ca, 2010.

[12] Utah State University, Terrain Analysis Using Digital Elevation Models (TauDEM), Available at: http://hydrology.neng.usu.edu/taudem/, 2009.

[13] S.K. Jenson, J.O. Domingue, Extracting Topographic Structure from Digital - Elevation Data for Geographic Information System Analysis, Photogrammetric Engineering and Remote Sensing, 54, 1988, pp.1593-1600.

[14] D.M. Mark, Network Models in Geomorphology, in: M.G. Anderson (Ed.), Modelling in Geomorphological Systems, John Wiley and Sons, New York, 1988, pp.73-97.

[15] D.G. Tarboton, A New Method for the Determination of Flow Directions and Contributing Areas in Grid Digital Elevation Models, Water Resources Research, 33, 1997, pp.309-319.

[16] R. Vogel, C. Bell, N. Fennessey, Climate, Streamflow and Water Supply in the Northeastern United States, Journal of Hydrology, 198, 1997, pp.42-68.

[17] J. E. Nash, J. V. Sutcliffe, River Flow Forecasting Through Conceptual Models. Part 1: A Discussion of Principles. Journal of Hydrology, 10 (3), 1970, pp.282–290.

[18] United States Geological Survey, The National Map Seamless Server, Earth Resources Observation - National Elevation Dataset (NED) 1 Arc Second, Available at: http://seamless.usgs.gov/products/1arc.php, 2008.

[19] Canada, Department of Natural Resources, GeoGratis - Atlas of Canada 1,000,000 National Frameworks Data, Hydrology Drainage Areas, Available at: www.geogratis.ca, 2009.

[20] Canada, Department of Environment, Canadian Climate Normals or Averages 1971-2000, Available at: http://climate.weatheroffice.ec.gc.ca/climate_normals/index_e.html, 2009.

[21] World Climate, Available at: www.worldclimate.com, 2005.

[22] Canada, Department of Environment, Water Survey, Available at: http://scitech.pyr.ec.gc.ca/waterweb/formnav.asp?lang=0, 2006.

[23] D. Nagel, J. Buffington, D. Isaak, Comparison of Methods for Estimating Stream Channel Gradien Using GIS, USDA Forest Service, Rocky Mountain Research Station Boise Aquatic Sciences Lab, Boise, Idaho, 2006.

[24] United States, Department of Energy, Feasibility Assessment of the Water Energy Resources of the United States for New Low Power and Small Hydro Classes of Hydroelectric Plants, Cat. No. DOE/1D-11263, Idaho National Laboratory, 2006.